2007

Flow of Sub-Cooled Cryogens through a Joule-Thomson Device: Investigation of Metastability Conditions

John M. Jurns
Cleveland State University

FLOW OF SUB-COOLED CRYOGENS THROUGH A JOULE-THOMSON DEVICE – INVESTIGATION OF METASTABILITY CONDITIONS

JOHN M. JURNS

Bachelor of Science Civil Engineering

State University of New York at Buffalo

June, 1978

submitted in partial fulfillment of requirements for the degree

MASTER OF SCIENCE IN MECHANICAL ENGINEERING

at the

CLEVELAND STATE UNIVERSITY

December, 2007

This thesis has been approved

for the Department of **MECHANICAL ENGINEERING**

and the College of Graduate Studies by

_____

Professor Jerzy T. Sawicki, Thesis Committee Chairperson

_____

Department / Date

_____

Professor Edward G. Keshock

_____

Department / Date

_____

Professor Asuquo B. Ebiana

_____

Department / Date

_____

Professor Hanz Richter

_____

Department / Date

_____

Dr. Mohammad M. Hasan

_____

Department / Date

ACKNOWLEDGEMENT

We would like to acknowledge the NASA Glenn Research Center in general, and the NASA GRC Propulsion and Propellants branch in particular for their support of this work and the for the use of the NASA GRC Creek Road Complex cryogenic test facilities. We would also like to acknowledge Dr. Mohammad Mojibul Hasan of the NASA Glenn Research Center for initially identifying the potential issue of metastable flow in Joule-Thomson “Visco Jet” devices, and for his direction and support of this work.

FLOW OF SUB-COOLED CRYOGENS THROUGH A JOULE-THOMSON DEVICE – INVESTIGATION OF METASTABILITY CONDITIONS

JOHN M. JURNS

ABSTRACT

Cryogenic fluid systems are fundamental to space flight architecture. Due to the unique properties of cryogenic fluids and the environments in which they operate for space flight, cryogenic fluid management systems must be developed to maintain these fluids at conditions in which they can be utilized. Liquid oxygen boils at 90 K, and liquid hydrogen boils at 20 K. Significant care must be taken to provide a thermal management system that prevents heat entering these fluids with consequential adverse effects on the performance of the cryogenic fluid systems. One critical component of a cryogenic thermal management system is a Joule-Thomson device. This one small component provides the driving force not only for the production of cryogenic fluids, but for the effective management of thermal loads in many cryogenic fluid systems including those used in space flight architectures.

As a fundamental understanding of the Joule-Thomson effect and J-T devices is critical to the effective design of cryogenic fluid management systems, the intent of this work is to examine J-T devices as they relate to space flight systems. This work will examine where these devices are used in space based cryogenic fluid management systems. It will consider research conducted to date that examines both the fundamental fluid physics behind how these devices operate and their application in real systems. Finally, it will report on the potential impact that fluid metastability has as it relates to J-T devices for certain cryogenic fluids.

An analytical assessment is made of the stability limits of single phase cryogenic fluids as a J-T device operates on them. This is compared to experimental results for tests conducted in liquid oxygen, and liquid methane. Results show that several factors influence the performance of J-T devices, and that the metastability of single phase cryogenic fluids below the saturation line must be considered in the design of cryogenic fluid management systems.

TABLE OF CONTENTS

NOMENCLATURE

c_p – Specific heat

h – Enthalpy

k_B – Boltzmann Constant

Lohm – Liquid ohm, measurement of Visco Jet flow resistance

mdot – Mass flow rate

p – Pressure

Q – Heat

R – Gas constant

S – Specific Gravity

T – Temperature

v – Specific volume

v_f – Liquid specific volume

v_g – Vapor specific volume

v_m – Specific volume at the root of a cubic p-v-T equation between v_f and v_g

X – Fluid quality

μ_{JT} – Joule-Thomson coefficient

ρ – Fluid density

σ – Surface tension

sp – spinodal

sat – saturated

LIST OF TABLES

LIST OF FIGURES

Figure Page

CHAPTER I

INTRODUCTION

A cryogenic fluid system is a fundamental component of virtually every space flight vehicle that leaves the confines of earth and travels to space. Whether it is a launch vehicle carrying a satellite to geosynchronous orbit, the satellite itself, a space station in low earth orbit, a science mission to the outer planets, or a lunar lander carrying astronauts back to the surface of the Moon, it would not be able to carry out its mission unless there were cryogenic fluids on board. When one speaks of a cryogenic fluid system, what essentially is meant is a container to hold a cryogenic fluid along with the ancillary components required to maintain that fluid at or below its vapor pressure. These components typically include insulation surrounding the tank to minimize heat leaking into the container, a system to pressurize the container as required, usually with an inert gas such as helium, a pump or other device to deliver the cryogenic fluid to an engine or other system, a vent system to relieve excess pressure from the container, and a heat exchanger system to either add heat to, or to extract heat from the cryogen. One small yet critical component of a heat exchanger system is a Joule-Thomson device. This seemingly insignificant item, which is essentially nothing more than an orifice in a pipe, is actually the critical component that allows the system to reject unwanted heat from the cryogenic fluid.

For a Joule-Thomson device to perform effectively in a cryogenic fluid thermal management system, pressure drop as a result of flow across the device must result in expansion of the liquid cryogen into the two phase region. Otherwise, there will be no accompanying temperature drop to provide the differential temperature required to drive the rejection of heat from the system. This observation is corroborated by liquid nitrogen (LN_2)[1] and liquid hydrogen (LH_2)[2] data from research conducted by the NASA Glenn Research Center in Cleveland, Ohio.

If cryogenic fluids are stored as saturated liquids, any heat entering the system converts liquid to vapor. It is therefore desirable to store a cryogenic fluid as a sub-cooled liquid. Subcooling the liquid is typically done by pressurizing the storage container with a non-condensable gas – typically gaseous helium (GHe). One operational issue that arises as a result of storing cryogenic fluids in the sub-cooled state is that the liquid then enters the Joule-Thomson device sub-cooled. As cryogen flows through the Joule-Thomson device, the pressure drop is isenthalpic until it crosses the two phase line. Further drop in pressure should result in phase change, and a resultant drop in temperature. However, a drop in pressure below the two phase line may, in some situations, still result in single phase flow of a metastable liquid, rather than two-phase liquid-vapor flow. That is, following a constant temperature line, the pressure can drop below the point at which transition to two-phase is expected, and even down to some minimum point beyond which the liquid cannot remain single phase. This theoretical limit can be predicted analytically, but actual minimum pressures where liquid no longer remains metastable are

typically higher than this value[3,4,5,6].

The significant question of practical importance is – how far below the two phase line might the liquid remain single phase? This is important to know for several reasons:

1. Designers may not assume that one needs only to drop pressure to the saturation line to get two phase flow and the accompanying temperature drop (ΔT).
2. The amount of initial sub-cooling of the liquid may be very significant with respect to the performance of the Joule-Thomson device in achieving a temperature drop which will reject heat from a system.
3. There are a number of different devices that can be used for J-T expansion. The type of J-T device used in a given system may have an impact on the minimum pressure the sub-cooled metastable fluid reaches before transition to two phase flow occurs.

The object of the present study is to determine analytically the theoretical minimum temperature a fluid may drop below the two phase line, and determine experimentally how close to these limits several cryogenic fluids might approach in a typical system. The fluids to be considered are liquid oxygen (LO_2) and liquid methane (LCH_4). A series of tests with varying degrees of sub-cooling on the inlet side and various downstream pressures were performed to determine how far below the saturation line the flow could go before becoming two phase with an accompanying temperature drop. These tests were carried out under several test programs at the NASA Glenn Research Center in Cleveland OH, at their cryogenic test research facilities[7].

1.1 J-T Effect

The Joule-Thomson (J-T) effect is a process in which the temperature of a real gas is either decreased or increased by letting it expand freely at constant enthalpy, as described in thermodynamics or physics textbooks. When a real gas expands freely at constant enthalpy, the temperature may either decrease or increase, depending on the initial temperature and pressure (see Figure 1). For any given pressure, a real gas has a *Joule-Thomson inversion temperature*, above which expansion at constant enthalpy causes the temperature to rise, and below which expansion at constant enthalpy causes cooling.

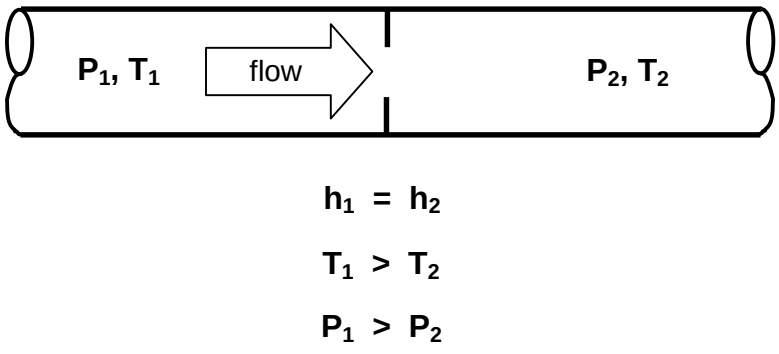

Figure 1 – Flow across a J-T orifice resulting in temperature drop

Applying the First Law of Thermodynamics for steady flow through an expansion device (a valve, orifice or other flow restriction), for zero heat transfer and zero work transfer, and negligible kinetic and potential energy changes, the enthalpy upstream equals the enthalpy downstream. That is:

$$h_1 = h_2 \tag{1}$$

Plotting lines of constant enthalpy on a graph of temperature versus pressure would reveal a region where the expansion through a J-T device produces an increase in temperature,

and a region where expansion would produce a decrease in temperature. The curve that separates these two regions is called the *inversion curve*. Figure 2 shows the inversion curve for gaseous methane passing through the maxima of lines of constant enthalpy.

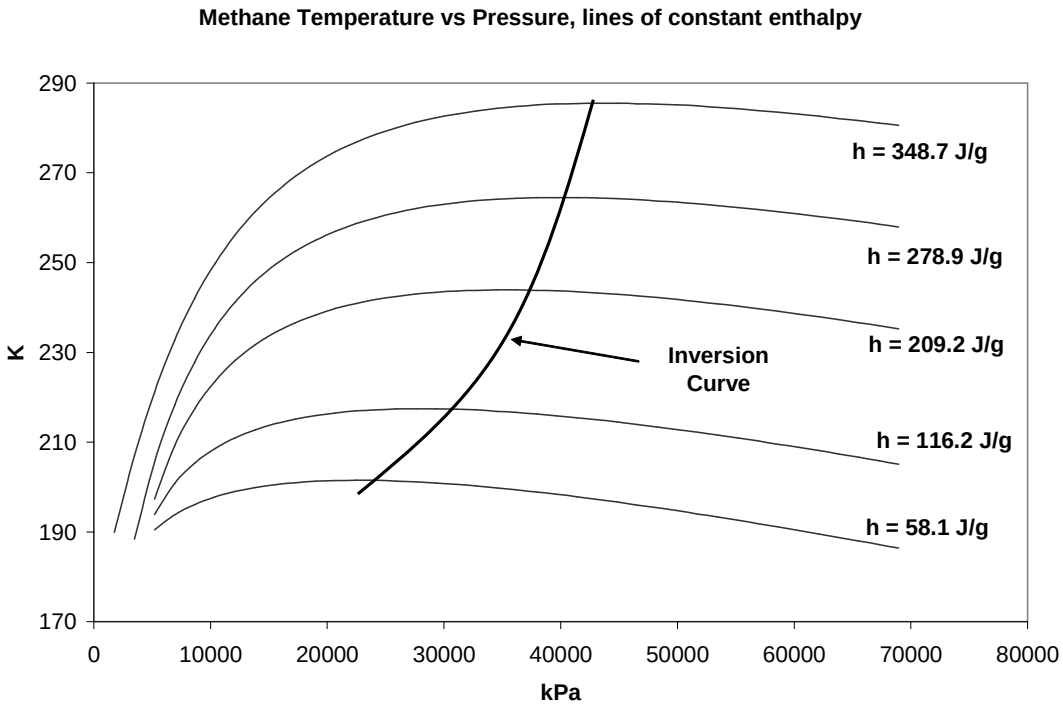

Figure 2 – Joule-Thomson Inversion Curve for Methane

In many cryogenic systems, the Joule-Thomson effect is used to produce low temperatures by performing isenthalpic expansion (pressure drop) to the left of the inversion curve.

The effect of change in temperature from isenthalpic change in pressure is represented by the Joule-Thomson coefficient, μ_{JT}.

$$\mu_{JT} = \left(\frac{\partial T}{\partial p} \right)_h \tag{2}$$

Note that the Joule-Thomson coefficient must be positive for a net temperature decrease during expansion, i.e. a temperature decrease resulting from a pressure decrease would result in a positive coefficient.

1.1.1 Devices

A Joule-Thomson device can be built in any number of physical configurations. The only requirement for the device is that it provides a restriction to flow of fluid through a pipe. This restriction could be provided by an orifice, porous plug, throttling valve, or any other similar device. Orifices and porous plugs have the advantage of having no moving parts. However, this may restrict their operating range. A throttling valve may provide pressure drop over a greater range of flows, but has the disadvantage of having moving parts. In cryogenic systems, careful attention must be paid to providing hardware that will perform reliably and without failure in the extreme cold temperature environment.

1.1.2 History

The J-T effect was discovered as one of the results of collaboration between James Prescott Joule and William Thomson (Lord Kelvin) in the 1850's, where they conducted research laying much of the groundwork in classical thermodynamic and kinetic theory[8]. Carl von Linde used the J-T effect in developing refrigeration cycles, and in 1895 liquefied air using J-T expansion and counter-flow heat exchangers[9]. This heralded the beginning of the air separation industry and modern cryogenics. Without this

fundamental work and the development of technology for liquefying and distilling air, modern rockets and the entire space industry would have never developed. (An interesting side note is that both Joule and von Linde were interested in developing technology to support the brewing industry – Joule investigated replacing steam engines with electric motors in breweries, and von Linde applied his refrigeration technology to German breweries and even Guinness!)

Modern rocketry was successfully developed based on the availability of cryogenic oxidizer and fuels. The higher density of liquid oxygen and hydrogen allows rockets to carry both fuel and oxidizer as relatively low pressure sub-critical fluids much more efficiently than if they were stored as high pressure gas. Early on in the United States space program, not much thought was given to conditioning cryogenic fluids, as their use was typically limited to very short durations. Propellant tanks would be loaded on the launch pad. Shortly thereafter, the rocket was launched, and the cryogenic oxidizer and propellant would be used up literally in a matter of minutes by the time the spacecraft reached orbit.

However, at the dawn of the Apollo era with the advent of longer duration space missions, managing cryogenic fluid conditions became a much more important issue. Whereas cryogenic storage in early rockets had only to be adequate for short term use, now cryogens for propulsion, on-board power and life support needed to be maintained for days or weeks duration. Systems and techniques needed to be developed to effectively manage fluid conditions and minimize heat entering these cryogenic systems.

As early as the 1960's cryogenic thermal conditioning systems were being developed for the Apollo program[10]. Since that time, there has been much work done in the aerospace industry developing cryogenic thermal management technology. Improved insulation systems to minimize heat leak into a cryogenic system[11], de-stratification and fluid mixing techniques[12,13], and active thermal control[14] have all contributed to improving long-term cryogenic storage.

Joule-Thomson devices started showing up as system components in cryogenic thermal conditioning systems in the 1970's[15,16]. By the 1980's, NASA had a robust cryogenic fluid management research program that included work on Thermodynamic Vent Systems incorporating Joule-Thomson devices[1,2,17,18].

1.2 J-T Devices in Space-Based Cryogenic TVS Systems

Long term storage of subcritical cryogenic fluids in space presents many challenges arising from a micro-gravity environment and ambient heat leak into the system. These factors result in thermal stratification of the fluid in storage tanks, formation of undesirable liquid/vapor mixtures and excessive tank pressure rise. Ambient heat leak into the system can be minimized, but not totally eliminated. Therefore, a means of minimizing thermal stratification and rejecting environmental heat is required. Heat rejection in space based cryogenic systems is provided by means of a *Thermodynamic Vent System* (TVS)[19]. These systems are generally divided into *active TVS* and *passive TVS* categories, the difference between the two architectures being the active TVS system requires a pump to provide fluid mixing[20]. Figure 3 shows a schematic representation of both (passive and active) architectures. However, a J-T device is common to both

systems, and understanding how J-T devices perform is critical to the design of the overall TVS system. In both active and passive TVS, a small amount of tank liquid is withdrawn (continuously or intermittently), and passed through a J-T device, resulting in a lower temperature and lower pressure two-phase fluid. This two-phase mixture then flows through a heat exchanger to cool the bulk tank fluid. The fluid mixture is completely evaporated in the heat exchanger, and then either vented overboard directly, or passed through vapor-cooled shields to intercept heat leak into the tank. It is apparent that the advantage of this system is to vent only vapor from the tank, thereby providing the maximum amount of heat rejection with the minimum loss of fluid from the tank.

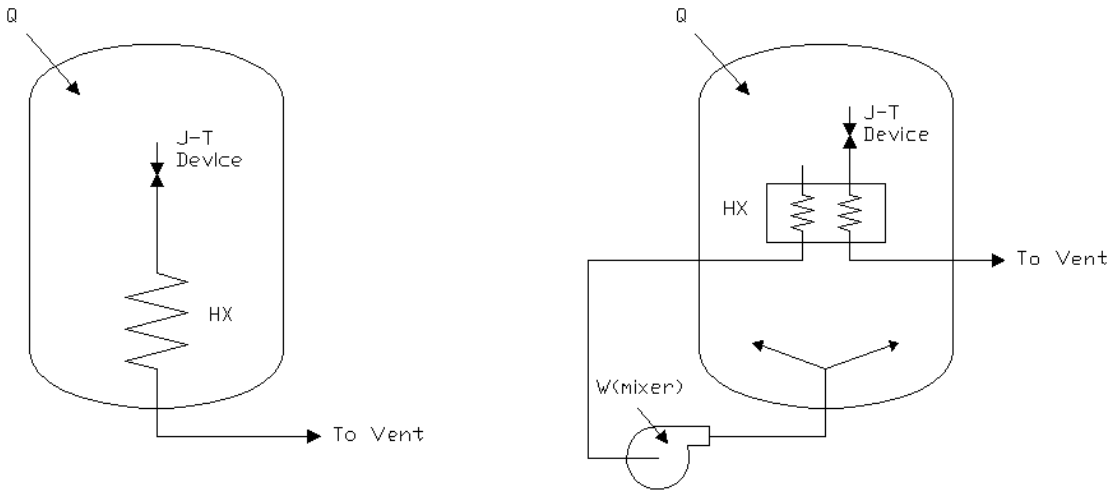

Passive TVS Active TVS

Figure 3 – Passive and Active TVS cooling schematics

CHAPTER II

PREVIOUS RESEARCH

2.1 Cryogenic Propellants

Research on Joule-Thomson devices in both LN_2 and LH_2 was conducted at the NASA Lewis Research Center (now the NASA Glenn Research Center) by Papell et al [1,2] in the early 1990's. They obtained flow rates, pressure drop and temperature drop data in LN_2 and LH_2 for a series of multiple orifice Joule-Thomson devices (Visco Jets [TM]) over a range of conditions. For LN_2 tests, inlet pressures ranged from 207 to 414 kPa, inlet temperatures from 65 to 91 K, outlet pressures from 19.3 to 385 kPa, outlet temperatures from 65 to 91 K, and flow rates from 0.18 to 1.8 kg/hr of nitrogen. For LH_2 tests, inlet pressures ranged from 186 to 448 kPa, inlet temperatures from 19 to 25.5 K, outlet pressures from 17.2 to 418.5 kPa, outlet temperatures from 15.5 to 25.5 K, and flow rates from 0.007 to 0.44 kg/hr of LH_2.

Visco Jets were originally designed as a miniature hydraulic flow component using the multiple orifice concept to induce a pressure drop in a line. The flow path for this device includes many orifices in series containing spin chambers that induce significant pressure drops. Figure 4 shows a detail of one of the several plates stacked in a Visco Jet, and the flow path.

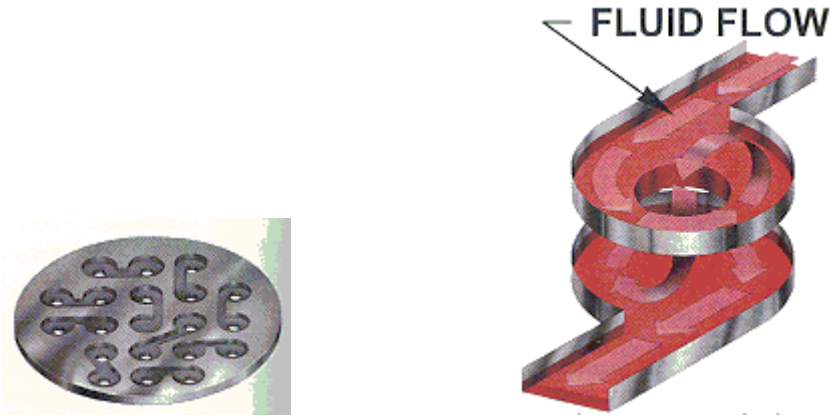

Figure 4 – Detail of the Lee Company Visco Jet

The advantage of this design results from having multiple larger holes instead of a single smaller orifice. The design provides the same pressure drop as a smaller single orifice with a much larger flow. The larger holes in the Visco Jet reduce the possibility of clogging due to solid contaminants in the line. The onset of cavitation is also minimized by the reduced velocity in the jet due to the larger size holes. The resistance to flow in Visco Jets is measured in liquid ohms – or "Lohm", a term coined by the manufacturer. This term is included in an equation that predicts single phase liquid flow rates for many fluids[21]. The form of the equation is:

$$\dot{m} = \frac{10000}{Lohm} * \left(\Delta P * S\right)^{0.5} \tag{3}$$

The Visco Jet multiple orifice design inherently reduces the onset of cavitation with hydraulic fluids. However, with cryogens stored at or near saturated conditions, it is inevitable that some flashing will occur, leading to a reduction in flow. Papell's work resulted in an empirical factor to correct flow for cryogens based on the quality of the flow exiting the Visco Jet. The modified correlation was determined to be:

$$\dot{m} = k * \frac{10000}{Lohm} * (\Delta P * S)^{0.5} * (1 - X) \tag{4}$$

where X is the fluid quality and k is an empirical constant. Exit flow quality was determined using isenthalpic expansion calculations:

$$h_t = X h_g + (1 - X) h_l \tag{5}$$

where h_t is inlet enthalpy, and h_g and h_l are saturated and liquid enthalpies at the outlet pressure, respectively. Reviewing data from Papell's report hinted at the potential issue of metastable liquid flow at the Visco Jet orifice. His tests were conducted by establishing a fixed inlet pressure and temperature for the fluid, and varying the downstream pressure. As the downstream pressure varied, typically the liquid cryogen flow through the Visco Jet would remain isothermal until the downstream pressure dropped below saturation conditions. At this point, the fluid temperature would drop, indicating the existence of two-phase flow, with the downstream temperature essentially following the temperature curve for saturated fluid. However, in a few cases, data were shown below the saturation line in which no temperature drop occurred, indicating the absence of phase change. Figures 5 and 6 show the data with these points noted.

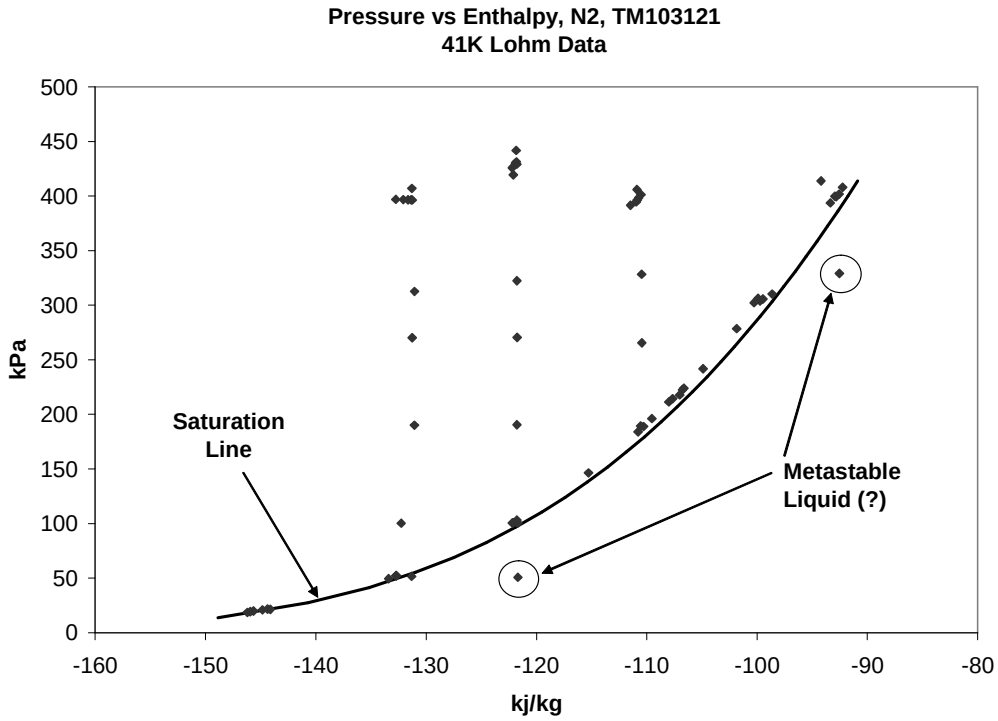

Figure 5 – LN_2 Visco Jet Data showing possible metastable liquid points

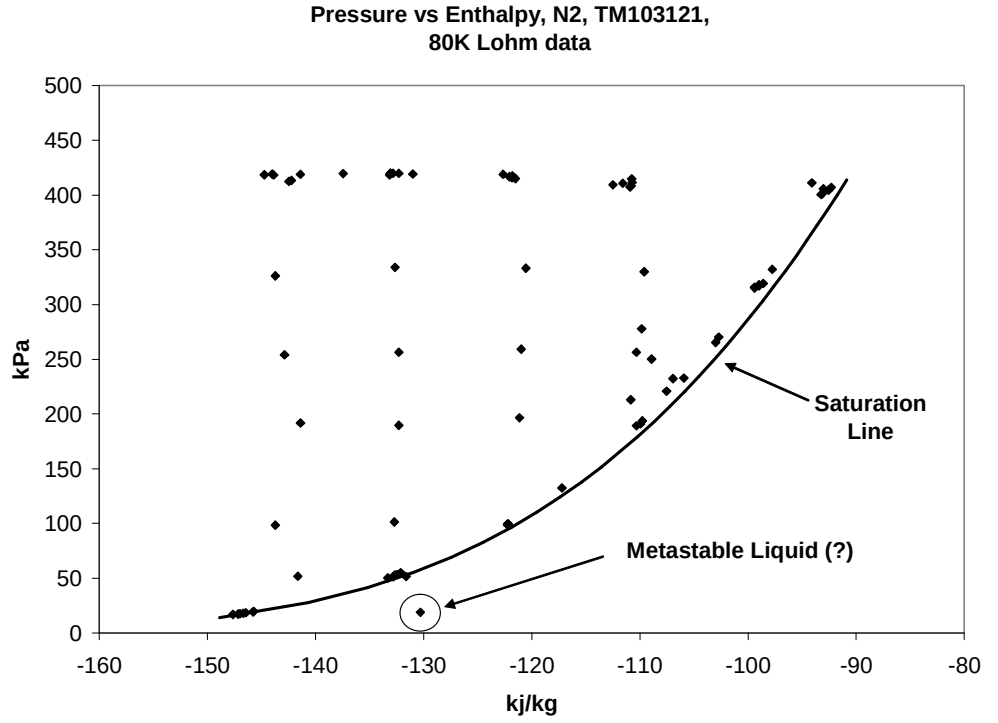

Figure 6 – LN_2 Visco Jet Data showing possible metastable liquid points

Further work with Visco Jets was performed by LeBar[22] and presented results of Visco Jet tests in liquid hydrogen. Tests were conducted on Visco Jets with Lohm ratings from 1,600 to 243,000 Lohm. LeBar concluded that flow rates from Visco Jets may vary considerably from predictions, and appears to be configuration dependent. No data was presented on fluid conditions downstream of the Visco Jets.

Jurns and Lekki[23] reported in 2006 on clogging of Joule-Thomson Devices in Liquid Hydrogen. This investigation focused on a phenomenon that was originally observed in some of Papell's 1992 Visco Jet tests. It was discovered that Joule-Thomson devices became clogged when transferring liquid hydrogen, operating within a temperature range from 20.5 to 24.5 K. Blockage did not exist under all test conditions, but was found to be sensitive to the inlet temperature of the LH_2. It was proposed that the clogging was due to trace amounts of neon in the LH_2 supply[24]. Neon freezes at 24.5 K at one atmosphere pressure, and it was postulated that between 20.5 and 24.5K, the neon existed in a metastable supercooled liquid state. When impacting the face of an orifice, liquid neon solidified and accumulated, blocking flow over time. The test program attempted to obtain visual evidence of accretion of neon in the orifice. Tests were performed with LH_2, and obtained similar results to the 1992 tests.

Baidakov and Skripov[6] conducted experimental work in 1992 with a number of cryogens, including hydrogen, nitrogen, oxygen, neon, argon, and methane. They investigated metastability by evaluating superheated liquids. Cryogenic liquids are readily superheated because they contain little dissolved gas or suspended solids (possible

nucleation sites). The focus of this work was to try and address the concern of eliminating the super heat in superheated liquids that might cause large hydraulic shock (explosive boiling). Their studies were predicated on the fact that in the absence of other factors initiating phase transition, homogenous nucleation defines the *upper* limit of the metastable state. Experimental investigations were carried out to compare with theory. Their results showed good agreement with theory, and showed significant excursion into the metastable region for cryogens. Table I shows results from some of their tests.

Table I – Maximum superheat temperature achieved for metastable cryogens per Baidakov et al

Fluid	Saturation Temperature (K)	Maximum Superheat Temperature Achieved (K)
N_2	77	110
O_2	90	135
CH_4	117	166

The implication of this work for metastable superheated fluids in space flight applications was further investigated and reported by Hasan et al[26] in 1993.

Hasan[26] reported in 1993 on a space flight experiment using Freon 113 as a surrogate fluid to study explosive boiling in a microgravity environment. They determined that for very low heat fluxes (0.2 to 1.2 kW/m^2), a high degree of liquid superheat can be sustained for a long duration in microgravity. The unique issues relating to pressure control in microgravity have to do with the liquid-vapor interface. In a microgravity environment, surface tension forces tend to dominate in a fluid, resulting in (for a wetting

fluid) liquid wetting the surface of a container, with the liquid-vapor interface located in the middle of the fluid. This presents a unique thermal problem, as for a partially full tank, there may not be direct contact between the tank wall and the vapor region. Heat transfer from the tank wall is transferred directly to the liquid and then to the vapor. As a consequence, the liquid may end up superheated. A great enough degree of super heat could result in explosive boiling, and significant pressure rise in the container. Like Baidakov and Skripov's work, this investigation deals not with subcooled liquid, but with superheated liquid. As such, the relation to the present work is not directly applicable. However, Hasan does make several relevant points. First of all, the presence of a superheated cryogen is more likely in a microgravity environment (with possibly significant negative impact on container pressure in the case of explosive boiling). Secondly, even relatively small heat fluxes can result in superheated liquid due to the location of the vapor ullage. These observations point to the importance of understanding the nuances of cryogenic fluid thermal control in space. Hopefully, our work will provide additional insight into how to best design thermal control systems to deal with these issues.

Simoneau[27] conducted studies on the maximum two phase flow rates of sub-cooled nitrogen through a sharp edged orifice. This work evaluated flow through an orifice with sub-cooled inlet and two phase exit conditions. Fluid conditions were well below critical values ($95 < T < 130K$, $800 < P < 6750$ kPa). Tests varied downstream pressure and evaluated the asymptotic behaviors of flow rates as minimum back pressures were approached. They showed that as back pressures were lowered below saturated pressure;

orifice exit temperatures decreased and corresponded to saturation temperatures for that pressure. Of course, this is what one would typically expect, and agrees by in large with Visco Jet data from Papell. Simoneau states that some others[28,29] postulated that no vaporization occurs right at the orifice, but flow passes through as metastable liquid, and flashes downstream. Simoneau's work left it at this, and did not examine extensively downstream conditions. However, one interesting conclusion is that if the difference between saturation pressure and orifice downstream pressure is large enough, the metastable jet vaporizes sufficiently close to the orifice to interfere with the flow and reduce the flow coefficient. This conclusion is consistent with Baidakov & Skripov's[6] assertion that "the depth of penetration ... depends on the intensity of process". It is also consistent with Papell's[2] observation of decreased flow through a Visco Jet when downstream conditions were two phase.

2.2 Work done near critical state

Simoneau, Hendricks and Ehlers[30] also conducted additional research with liquid nitrogen choked flow, with the emphasis on critical region (pressures up to 9650 kPa and temperatures from 88 – 279 K). This work is not directly applicable to the present work, as the present work deals with fluids much closer to saturation conditions. However, their conclusions do mention sub-cooled and saturated liquids and refer to Henry, Grolmes and Fauske[31] for treatment of LN_2 in this region.

Henry, Grolmes and Fauske[31] discuss flow of saturated and subcooled liquids through nozzles and orifices, and report some results for LN_2 flow for fluid close to the critical

state. Their discussion provides some relationships for calculating flow, and asserts that saturated or subcooled liquids discharging through a sharp-edged orifice behave in a completely metastable manner. Again, they do not provide any detail of the fluid downstream conditions, but limit their discussion to flow rates.

Although flows through orifices near the critical state is not directly applicable to this work, it should be mentioned that recently proposed architectures for future space flight systems are considering storing cryogenic propellants at pressures as high as 2,400 kPa, and investigating the possibility of metastable liquid flows through J-T devices at these conditions could provide useful data for designers.

It is evident from the literature and research conducted in cryogens that there is a solid foundation of both analytical and experimental treatment of sub-cooled flow of cryogens through an orifice. However, much of the theory and work to date focuses not so much on downstream conditions as on matters of flow rate, choked flow for two phase fluids, and has only a passing nod to metastability downstream. Also, much of the work is based on idealized conditions and test sections, as opposed to real world systems. The present work, although not as theoretically rigorous, attempts to examine more complicated Joule-Thomson geometries (i.e. – multiple orifice Visco Jets), with the hope of providing some realistic valuable data for designers.

CHAPTER III

POTENTIAL PROBLEMS – 2 phase transition, choking, clogging

The amount of heat that can be removed from a system using a J-T device depends not only on the pressure drop and resultant temperature drop across the device, but also on the mass flow through the device. For example, considering either of the two TVS systems shown in Figure 3, the total amount of heat being removed from the system is:

$$Q = \dot{m} c_p \Delta T \tag{6}$$

Where

mdot = mass flow rate of cooled fluid venting

c_p = Heat capacity of venting fluid

ΔT = Temperature difference between bulk liquid and J-T cooled fluid in vent line

Obviously, if the mass flow of venting fluid is decreased, the total amount of heat that can be rejected from the system also decreases. Mass flow through the J-T device can be limited by choking through the orifice. Flow downstream of the device may be limited by critical two-phase flow conditions[32]. Simoneau[27] examined the maximum flow rate of liquid nitrogen through a sharp edged orifice. They referenced earlier work by Benjamin

and Miller[28] and Bailey[29] that postulated that no vaporization occurs at the orifice, but that flow passes through as a liquid in a metastable state and flashes downstream. Simoneau's work suggested that the flow of single phase liquid passing through a sharp edged orifice reaches a limit as downstream pressure decreases due to a metastable jet of liquid vaporizing sufficiently close to the orifice to interfere with flow. Also, for liquid hydrogen, it has been shown that a J-T orifice can become clogged under certain conditions, presumably due to metastable impurities in the liquid which solidify out in the orifice[23].

CHAPTER IV

PROPOSED WORK FOR THIS EFFORT

It has been established that there is a solid foundation of both analytical and experimental treatment of sub-cooled flow of cryogens through an orifice. However, much of the theory and work to date focuses not so much on downstream conditions as on matters of flow rate, choked flow for two phase fluids, with limited emphasis on metastability downstream of the orifice. Also, much of the work is based on idealized conditions and test sections, as opposed to real world systems. The present work attempts to examine more complicated Joule-Thomson geometries (i.e. – multiple orifice Visco Jets) with particular emphasis on characterizing performance for these J-T devices, examining behavior around the two phase transition line, and determining the practical stability limits for metastable cryogenic liquids with comparison to their spinodal conditions.

4.1 J-T Effect

For a Joule-Thomson device to perform effectively in a cryogenic fluid thermal management system, pressure drop across the device must result in expansion into the two phase region. Otherwise, there will be no accompanying temperature drop. This expansion of the cryogenic fluid into the two phase region and its accompanying

temperature drop provides the differential temperature between the expanded fluid and the surrounding environment to drive heat rejection from the system. In most sub-critical cryogenic fluid systems, it is desirable to store the cryogen in a subcooled state for a number of reasons. Maintaining the liquid sub-cooled allows it to absorb heat from the environment without boiling and a resulting in undesirable pressure rise. Sub-cooled liquid is also necessary to provide adequate net positive suction pressure (NPSP) to turbo-pumps feeding rocket engines. Insufficient NPSP would result in pump cavitation, resulting not only in a decrease in engine performance, but also possibly catastrophic damage to turbo-machinery. Sub-cooling may be accomplished by several means, but for space based cryogenic systems is typically done by pressurizing the ullage volume of a container with GHe. This results in the tank vapor volume consisting of a mixture of helium and vapor phase fluid from the stored cryogen. The partial pressure of the cryogen is less than the total pressure in the tank, allowing the cryogen to absorb heat with a resulting temperature rise before it would boil. Take for example LCH_4. A volume of LCH_4 is stored under its own vapor pressure at 103.4 kPa has a saturation temperature of 111.9 K. If the volume were then pressurized to 137.9 kPa with GHe, the liquid would initially remain at its saturation temperature of 111.9 K. However, as the saturation temperature of LCH_4 at 137.9 kPa is 115.5 K, the LCH_4 could absorb additional heat without boiling until its temperature increased by 3.7 K to 115.5 K. As is demonstrated, pressurizing a tank with GHe provides a good short term solution for subcooling stored cryogens. However, heat leaking into the system will eventually result in pressure rise. This pressure rise could be eliminated by venting off some of the vapor. The downside of this is that venting vapor would also vent off some of the GHe, resulting

in a lower partial pressure of helium in the vapor space to suppress boiling. A solution to this problem of venting vapor is to utilize a TVS system as described in section 1.2. One operational issue that arises in the function of the TVS system is that the cryogenic liquid typically enters the Joule-Thomson device sub-cooled, due to GHe pressurant. As sub-cooled cryogen flows through the Joule-Thomson device, the pressure drop is isenthalpic until it crosses the two phase line. Further drop in pressure should result in phase change, and a resultant drop in temperature. Based on the downstream pressure, the temperature is predicted based on standard thermodynamic tables. Note for example the pressure versus enthalpy chart shown in Figure 7. LCH_4 with a temperature of 111.1 K follows a line of constant enthalpy as the pressure is reduced from 275 kPa, crossing the liquid to vapor transition line at approximately 97 kPa. With further reduction in pressure, the fluid would follow the saturation line. For example in Figure 7, dropping the pressure down to 34.6 kPa would result in a fluid temperature of 100.0 K.

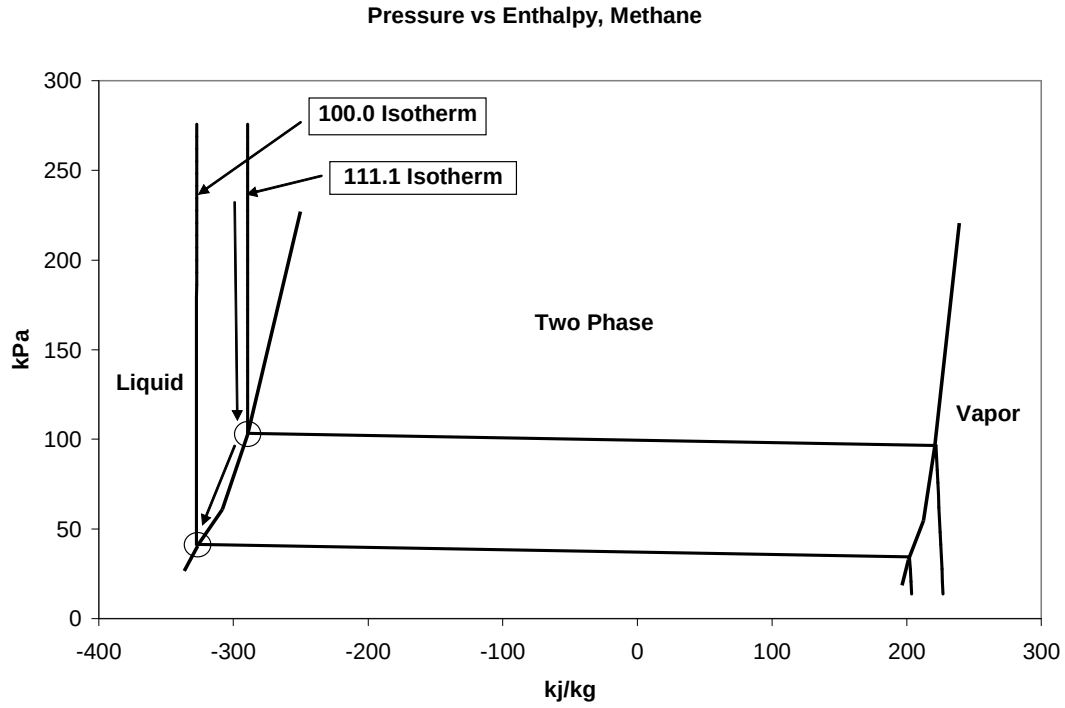

Figure 7 – Temperature drop of saturated LCH_4 from 97.0 kPa to 34.6 kPa

4.2 Metastable Cryogenic Liquids

It is widely known and described in the literature[6] that liquids can be both cooled below their freezing temperatures without solidifying (supercooled liquid), and heated above their boiling point without vaporizing (superheated liquid). In both of these cases, the fluid remains homogenous beyond the phase equilibrium line. Fluids that remain homogenous in this region are referred to as *metastable*. The limit beyond which fluids can no longer remain homogenous is called the spinodal limit. For subcritical fluids, the *spinodal curve* represents the stability boundary of the single phase state in the two phase region. This limit can be described in terms of an isotherm as it passes through local maxima and minima defined by

$$\left(\frac{\partial P}{\partial v}\right)_{cons\tan tT} = 0 \qquad (7)$$

This theoretical boundary cannot be approached absolutely by real fluids due to molecular level fluctuations in the fluid[3]. Nevertheless, there have been a large number of experiments conducted[6] that point to the existence of this spinodal line.

The location of the spinodal curve is of particular importance to us in relation to the function of a TVS. In a TVS, liquid is passed through a J-T device where is it expanded to a lower pressure. Thermodynamically, the liquid follows an isothermal path until it reaches the J-T device. As it expands, the fluid follows the phase equilibrium line until it reaches the saturation temperature at the downstream pressure, resulting in a temperature drop and subsequent phase change as previously described (refer to Figure 7).

Phase change is critical to the function of the J-T device, as without it there would be no temperature drop and consequently no cooling provided to the cryogenic system. If indeed the fluid passing through a J-T device does not follow the saturation curve to a lower temperature as pressure drops, but remains as a single phase metastable fluid, the TVS will not function as required. The spinodal line as shown in Figure 8 therefore represents the potential "worst case" pressure that a metastable fluid could drop to without phase change and temperature drop.

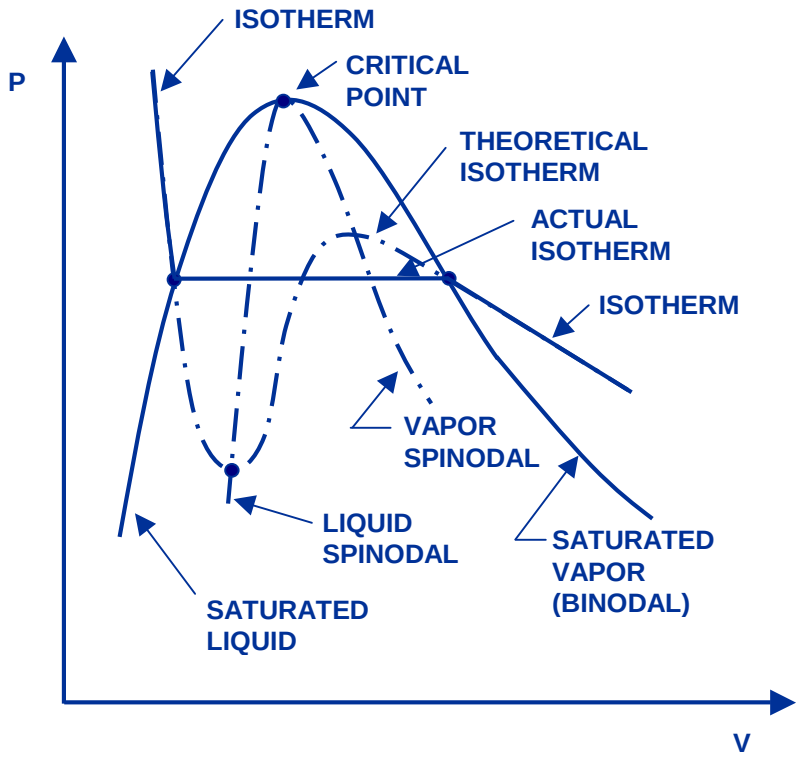

Figure 8 – Typical real fluid isotherm showing saturated liquid and spinodal lines

Empirical relationships[3,6] have been developed to estimate the spinodal line. These relationships, although approximate, provide a reasonably accurate estimate of the spinodal.

$$p_{sp} = p_{sat} - \frac{C\sigma^{1.5}}{(k_B T)^{0.5}\left(1 - \frac{\rho_v^{sat}}{\rho_l^{sat}}\right)} \tag{8}$$

The constant "C" has several reported values

Reference	C
Baonza et al [25]	1.32
Lienhard et al [4]	1.2064

Saturation pressure and spinodal pressure versus specific volume are plotted for methane and oxygen in Figures 9 and 10. Both plots show the spinodal pressure dropping

precipitously below zero as the specific volume decreases. The negative spinodal pressures indicate that the fluid is actually under tension.

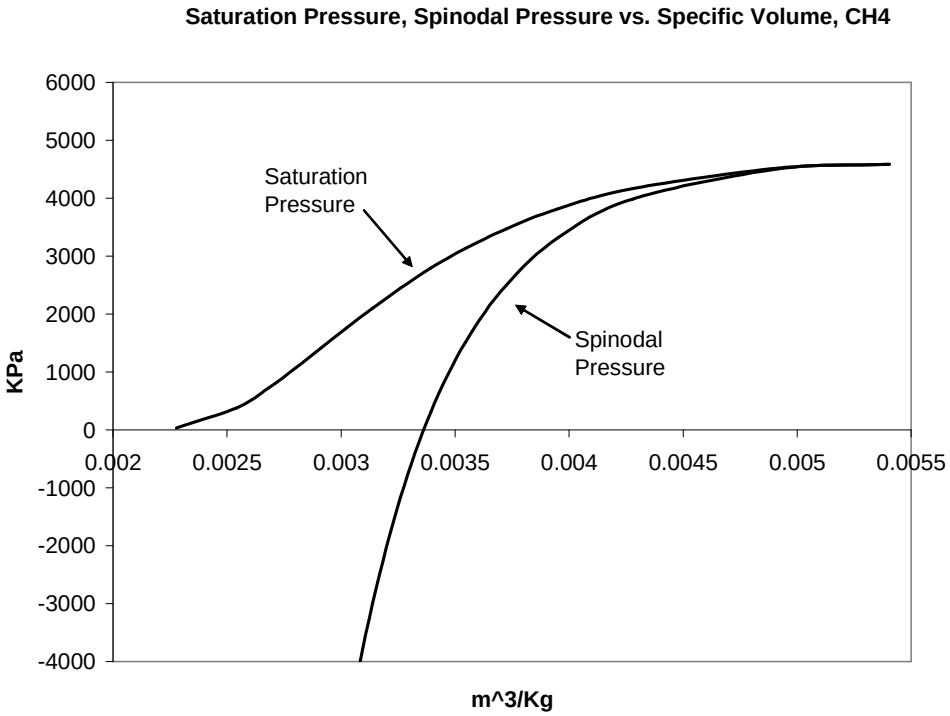

Figure 9 – Saturation and Spinodal Pressure vs. Specific Volume for Methane

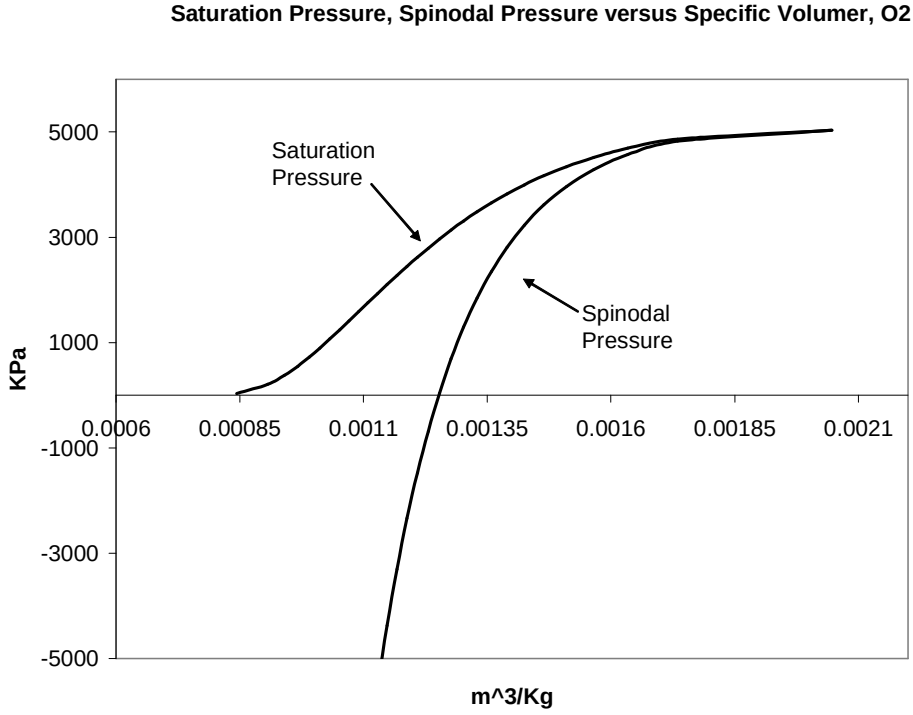

Figure 10 – Saturation and Spinodal Pressure vs. Specific Volume for Oxygen

Practically speaking, the spinodal limit is only approached experimentally by use of extremely sensitive experimental hardware, and not typical flight hardware. However, for real systems, it is still important to determine if fluid traverses into the metastable region, and if so, to what extent. Also, it is of interest to determine if the phenomena might depend on either the type of J-T device, or possibly the rate of the process.

CHAPTER V

EXPERIMENTAL FACILITIES

5.1 Low pressure LCH_4 facility

Low pressure LCH_4 Visco Jet testing was performed at the CCL-7 cryogenic test facility at the NASA Glenn Research Center Creek Road Complex in Cleveland, Ohio[7]. This test facility specializes as a low-cost small scale screening facility for concept and component testing. In addition to component screening, the facility can perform propellant transfer as well as vent flow tests. CCL-7 safely handles 1135 L of LH_2 and LN_2, 455 L of LCH_4, and 909 L of LO_2. GH_2, GO_2, GHe and GN_2 are available on-site. Figure 11 shows a simplified schematic diagram of the CCL-7 test facility.

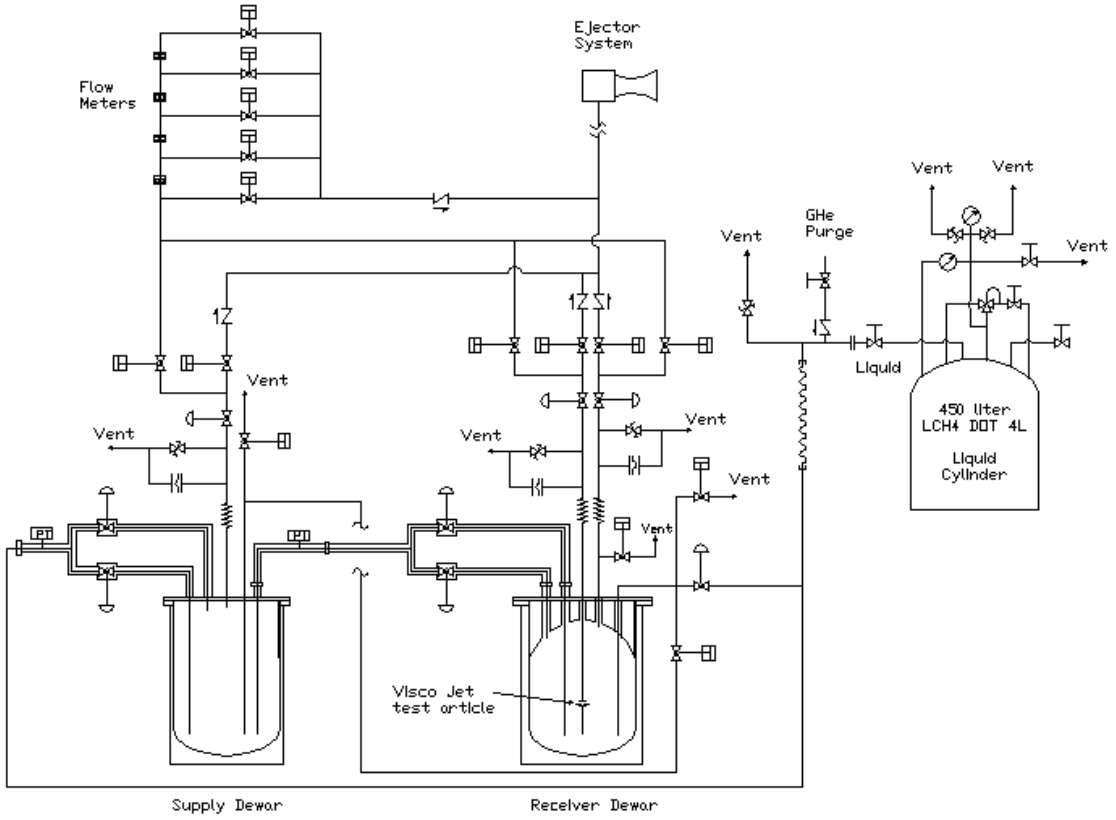

Figure 11 – CCL-7 cryogenic test facility simplified schematic diagram

5.1.1 Capabilities/capacities

CCL-7 testing can be performed in either a Supply or Receiver dewar at the facility; although the supply dewar is generally used for propellant conditioning. The Supply dewar is a vertical cylinder with a 55.9 cm diameter and 135.9 cm height. It has a 320 L internal volume and an operating pressure of 276 kPa. An instrument rake equipped with silicon diodes provides temperature measurements and liquid level indication.

Three interchangeable Receiver dewars are available at CCL-7. They all have a smaller liquid volume than the Supply dewar. The receiver dewars all have a common stationary lid. Fluid supply and vent as well as instrumentation pass through this stationary lid. The

diameter of the Receiver dewars is 55.9 cm. The bodies of these test dewars are raised and lowered on a lift and secured with an o-ring seal to a flanged lid by 12 bolts. The removable Receiver dewar allows for ready access to the test hardware with a minimum of down time between hardware re-configuration. All Receiver dewars are vacuum jacketed. An instrument rake equipped with silicon diodes provides temperature measurements and liquid level indication for the dewars. The first dewar has the highest working pressure, 372 kPa. Its overall length is 81.3 cm, with a resulting internal volume of 158.5 L. The second tank is 106.7 cm long and has an internal volume of 226.5 L. A window in the sidewall is located 54.6 cm from the bottom of the dewar. It has a working pressure of 172.4 kPa and 3 pressure taps in the bottom of the dewar. The third Receiver dewar is identical to the second dewar except the window in the sidewall is 76.2 cm from the bottom. The dewars with sidewall windows have been used to view tank internal hardware. Light from a fiber optic light source is supplied through the window on the dewar lid and a camera is available to record images inside the receiver dewar through the window.

Cryogen is transferred to the test facility through a 19 mm diameter vacuum jacketed hose and piping from a roadable dewar parked at the test cell. Cryogens are transferred into the Supply dewar, and from there to the Receiver dewar. The Supply and Receiver dewars can vent either directly to atmosphere or through a series of air ejectors. The air ejectors are venturi devices that use compressed air as a motive fluid to create suction in the dewar vent piping. The ejectors allow the dewars to operate at a minimum pressure of approximately 17.2 kPa. The Supply dewar vent valve is an open loop proportional valve

that can be set at 0 – 100% open. The Receiver dewar vent valve is operated either open loop, or with a PID loop in the PLC control system, and can control backpressure in the Receiver dewar to within ±0.34 kPa. A separate vent line with an open loop proportional valve is available for test articles installed inside the Receiver dewar. Gasses evolved during testing from the dewars and test articles can vent directly to atmosphere, or to a series of four mass flow meters. The mass flow meters have a combined range of 0 – 24000 SLPH. Test articles installed inside the receiver tank also have an independently controlled pressurization system for added flexibility.

5.1.2 Control

A PLC with a Wonderware© HMI (Human Machine Interface) controls the facility. Interlocks, alarms and shutdowns are used to protect the research hardware and the facility and operator controlled open-loop processes are used to provide flexibility. The control system is independent from the data system but data can be shared between the two systems through standard communication protocols.

Test operations are conducted from a remote control room. Checkout can either be performed locally at the facility or in an interconnect room located at a remote building. The test area has been designed to NEC Class 1, Division 2, Group B and is suitable for propellant testing. Components including the data acquisition hardware, the PLC and flow meters that are not rated for the environment are installed inside purged/pressurized cabinets per NEC code.

5.1.3 Instrumentation

CCL-7 has a state of the art LabVIEW© based data collection system. Up to 320 channels of data at can be collected at a nominal rate of 1 Hz. Many of the facility channels are pre-configured for standard instruments including thermocouples, pressure transducers, and silicon diodes. Modular jack-type field connections at instrument cabinet facilitate installation and checkout of research hardware.

5.2 Higher pressure LO_2 facility

NASA Glenn Research Center also has a cryogenic test facility named SMiRF (Small Multipurpose Research Facility)[7]. This facility provides the ability to simulate space, high altitudes and launch pressure environments, to conduct calorimetric tests on prototype insulation systems and to safely handle gaseous and cryogenic propellants. Operations at this facility have an established track record of safely handling 5,678 L LH_2 and 7,571 L of LN_2 simultaneously. Recent augmentations to this facility have resulted in the capability to test with LO_2 and LN_2 at pressures up to 1724 kPa. Gaseous hydrogen (GH_2), gaseous oxygen (GO_2), gaseous helium (GHe) and gaseous nitrogen (GN_2) are also available on-site. Visco Jet tests as part of a larger cryogenic research program[33] were conducted in this facility.

5.2.1 Capabilities/capacities

The test facility consists of an interconnect room (used for instrument and control terminations and check out), a shop area (for build up and bench work), and the test cell. The test cell has been designed to National Electric Code (NEC) Class 1, Division 2,

Group B and is suitable for propellant testing. The interconnect room and shop area are pressurized during tests to meet NEC requirements.

The center of the SMiRF test cell is a cylindrical space simulation vacuum chamber. The 7.45 m^3 vacuum chamber shown in Figures 12 and 13 accommodates test articles as large as 183 cm in diameter and 229 cm high. The SMiRF vacuum system includes mechanical and diffusion vacuum pumps, and can maintain a vacuum environment of 6.7 x 10^{-4} Pa in the chamber. The vacuum system also allows the chamber to be evacuated to simulate a launch vehicle (i.e. - the Space Shuttle) ascent pressure profile (from atmospheric pressure to 1.33 Pa in 2 minutes). Chamber pressure can be maintained at intermediate values as required by research programs. A programmable thermal shroud is available for use at the facility. The shroud limits the dimensions of the test article to a maximum diameter of 112 cm. The shroud can simulate lunar or Martian diurnal temperature profiles and operate over a temperature range of 110 to 360 K with ramping capabilities of 0.1 K per minute over the entire range. Gas composition in the vacuum chamber is continuously monitored with a mass spectrometer based residual gas analyzer that detects species in the 0-200 amu range.

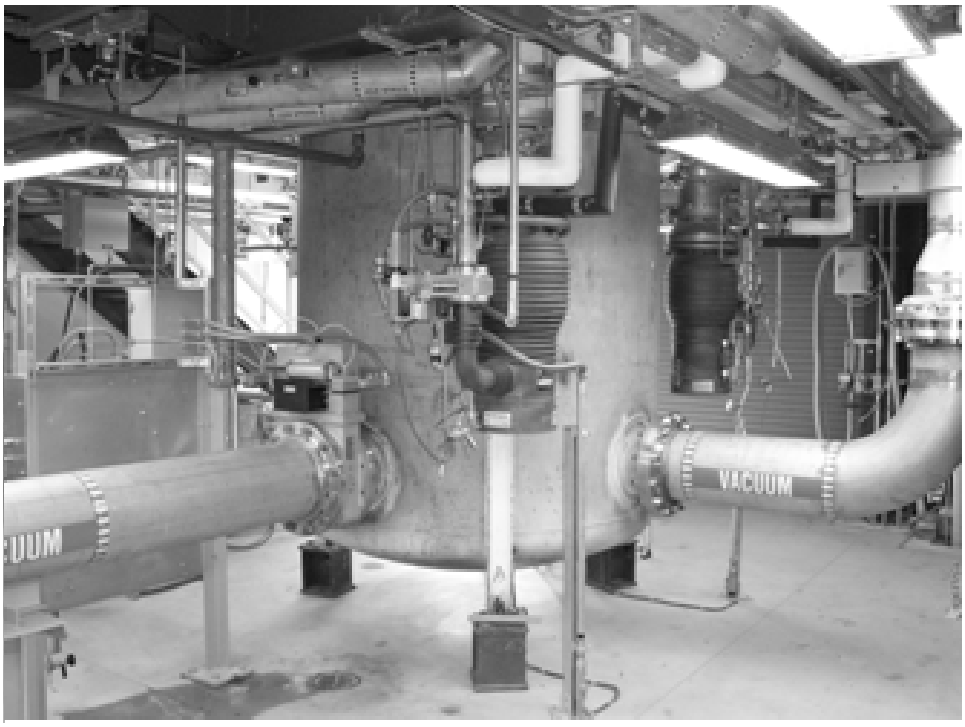

Figure 12 – Bottom view of SMIRF vacuum chamber

Figure 13 – Top view of vacuum chamber

Test articles are suspended from the vacuum chamber lid, and then placed inside the vacuum chamber when the lid is attached to the chamber. Figure 14 shows the test tank used for these tests suspended from the vacuum chamber lid during build up. This tank was 122 cm diameter, 160 cm overall height 304 stainless steel pressure vessel with a maximum working pressure of 1724 kPa. All electrical and fluid connections pass through the lid of the vacuum chamber as shown in Figure 13. The facility supply/vent systems limit the maximum working pressure of test articles in the vacuum chamber to 1965 kPa. Mechanical vacuum pumps can also provide sub-atmospheric pressure conditions to the research hardware located inside the vacuum chamber if required, as well as providing backing for the SMiRF chamber diffusion pumps.

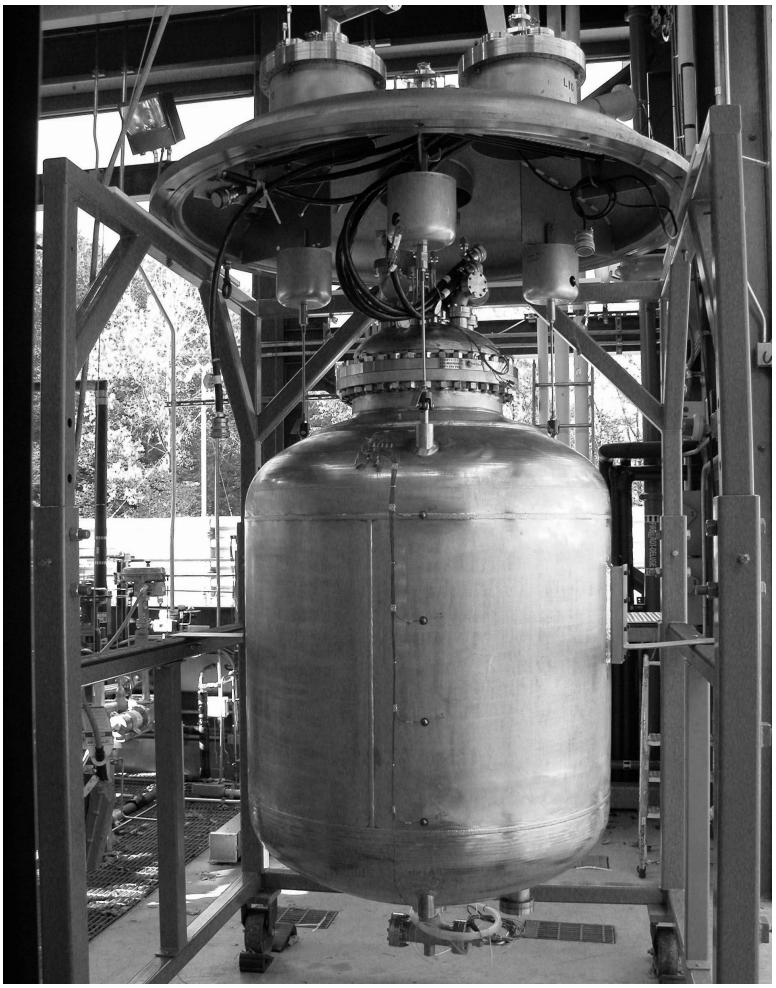

Figure 14 – 1.4 m^3 LO_2 test tank suspended from SMIRF Vacuum chamber lid during build up

The facility boasts four independently controllable cryogenic liquid fill/drain lines and three independent vent systems. The fill systems consists of 19 mm main supply line that branches into four independent fill paths. In the past, the independent fill lines have been used to fill multiple tanks within the vacuum chamber with different liquid cryogens. The 51 mm diameter main vent is the most commonly used vent system. It can either vent directly to the atmosphere or the backpressure of the control research hardware to

within ±0.13 kPa by modulating a series of five parallel control valves. One of five mass flow meters with a range of 0.57 to 90,600 Standard Liters per Hour (SLPH) can measure gas vent rate. The flow meters are typically used to establish baseline heat flow into the test articles installed in the vacuum chamber by measuring boil-off in the test article. A secondary 25 mm diameter vent system can be controlled to within 1.4 kPa of the set point or directly vented. A differential pressure controller maintains pressure levels in the main and secondary vents. The controller is referenced to a gas volume in an isothermal bath. A tertiary vent system, also 25 mm diameter, can be controlled to within 6.9 kPa or vented directly to atmosphere. Figure 15 shows a simplified cryogenic supply and vent schematic.

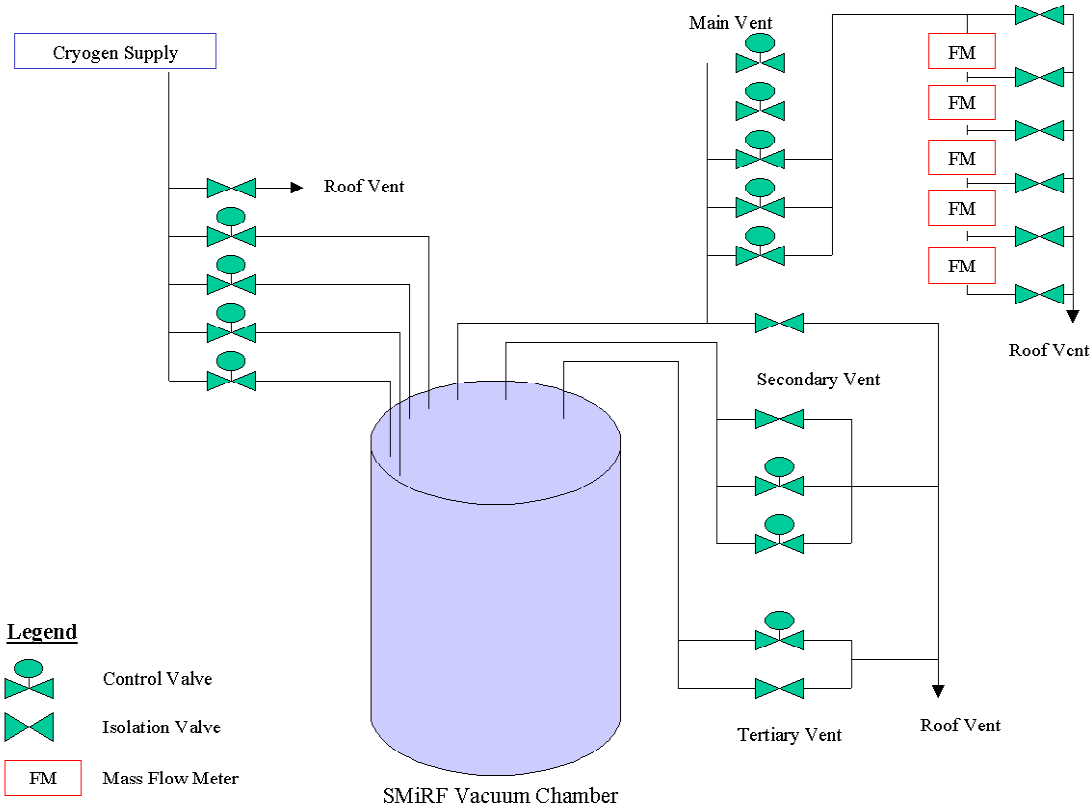

Figure 15 – Simplified schematic of SMIRF facility supply and vent systems

5.2.2 Control

A programmable logic controller (PLC) with a Wonderware© HMI (Human Machine Interface) controls the facility. Interlocks, alarms and shutdowns protect the research hardware and the facility, and operator controlled open-loop processes provide testing flexibility. The control system is independent from the data system, but data can be shared between the two systems through standard communication protocols.

5.2.3 Instrumentation

SMiRF has a state-of-the-art LabVIEW© based data collection system. Up to 425 channels of data can be recorded at a nominal rate of 1 Hz. An additional 24 channels can be recorded at rates of 0.1 Hz. Many of the facility channels are pre-configured for standard instruments including thermocouples, pressure transducers, and silicon diode thermometers. Modular jack-type field connections at instrument cabinets located throughout the facility enable installation and checkout of research hardware.

CHAPTER VI

DESCRIPTION OF EXPERIMENT

6.1 LCH_4 tests

A series of tests with varying degrees of sub-cooling on the inlet side and various downstream pressures was performed to determine how far below the saturation line the flow through a Visco jet Joule-Thomson device might reach as a metastable superheated liquid before transitioning to two phase with an accompanying temperature drop. These tests were performed at the NASA Glenn Research Center CCL-7 cryogenic test facility described in detail in section 7.1. The test facility was configured for LCH_4 testing. A Visco Jet was installed in the CCL-7 Receiver dewar. The dewar was partially filled with LCH_4 and conditioned to a certain temperature as determined by the test matrix shown in Table II. LCH_4 flowed out of the dewar through the Visco Jet. Silicon diode temperature sensors were located in the outflow line, upstream and downstream of the Visco Jet. A schematic diagram of the test configuration is shown in Figure 16. Note that the Visco Jet and temperature sensors were wrapped with insulation to prevent false temperature readings from the bulk LCH_4. Liquid methane was transferred to the dewar through a 19 mm diameter vacuum jacketed hose and piping from a portable 450 L liquid methane vacuum jacketed dewar.

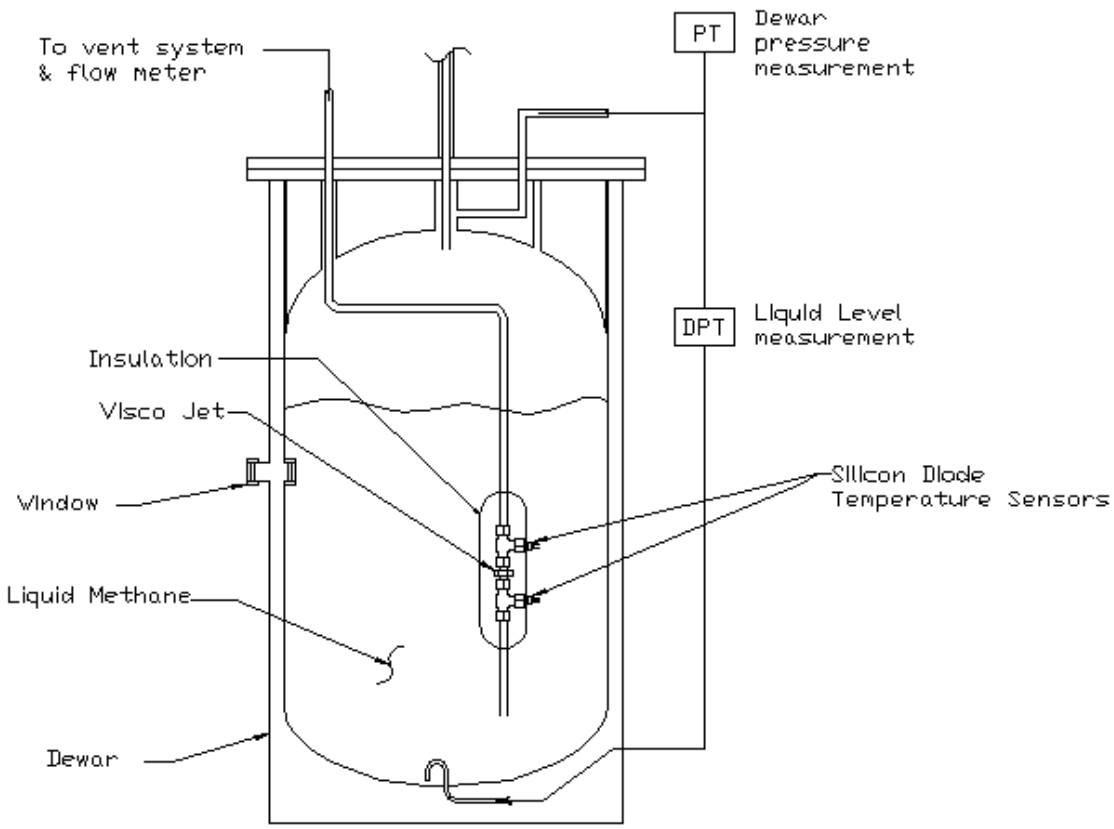

Figure 16 – Visco Jet with Silicon Diode temperature sensors in Receiver dewar

6.2 Test conditions

Test conditions were established to assure that the LCH_4 would enter the Visco Jet as single phase liquid, and that the downstream pressure could be varied so as to allow the exiting fluid to cross the two phase transition line. The Visco Jet outlet pressure was controlled to be initially above the transition line, after which the downstream pressure was gradually reduced to a level below the transition pressure. Figure 17 is a plot of Visco Jet outlet pressure versus liquid enthalpy for LCH_4 between approximately 34.5 and 206.8 kPa. Lines of constant temperature are shown for a number of isotherms between 97 and 122 K. Table II shows the specific conditions for the tests performed.

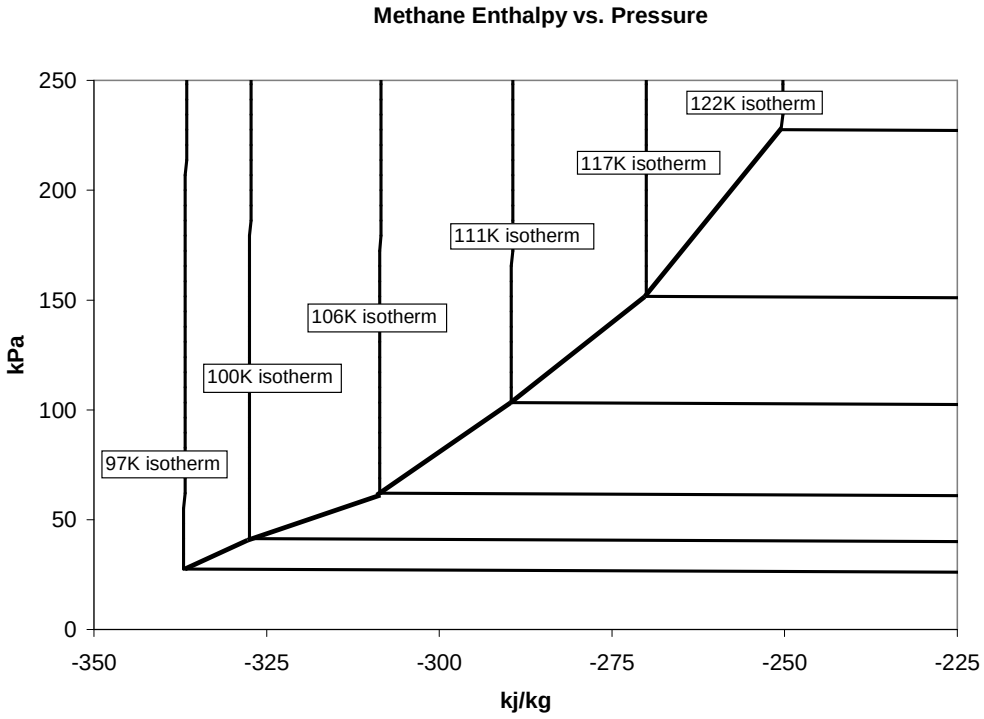

Figure 17 – Plot of pressure vs. liquid enthalpy for LCH_4

Table II - Test Matrix for determining minimum pressure of metastable subcooled liquid methane

Visco Jet	Lohm Rating	Tank Pressure (kPa)	2 Phase transition press (kPa)	Minimum Downstream Press (kPa)	Bulk Fluid Temp. (K)
VXLA 2500 820D	8,200	151.6	76.5	20.7	105.5
VXLA 2500 820D	8,200	151.6	121.3	20.7	112.8

6.3 Test procedure

For the LCH_4 Visco Jet testing, the Visco Jet Joule-Thomson device was installed in an outflow line in the Receiver dewar as shown in Figure 16. The dewar was filled with LCH_4 approximately 31.75 cm deep. Liquid level was measured by means of a 0-7.5 kPa differential pressure transducer. This amount of liquid was sufficient to submerge the Visco Jet. The bottom of the inlet line was located approximately 10 cm above the

bottom of the dewar. After fill was complete, the temperature of the bulk LCH_4 was noted. Two series of tests were performed; the first series of test with the LCH_4 saturated close to the normal boiling point (NBP). The second series of test was performed with LCH_4 subcooled below the NBP. For the first series of tests, the LCH_4 was allowed to saturate at NBP conditions by simply venting the dewar to atmospheric pressure. This resulted in bulk LCH_4 temperature of approximately 112.2 K. For the second series of tests, the LCH_4 was subcooled by reducing the pressure in the dewar to approximately 53.8 kPa and allowing the liquid to boil. The pressure was reduced in the dewar by means of the test facility ejector system described in detail in section 5.1.1. For the subcooled tests, the bulk LCH_4 temperature was reduced to approximately 105 K. For both tests, once the desired LCH_4 temperature was attained, the dewar was then pressurized to between 137.9 and 151.7 kPa with GHe. A small constant bleed of GHe was fed to the dewar, and the pressure maintained by means of a proportional vent valve operated with a PID loop controller. The desired dewar pressure was input to the controller, and the vent valve modulated automatically to maintain dewar pressure to within ± 0.34 kPa of the set point.

Once the desired fluid conditions were attained and the dewar pressurized, flow was initiated through the Visco Jet. Liquid flowed through the Visco Jet from the bulk LCH_4 and then out of the dewar, through a heat exchanger which vaporized and warmed the LCH_4, through a proportional valve, a mass flow meter, and finally out the ejector to atmosphere. Figure 18 shows a simplified schematic of the flow path of methane. The pressure on the downstream side of the Visco Jet was varied by modulating the control

valve between 0 – 100% open while maintaining the flow to the ejector. Using this operating scenario, the Visco Jet downstream pressure could be varied between 56.5 and 120.6 kPa.

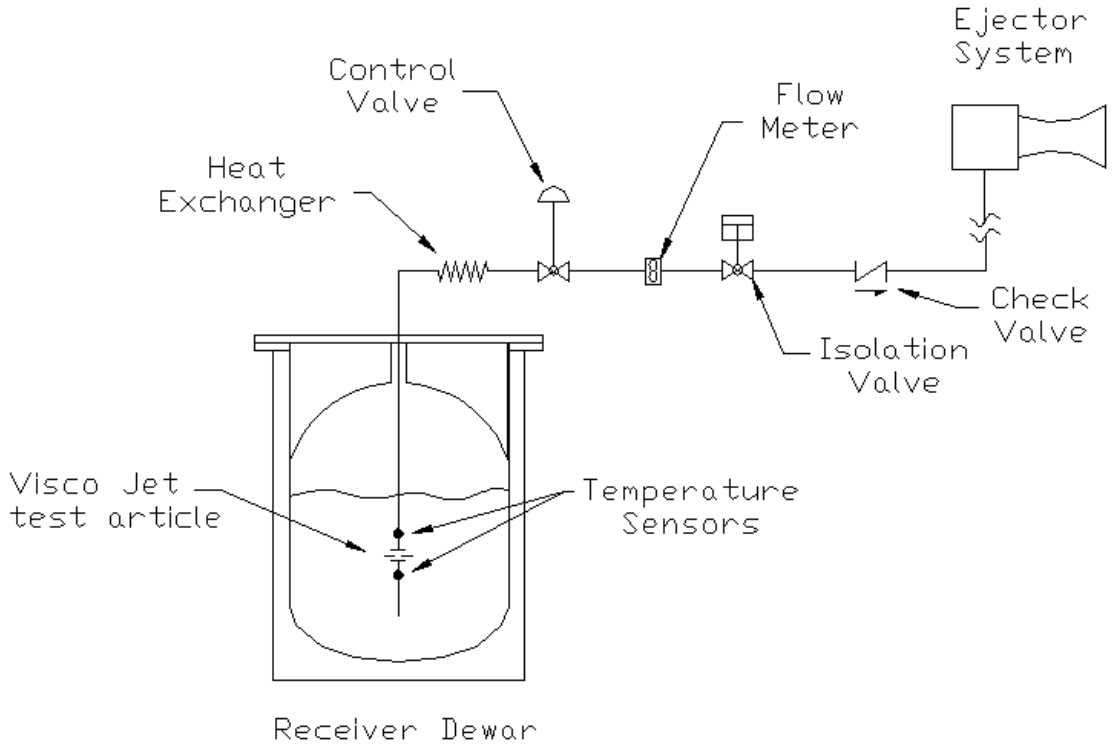

Figure 18 – Visco Jet outflow line simplified schematic diagram

Table III shows the actual test conditions attained for the two test series.

Table III – LCH_4 Visco Jet test conditions

8,200 Lohm Visco Jet	**Sub-cooled LCH_4**	**NBP LCH_4**
Dewar ullage pressure (kPa)	137.9	151.0
Bulk LCH_4 temperature (K)	105.7 – 106.0	112.9 - 113.0
Visco Jet inlet temperature (K)	105.7 – 106.0	112.9 - 113.0
Visco Jet outlet Temperature (K)	105.7 – 106.0	106.5 – 112.7
Visco Jet outlet pressure (kPa)	57.9 – 97.2	60.0 – 126.9
Flow Rate (slpm)	0-33	11 - 36

6.4 LO_2 tests

A second series of tests with varying degrees of sub-cooling on the inlet side and constant downstream pressures was performed to determine how far below the saturation line the flow through a Visco Jet Joule-Thomson device would persist as a metastable superheated liquid before transitioning to two phase with an accompanying temperature drop. These tests were performed at the NASA Glenn Research Center SMiRF cryogenic test facility described in detail in section 5.2. The test facility was configured for LO_2 testing. Six Visco Jets with a range of Lohm ratings were installed in the 1.4 m^3 SMiRF test tank. The dewar was partially filled with LO_2 and conditioned to a certain temperature per the test matrix shown in Table IV. LO_2 flowed out of the test tank through the Visco Jets. Silicon diode temperature sensors were located in the outflow lines, upstream and downstream of the Visco Jets. A schematic diagram of the test configuration is shown in Figure 19. Note that unlike previous LCH_4 tests at CCL-7, Visco Jet and temperature sensors were not wrapped with insulation to prevent false temperature readings from the bulk LO_2. Liquid oxygen was transferred to the test tank through 25 mm diameter vacuum jacketed piping from a portable 13,600 L LO_2 vacuum jacketed trailer.

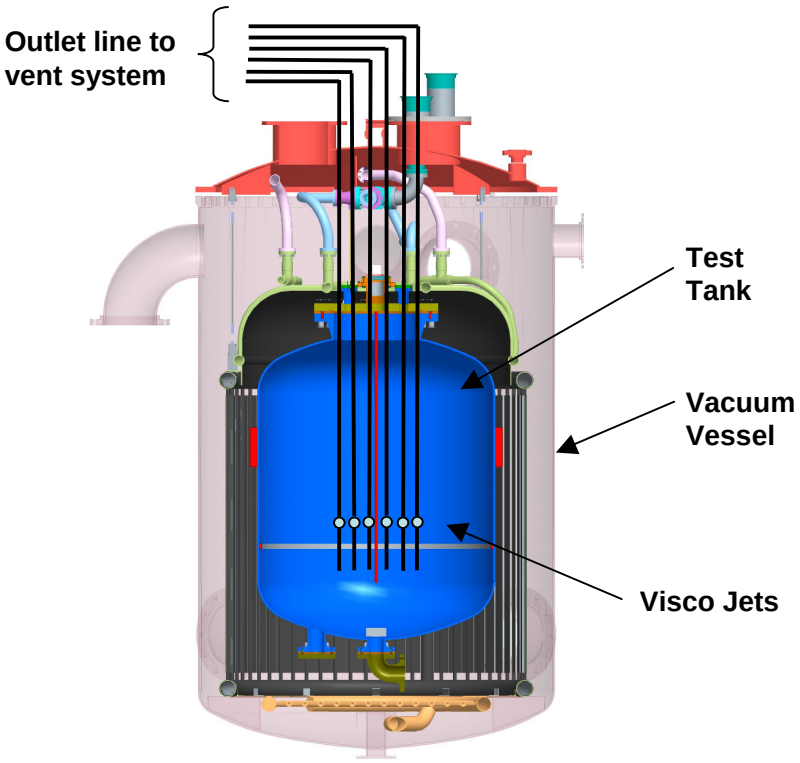

Figure 19 – Visco Jet in SMIRF Test Tank

6.5 Test conditions

Test conditions were established to assure that the LO_2 would enter the Visco Jet as single phase liquid. As the SMIRF test tank had a higher working pressure, tests could be performed with a wider range of conditions. To establish liquid conditions, the test tank was filled approximately 30% to cover the Visco Jets while venting the tank to atmosphere. This resulted in LO_2 saturated at close to NBP conditions. Unlike CCL-7, the facility was not configured to allow us to subcool the liquid below atmospheric pressure. The tank was pressurized with gaseous helium to the pressures shown in Table IV. The liquid would either remain close to its NBP temperature, or could be warmed up by maintaining tank pressure and bubbling warm gaseous oxygen into the liquid. The

piping downstream of the Visco Jets vented to atmosphere through open/close isolation valves. With this configuration, the downstream pressure could not be varied as was done with the proportional valve in the CCL-7 LCH4 test series. That is, the downstream pressure would drop below the two phase transition line, but could not be brought through the transition line in a controlled manner. Figure 20 is a plot of pressure versus liquid enthalpy for LO_2 between approximately 103.4 and 1379 kPa. Lines of constant temperature are shown for a number of isotherms between 86.1 and 122.2 K. Table IV shows the specific conditions for the tests performed.

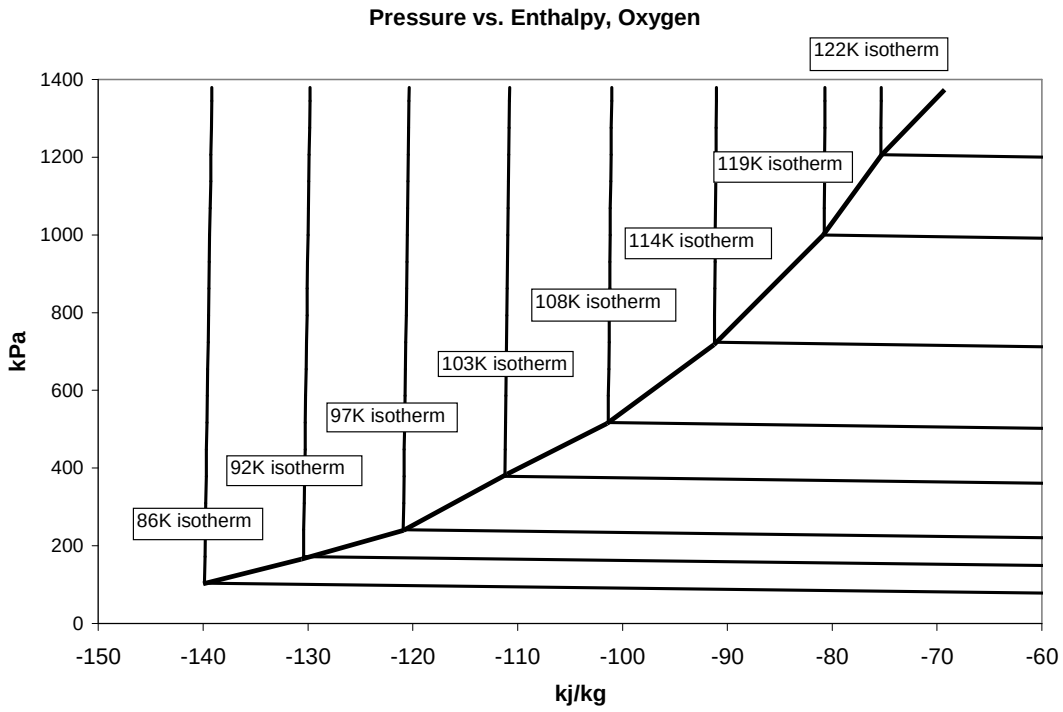

Figure 20 – Plot of pressure vs. liquid enthalpy for LO_2

Table IV - Test Matrix for determining minimum pressure of metastable subcooled liquid oxygen

Visco Jet	Lohm Rating	Tank Pressure (kPa)	2-phase transition pressure (kPa)	Minimum Downstream Pressure (kPa)	Bulk Fluid Temp. (K)
VDLA 4316 135T	1350000	141.3	142.0	101.3	93.5
JEVB 1815 313K	313000	141.3	143.4	102.7	93.7
JEVB 1825 102K	102000	142.0	144.1	103.4	93.7
VDCB 1845 112H	11200	142.7	142.7	104.1	93.6
VXLA 2500 330D	3300	143.4	142.0	104.1	93.5
JEVB 1825 102K	102000	835.6	786.7	102.7	115.7
VXLA 2500 330D	3300	835.0	763.9	104.1	115.2
VDLA 4316 135T	1350000	835.0	793.6	104.1	115.8
JEVB 1815 313K	313000	834.3	804.6	104.8	116.0
VDCB 1845 112H	11200	832.9	788.1	104.1	115.7
VXLA 2500 680L	680	832.9	790.8	120.0	115.7
VDLA 4316 135T	1350000	836.3	804.6	102.7	116.0
VDCB 1845 112H	11200	835.6	790.1	103.4	115.7
VDCB 1845 112H	11200	139.3	139.3	104.8	93.3
JEVB 1815 313K	313000	139.3	138.6	104.8	93.3

6.6 Test procedure

For the LO_2 Visco Jet testing, the Visco Jet Joule-Thomson devices were installed in an outflow line in the SMIRF test tank as shown in Figure 21. The test tank was filled with LO_2 approximately 91 cm deep. Liquid level was measured by means of a load cell system that weighed the amount of LO_2 in the tank. This amount of liquid was sufficient to submerge the Visco Jets. The Visco Jets themselves were located approximately 61 cm above the bottom of the test tank. The bottom of the inlet lines for each Visco Jet was located approximately 20 cm above the bottom of the test tank. After fill was complete, the temperature of the bulk LO_2 was noted. Two series of tests were performed; the first series of test with the LO_2 temperature approximately 93.3 K (saturated temperature for 137.9 kPa liquid). The second series of test was performed with LO_2 temperature

approximately 115.5 K (saturated temperature for 827.4 kPa liquid). For the first series of tests, the LO_2 temperature was attained by maintaining test tank pressure at 137.9 kPa while filling. For the second series of tests, the LO_2 was filled into the test tank at approximately atmospheric pressure. The tank vent system was set at 827.4 kPa which was maintained with a proportional valve operating with a PID loop that sensed test tank pressure. Warm gaseous oxygen was bubbled into the LO_2 to warm it up to approximately 115.5 K. For both tests, once the desired LO_2 temperature was attained, the dewar pressure was maintained by the proportional vent valve operating on a PID loop with the test tank pressure as the input to the PID control. If tank pressure dropped below the set point, GHe was used to re-pressurize the test tank.

Once the desired fluid conditions were attained and the dewar pressurized, flow was initiated through the Visco Jet. As with the LCH_4 tests, liquid flowed through the Visco Jet from the bulk LO_2 and then out of the test tank, through a heat exchanger which vaporized and warmed the LO_2, through an isolation valve, a mass flow meter, and finally out to atmosphere. As mentioned previously, the SMIRF facility did not include an ejector, so the Visco Jet outlet pressure could not be lower than atmospheric pressure. Figure 21 shows a simplified schematic of the flow path of oxygen. The downstream side of the Visco Jet was vented through an on/off valve. As the valve could not be modulated as in the LCH_4 tests, the outlet pressure immediately dropped to approximately 103.4 kPa when it was opened.

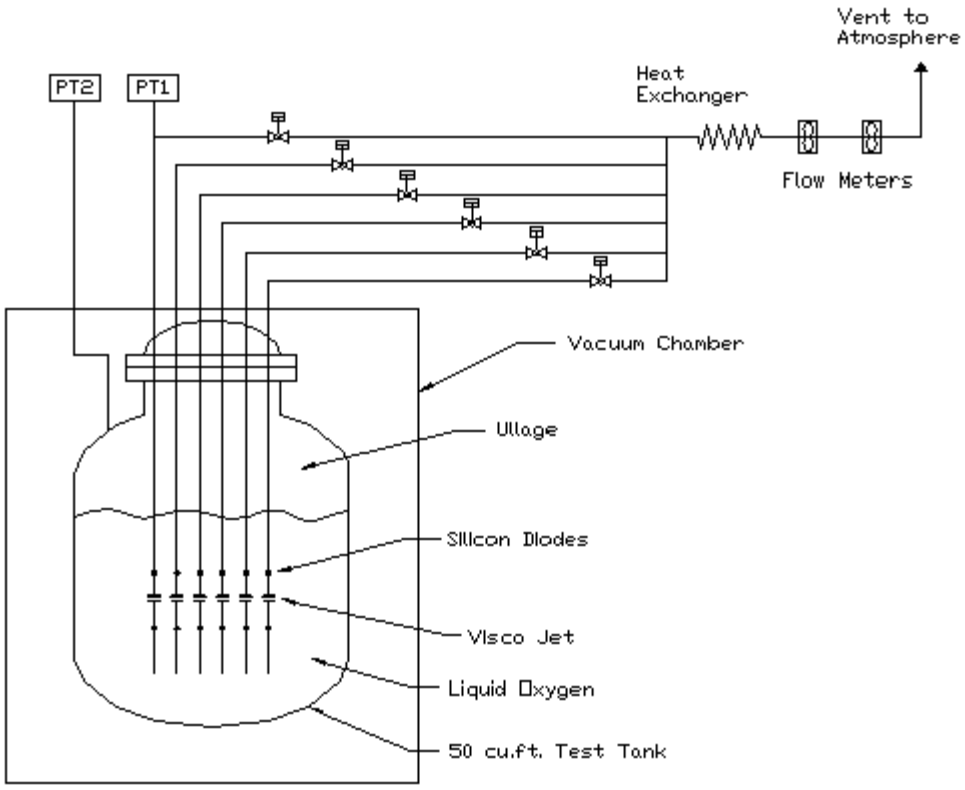

Figure 21 – Simplified Schematic of Visco Jets in SMIRF Test Tank

CHAPTER VII

ANALYTICAL DISCUSSION

It has been established[3-6] that cryogenic fluids can exist as metastable fluids to some extent below the saturation line. That is, following an isothermal line for decreasing pressure, the fluid may cross the two phase transition line and continue along an isothermal line as a single phase liquid until it reaches its theoretical limit at the liquid spinodal line. This liquid spinodal curve has been described previously in section 4.3, equation (8).

Consider fluid passing through the saturation curve along an isothermal path as shown in Figure 22. If point (A) is the beginning state, the path followed by the liquid crosses the saturation line at point (B). It continues to follow the curve to its theoretical minimum metastable liquid state at point (C), and follows on through points (D) and (E). It crosses the saturated vapor curve at (F), and exists as a stable vapor from points (F) to (G). The area of interest is the shape of the curve from (A) to (G). It is desired to follow the line from the saturated liquid point (B) to some practical lower limit (C). Point (C) is presumably some value significantly closer to the saturated liquid line than the metastable liquid limit (D). This curve takes the form of a cubic equation. There have been a number of methods proposed for determining its shape and where the minimum crosses

the spinodal line. These methods rely on a combination of existing data in the stable regime, some limited data available in the metastable regime, and the following additional constraints:

- Match known isotherms of fluid in the stable regime
- Must satisfy Maxwell-Gibbs requirement[3] that integral $\int_{sat\_liquid}^{sat\_vapor} vdp = 0$
- Must define spinodal line correctly (i.e. – the minimum stability point fits equation (8)

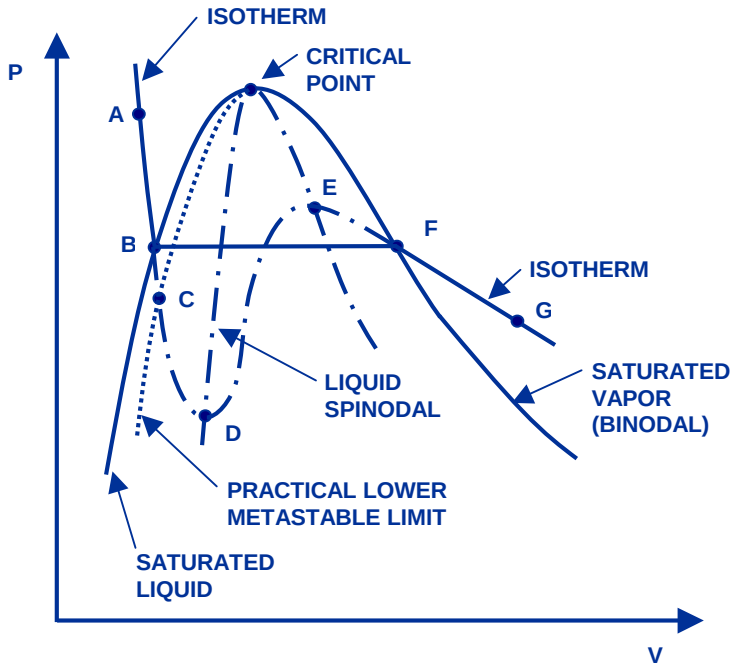

Figure 22 – P-V curve for a typical fluid showing saturation curve, spinodal curve and proposed practical lower metastable limit.

There are several references that discuss how this line can be defined. The Himpan cubic equation of state[34] represents the essential features of a correct equation of state and provides a good fit to real fluid data in the stable regimes. The Himpan equation is

shown in equation (9).

$$p = \frac{RT}{(\nu - \beta)} - \frac{\gamma}{(\nu - \alpha)(\nu - \delta)} \tag{9}$$

The constants α, β, γ, and δ are empirical constants and υ is the molar specific volume. These constants could be determined based on the criteria listed above and specific data from the metastable subcooled regime. Unfortunately, to date, literature searches have not uncovered values for these constants for the fluids and conditions (LO_2 & LCH_4). Annamali[35] also addresses this problem and has proposed the following equation to estimate the curve in the metastable region:

$$p = \frac{RT}{(\nu - \beta)} - \frac{\alpha}{\sqrt{T} * \nu * (\nu - \beta)} \tag{10}$$

where α, and β are empirical constants, and υ is specific volume.

Several others[36, 37] have had good success fitting cubic equations to predict surface tension and spinodal limits for individual isotherms in the metastable region. These equations may be useful in analyzing data from the experiments conducted as part of the present study.

The curves described by these equations predict the behavior of single phase fluids in the metastable region. In practical applications such as those found in typical cryogenic TVS systems, one would not expect to find a deep penetration of single phase fluids into the two phase region. However, data from the experiments conducted as part of the present study indicate that at least in some cases, there is penetration of single phase fluids into

the two phase region to some small extent. One might expect that an intermediate curve could be drawn between the saturation curve and the spinodal curve that would give the practical limits for metastable single phase fluids below the saturation line. It is likely that this curve would be influenced by the complexity of the J-T device. For example, a Visco Jet has multiple convoluted passages that the fluid would have to pass through during expansion. In comparison, a single orifice would provide a "cleaner" passage, and might more likely result in a deeper excursion below the saturation line.

For the tests conducted for the present study, Visco Jet J-T devices were utilized. Therefore, the data presented only represents conclusions that can be drawn from the specific configuration used in these tests.

CHAPTER VIII

EXPERIMENTAL TEST RESULTS

8.1 LCH_4 Tests

The general procedure for performing these tests has been outlined in section 6.3. The intent of these tests was to start with the Visco Jet outlet pressure greater than the saturation pressure of the bulk liquid methane. The outlet pressure would gradually be decreased to bring the outlet pressure through the saturation point for the bulk liquid. Data paid particular attention to was the outlet pressure and temperature. Presumably, as the pressure on the outlet of the Visco Jet decreased and passed through the pressure corresponding to the temperature of saturated liquid, further decreases in pressure would result in a corresponding decrease in temperature as explained in section 4.1. If the outlet temperature did not track with the outlet pressure but remained at or near the bulk liquid temperature, it could indicate that the liquid did not change state, but had remained as a metastable liquid. Therefore, to determine whether or not the outlet conditions indicated metastable liquid methane, the outlet temperature was compared to the temperature of saturated liquid based on outlet pressure.

Two different tests were performed in December 2006. The first test was performed with

warm LCH_4, with liquid temperature close to NBP conditions. The second test was performed with LCH_4 that was subcooled to approximately 105.3 K. A summary of the tests conducted is shown in Table V. Figure 23 plots inlet and outlet pressure of the methane as it flowed through the Visco Jet for the 112.9 K LCH_4 test. Figure 24 plots inlet and outlet temperature and outlet temperature corresponding to the outlet saturation pressure for methane as it flowed through the Visco Jet. Figures 25 and 26 show the same data for the 105.3 K subcooled liquid condition test.

Table V – Test Results for LCH_4 Visco Jet Clogging Tests

Data File	Visco Jet Lohm	LCH_4 condition	Bulk Liquid Temp (K)	Inlet Pressure (kPa)	Outlet Pressure (kPa)
CCL7_12.20.06	8200	saturated	112.9	151.0	60.6 – 124.1
CCL7_12.21.06	8200	subcooled	105.3	137.2	52.4 – 97.2

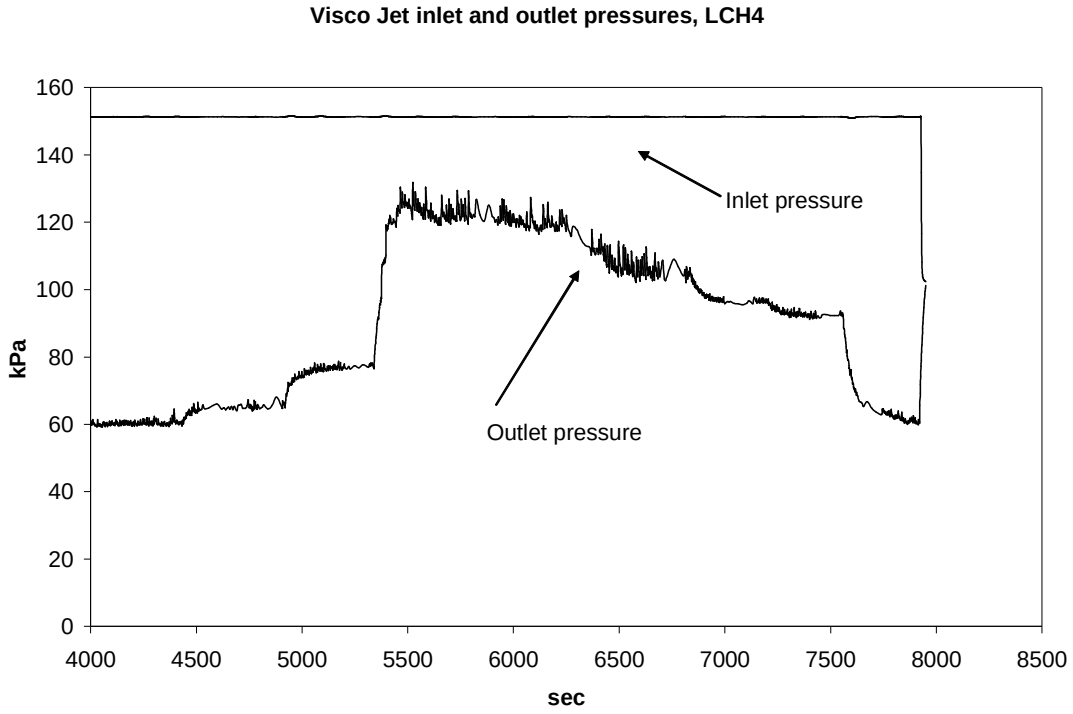

Figure 23 – Dewar inlet and outlet pressures for NBP LCH_4 test

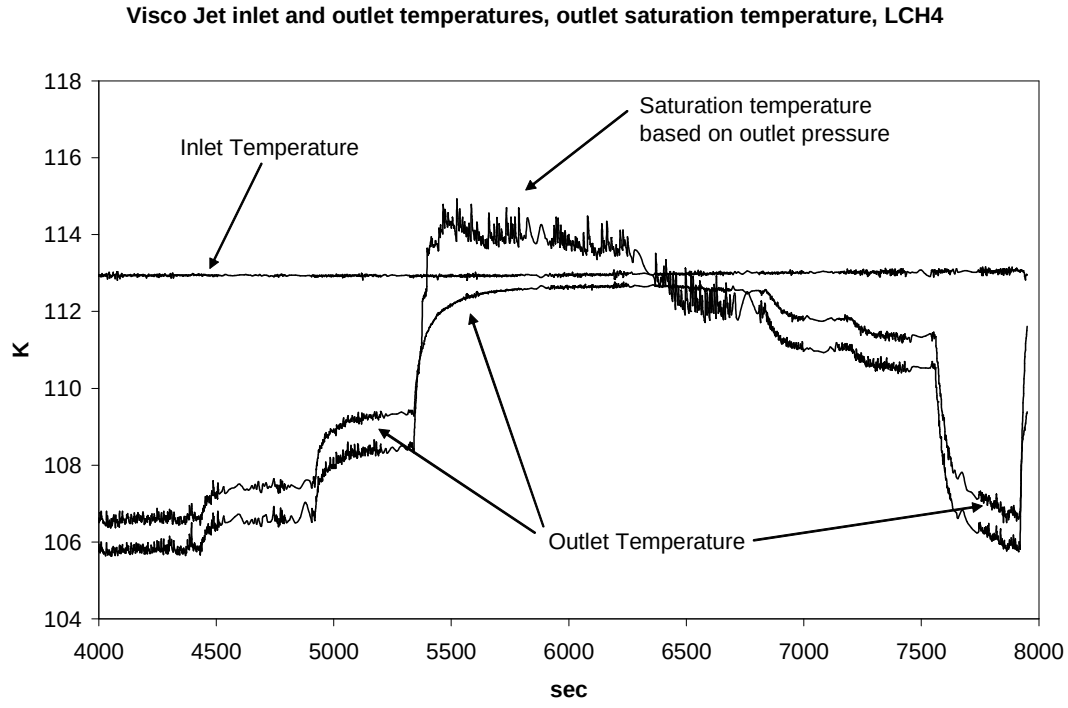

Figure 24 – Dewar inlet and outlet temperatures for NBP LCH_4 test

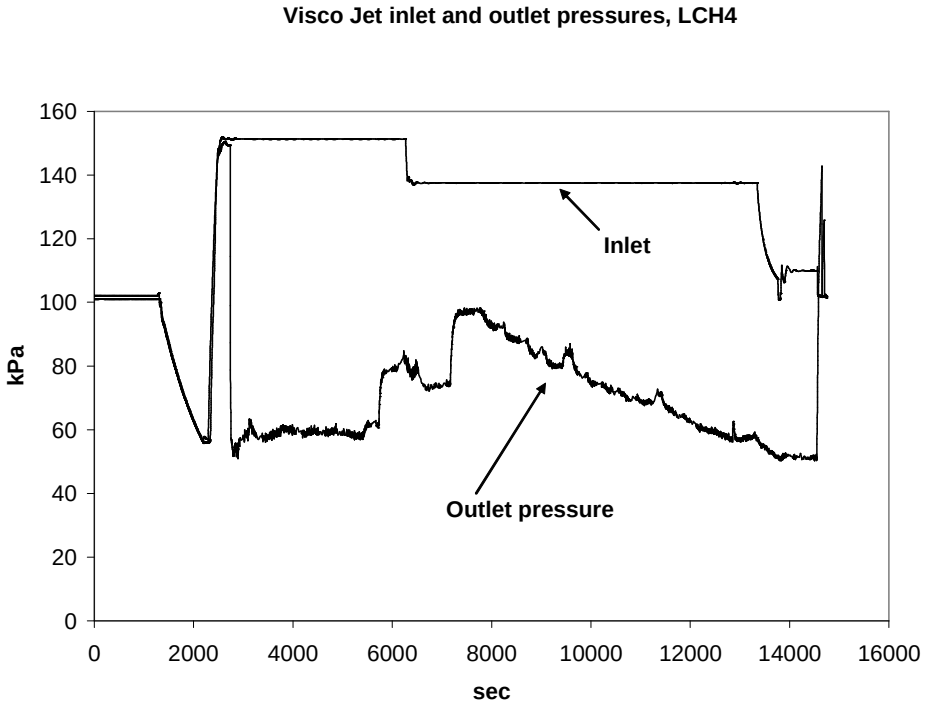

Figure 25 – Dewar inlet and outlet pressures for subcooled LCH_4 test

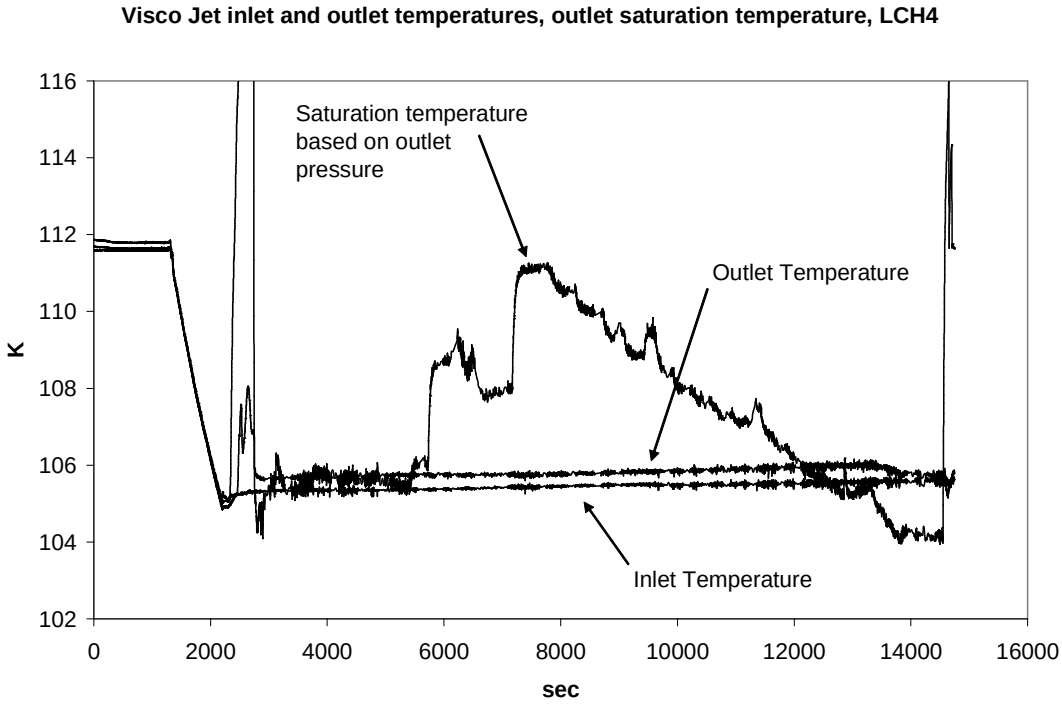

Figure 26 – Dewar inlet and outlet temperatures for subcooled LCH_4 test

For the NBP test, Figure 23 shows inlet pressure to the Visco Jet constant at approximately 151.7 kPa. The outlet pressure is initially sub-atmospheric, approximately 60.0 kPa. A valve in the outlet piping of the Visco Jet was throttled back, decreasing the flow, and increasing the outlet pressure to approximately 124.1 kPa. The outlet valve was then gradually opened, increasing the flow and decreasing the outlet pressure from 124.1 to 60.0 kPa (T=5500 to T=7900 seconds). It is noted that inlet temperature remains constant at approximately 112.8 K. The outlet temperature was initially about 106.1 K, which was consistent with the saturation temperature based on outlet pressure from T=4000 to T=5500. The outlet temperature was slightly warmer than the saturation temperature in this range (about 1 K), and one might conclude that this was metastable fluid. However, as the outlet fluid temperature was significantly less than the bulk fluid temperature upstream of the Visco Jet, it is unlikely that the fluid would have remained at some intermediate temperature between the bulk liquid and the downstream saturation temperature. It is much more likely that the outlet temperature fluid was tracking the saturation temperature and that the offset was due to either a temperature measurement or pressure measurement offset. At T=4500, the valve was throttled back. As flow decreased and outlet pressure increased, the temperature of the methane tracked closely with the saturation temperature, approaching the inlet fluid temperature at approximately T=6000. At T=5500, the valve was gradually opened up, decreasing outlet pressure and saturation temperature. At T=6500, the saturation temperature at the outlet dropped to the bulk liquid temperature. Between T=6500 and T=8000, the outlet temperature tracked the saturation temperature closely as before. That is – a fluid temperature at the

outlet of the Visco Jet that would indicate metastable conditions was not observed.

For the subcooled liquid test, Figure 25 shows inlet pressure to the Visco Jet constant at approximately 151.7 kPa from T=3000 to T=6500 and 137.9 kPa from T=6500 to T=13500 sec. The outlet pressure is initially sub-atmospheric, approximately 59 kPa. A valve in the outlet piping of the Visco Jet was throttled back, decreasing the flow, and increasing the outlet pressure to approximately 97 kPa from T=6000 to T=8000 sec. At T=8000, The outlet valve was then gradually opened, increasing the flow and decreasing the outlet pressure from 97 to 55 kPa at T=13500. It is noted in Figure 25 that the inlet temperature remains constant at approximately 105.5 K (subcooled liquid). The outlet temperature was initially about 106.1 K from T=3000 to T=6000, which was consistent with the bulk liquid temperature and the saturation temperature based on outlet pressure. The outlet temperature tracked well with the saturation temperature in this range. From T=6000 to T=8000, the valve gradually was throttled back. As flow decreased and outlet pressure increased, the saturation temperature based on outlet pressure increased accordingly, while the outlet temperature remained close to the bulk liquid temperature (approximately 106.1 K). At T=8000, the valve was gradually opened up, decreasing outlet pressure and saturation temperature. From T=8000 to T=12500, the saturation temperature dropped from 111.1 to 106.1 K, while the outlet temperature of the fluid remained approximately 106.1 K. In this range, the outlet pressure was still higher than the saturation pressure of the 106.1 K liquid, so one would expect no temperature drop. However, from T=12500 to T=13500, the outlet pressure continued to drop to a minimum of about 55 kPa, and the saturation temperature dropped correspondingly to 104 K.

However, it is noted that between T=12500 and T=13500, the Visco Jet outlet temperature remained above the corresponding saturation temperature. The expectation would be that the outlet temperature should track outlet saturation conditions, and drop to about 103.9 K. This observation is consistent with the existence of metastable warm liquid.

8.2 LO_2 Tests

The general procedure for performing these tests has been outlined in section 6.4. The intent of these tests was to start with the Visco Jet outlet pressure greater than the saturation pressure of the bulk liquid methane. The outlet pressure was then decreased to bring the outlet pressure through the saturation point for the bulk liquid. Data paid particular attention to was the outlet pressure and temperature. As with the LCH_4 tests, as the pressure on the outlet of the Visco Jet decreased and passed through the pressure corresponding to the temperature of saturated liquid, further decreases in pressure would result in a corresponding decrease in temperature as explained in section 4.1. If the outlet temperature did not track with the outlet pressure but remained at or near the bulk liquid temperature, it could indicate that the liquid did not change state, but had remained as a metastable liquid. As with the LCH_4 tests, the outlet temperature was compared to the temperature of saturated liquid based on outlet pressure to determine whether or not the outlet conditions indicated metastable liquid methane.

Two test series were performed in July and August 2007. The first test was performed with warm LO_2, with liquid temperature approximately 116 K. The second test was performed with colder LO_2 that has with liquid temperature approximately 93.5 K. A summary of tests is shown in Table VI. Figure 27 plots inlet and outlet pressure of the oxygen as it flowed through the Visco Jet for a typical LO_2 test for an 11,200 Lohm Visco Jet. Figure 28 plots inlet and outlet temperature and outlet temperature corresponding to the outlet saturation pressure for oxygen as it flowed through the Visco Jet.

Table VI – Test Results for LO_2 Visco Jet Clogging Tests

Data File	Visco Jet Lohm	LO_2 condition	Bulk Fluid Temp. (K)	Inlet Pressure (kPa)	Outlet Pressure (kPa)	2-phase transition pressure (kPa)
LOX JT001 7-31-07	1350000	Subcooled	93.6	141.3	101.4	142.2
LOX JT002 7-31-07	313000	Subcooled	93.7	141.3	102.7	143.7
LOX JT003 7-31-07	102000	Subcooled	93.7	142.0	103.4	143.9
LOX JT004 7-31-07	11200	Subcooled	93.6	142.7	104.1	142.6
LOX JT005 7-31-07	3300	Subcooled	93.5	143.3	104.1	142.0
LOX JT003 8-01-07	102000	Saturated	115.6	835.9	102.7	786.6
LOX JT005 8-01-07	3300	Saturated	115.2	834.8	104.1	764.0
LOX JT001 8-01-07	1350000	Saturated	115.8	835.0	104.1	793.5
LOX JT002 8-01-07	313000	Saturated	116.0	834.3	104.8	804.5
LOX JT004 8-01-07	11200	Saturated	115.7	833.1	104.1	788.0
LOX JT006 8-01-07	680	Saturated	115.7	832.9	120.0	790.7
LOX JT001 8-02-07	1350000	Saturated	116.0	836.3	102.7	804.5
LOX JT004 8-02-07	11200	Saturated	115.7	835.8	103.4	790.2
LOX JT002 8-02-07	313000	Subcooled	93.3	139.3	104.8	138.6

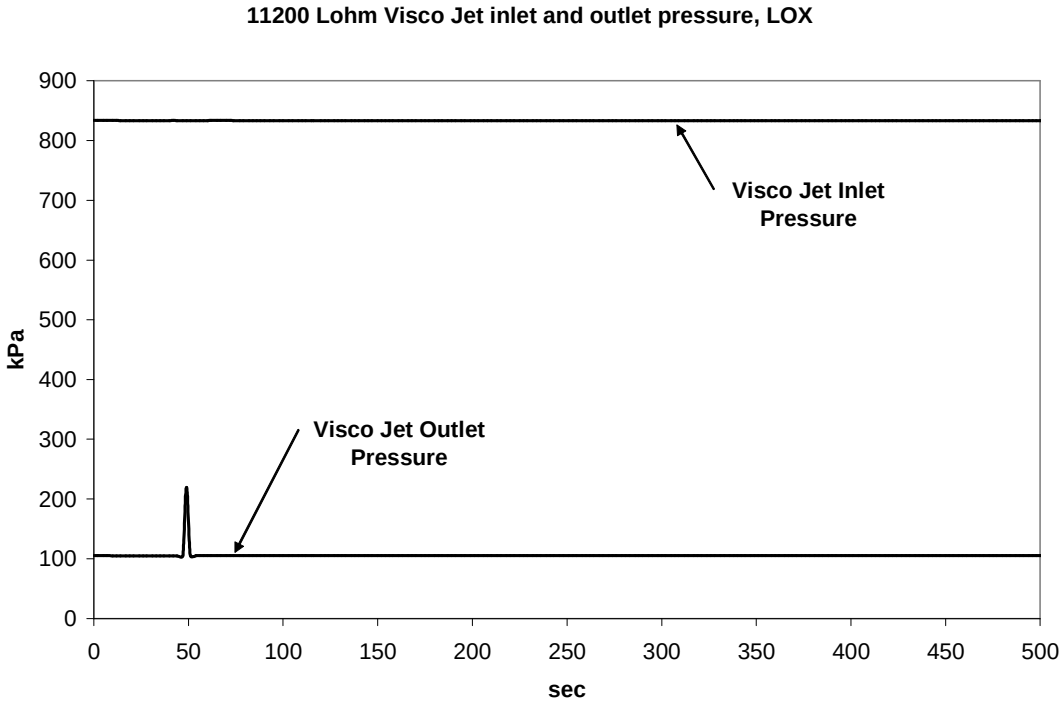

Figure 27 – Dewar inlet and outlet pressures for subcooled LO_2 test

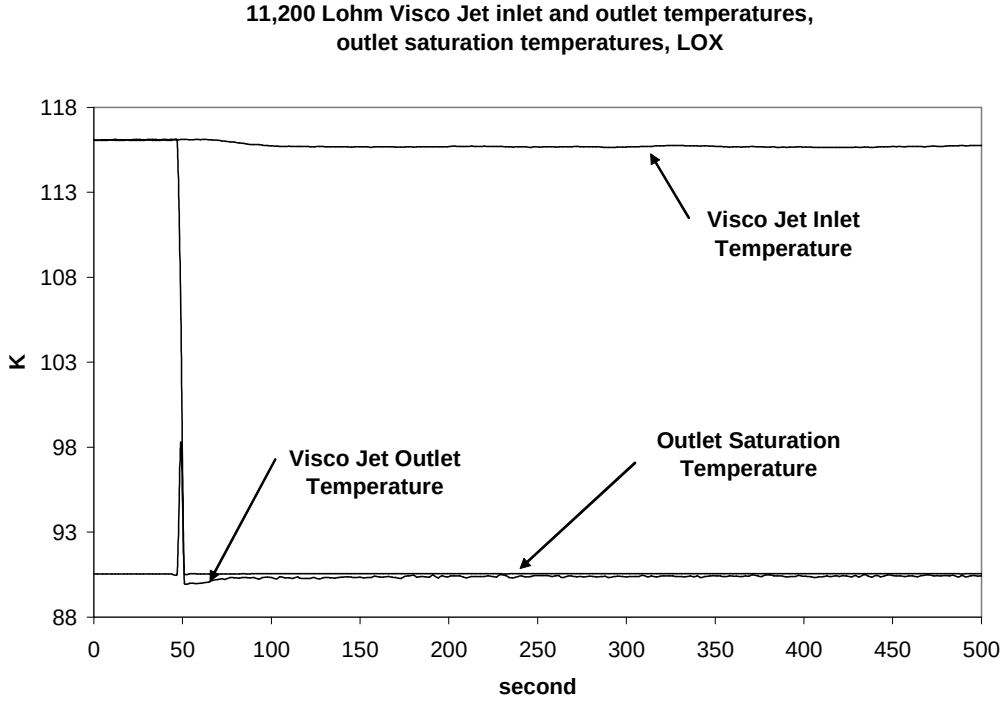

Figure 28 – Dewar inlet and outlet temperatures for subcooled LO_2 test

For the test run shown in Figures 27 and 28, Visco Jet inlet pressure remains constant at approximately 833 kPa. The outlet pressure is initially atmospheric, approximately 103 kPa. At time T=50, the outlet valve downstream of the Visco Jet was opened, initiating flow through the device. Note in Figure 27 the small rise in outlet pressure at T=50 as flow starts. The outlet pressure recovers almost immediately to atmospheric pressure and remains there for the duration of the test run. Note also in Figure 28 that the outlet fluid temperature drops immediately to slightly below the corresponding saturation temperature based on outlet pressure, and then recovers to track saturation temperature for the duration of the test run. It is noted that the response was immediate (within the limits of our data collection system), and it is noted that there was no temperature in the outlet stream that would indicate the presence of metastable warm liquid. This test result is typical of all test runs performed with LO_2. With some of the test runs where the flow rate was much smaller, it was noted that the outlet temperature was masked by the bulk fluid temperature. This was noted previously, and is due to the lack of any insulation on the piping downstream of the Visco Jet that would have insulated the outlet line from the influence of the bulk liquid temperature. Appendix 12.2 provides more detail for each of the other LO_2 test runs.

CHAPTER IX

DISCUSSION

9.1 General Observed Behavior

9.1.1 LCH_4 Tests

For both NBP and subcooled LCH_4 tests, initial test conditions started with outlet conditions close to one atmosphere. Increasing outlet pressure resulted in raising outlet temperatures close to inlet temperatures. For both tests, the outlet pressure was slowly decreased to bring outlet conditions below the saturation pressure based on bulk liquid condition. For NBP liquid, the outlet temperatures measured tracked saturation temperatures for measured outlet pressure. It is noted for the NBP test that the outlet pressure did not start very high above saturation pressure of bulk liquid. For the subcooled liquid test, once the outlet pressure was decreased below the saturation pressure for the bulk liquid, the outlet temperature did not track outlet saturation temperature based on outlet pressure. This persisted for about 1000 seconds (from T=12500 to T=13500 seconds). The outlet temperature did start to drop at T=13500, but still remained above the saturation temperature based on outlet pressure. In this timeframe, the flow was at a maximum for the entire test run. As the flow was higher, it is unlikely that outlet temperature was a false reading influenced by bulk fluid. If this

was the case, it would have been also observed in the NBP test. NBP temperatures tracked saturated temperatures based on outlet pressure, and did not appear to be influenced by bulk liquid temperatures. In hindsight, it would have been nice if an additional case with liquid subcooled to a lesser degree could have been run.

9.1.2 LO_2 Tests

Tests were performed at two conditions – 137.9 kPa inlet pressure with bulk liquid temperature 93.3 K and 827.4 kPa inlet pressure with bulk liquid approximately 115.5 K. For the 137.9 kPa test, the liquid was very close to the saturation temperature with respect to the tank pressure. Since the facility was not set up to allow for discharge to sub-atmospheric pressures, Bulk liquid was not subcooled very much with respect to the test tank pressure. However, for the 827.4 kPa tests, the liquid was subcooled approximately 0.8 K with respect to the test tank pressure. For both tests, outlet pressure was close to atmospheric. Refer to Table 4 for bulk liquid temperatures and two-phase transition pressures for the tests conducted. Figure 28 shows test results for a typical subcooled LO_2 test. From T=0 to T=50, both inlet and outlet temperatures were approximately 115.5 K. Outlet saturation temperature is based on the outlet pressure of approximately 103.4 kPa. At T=50, the outlet valve was opened, and flow was initiated through the Visco Jet. As can be seen from the plot, the outlet temperature immediately dropped to approximately 90 K, and recovered to about 90.3 K, very close to the saturation temperature of 90.6 K. This result was typical for all tests performed with LO_2. That is – the observed the outlet temperature was not elevated above the saturation temperature, but in each case, the outlet temperature tracked the saturation temperature based on the

outlet pressure, which indicated no apparent metastability of the outlet flow.

9.1.3 Summary of Test Observations

In summary, the following observations are made about tests with LO_2 and LCH_4:

1. For NBP LCH_4 tests, there were no observed apparent metastable conditions downstream of the Visco Jet.
2. For subcooled LCH_4 tests, some apparent metastable conditions were observed based on the downstream temperature remaining above the corresponding saturation temperature by approximately 2K for an extended period of time (approximately 1000 seconds). During this time, the outlet temperature started to decrease somewhat, but remained above the saturation temperature based on outlet pressure.
3. For both 93.5 K and 116 K liquid LO_2 tests, no apparent metastability downstream of the Visco Jet was observed.

9.2 Comparison with Theory

For LCH_4, a significant degree of liquid subcooling was achieved in one test, and not much subcooling in the other test. As noted previously, the warmer liquid test did not show any evidence of metastability downstream of the Visco Jet. However, apparent metastability was noted in the subcooled tests, where the outlet temperature remained above the outlet saturation temperature. It is noted that in these tests, the outlet conditions could be controlled due to the presence of a proportional valve. This valve allowed the transition through the phase transition point in a controlled manner.

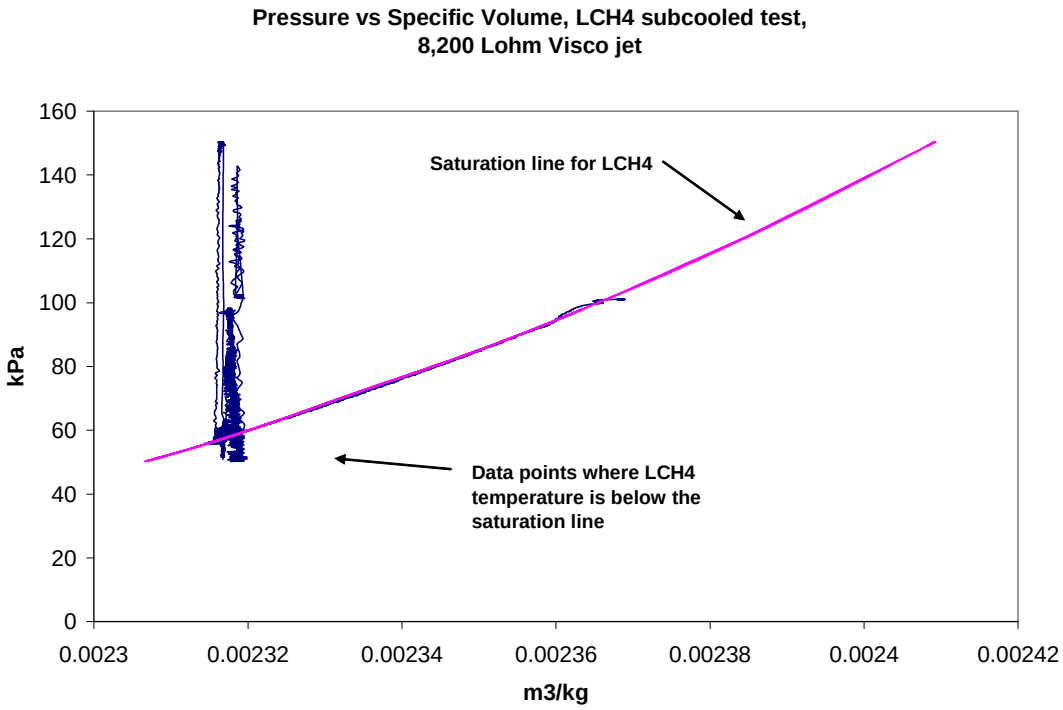

Figure 29 – Pressure vs. Specific Volume for subcooled LCH_4 test

(liquid temp. = 105.5 K)

For the subcooled LCH_4 test where observations indicated metastability, pressure versus specific volume was plotted as shown in Figure 29. Specific volume for test data is calculated based on the downstream liquid temperature. The pressure versus specific volume curve for saturation conditions is also shown. Note the excursion of data below the saturation line. This curve is compared to the general curve for saturated and spinodal pressure versus specific volume shown in Figure 22. For this particular test, one would desire to generate the curve described by points BDEF in the metastable region. This would allow comparison of how far into the metastable region the isotherm would extend with respect to the minimum spinodal point. Section 7.0 discusses fitting cubic equations to predict spinodal limits for individual isotherms in the metastable region. Per Biney[38],

consider fitting a cubic equation of the form:

$$\frac{p}{p_{sat}} = 1 - \frac{(v - v_f)(v - v_m)(v - v_g)}{(v + b)(v + c)^2} \tag{11}$$

Where v_f, v_g and p_{sat} are evaluated for the inlet fluid conditions (temperature = 105.3K). This equation is fit by assuming some reasonable value for v_m between v_f and v_g, and iterating on constants b and c to match the slope of the P vs. V curve in the liquid stable region. The resultant curve is shown in Figure 30. An expanded region of this curve in the stable liquid region is shown in Figure 31, showing that the cubic equation curve matches the slope of the stable liquid isotherm reasonably well. Figure 30 shows that for the methane 105.3K isotherm, the minimum spinodal pressure is in the vicinity of -60,000 kPa. Obviously, the data shown in Figure 29 only represents an excursion of a few degrees into the metastable region.

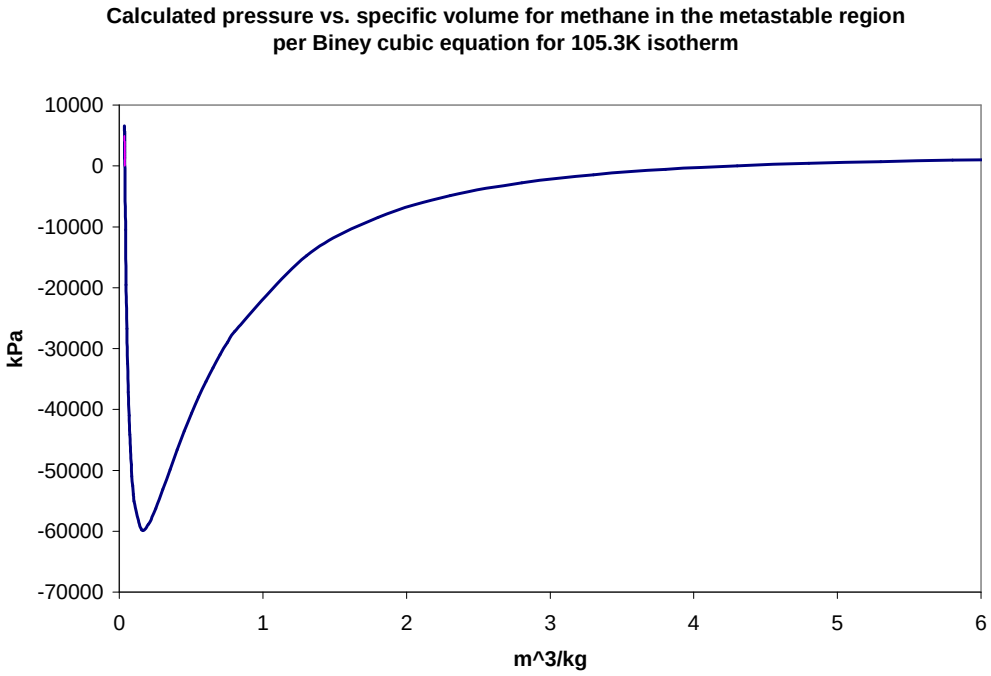

Figure 30 – Calculated press. vs. specific vol. in metastable regime, LCH_4 105.3K isotherm

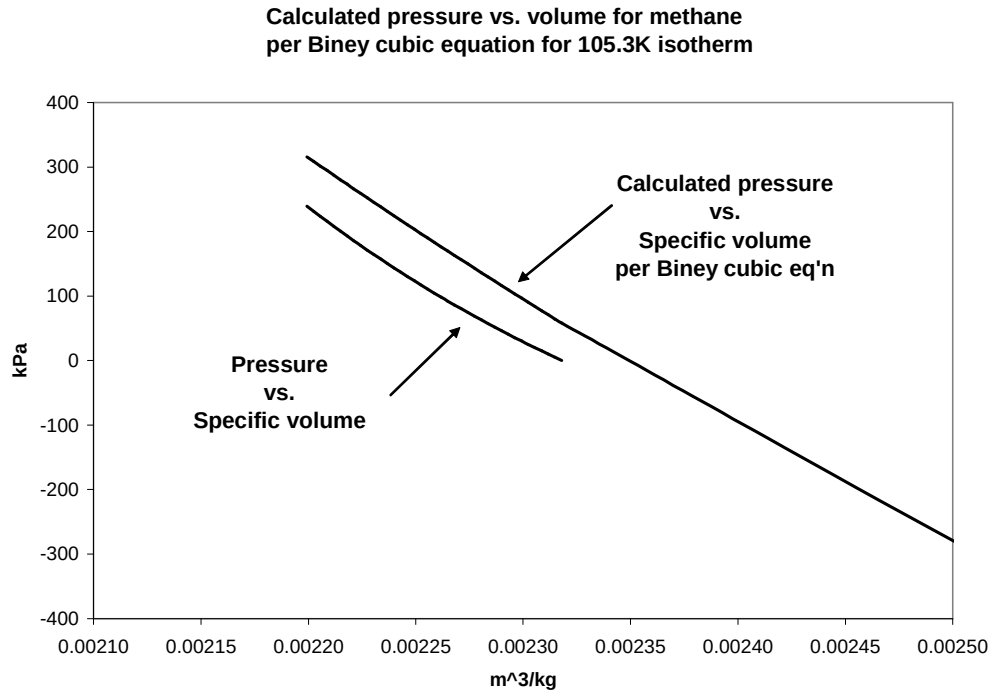

Figure 31 – P vs. V actual and per calculated cubic equation, LCH_4 105.3K isotherm

For LO_2, our bulk liquid conditions were almost at saturated conditions – not much subcooling. These conditions were a result of other test program requirements. In retrospect, it would have been nice if the tank pressure could have been bumped up some to further subcool the liquid with respect to the test tank pressure. Also, the test apparatus did not allow us to traverse through the two phase transition point smoothly as with the LCH_4 tests, but when initiating flow through the Visco Jet, outlet pressure immediately dropped to the minimum outlet pressure of 103.4 kPa. This may have an influence on whether or not metastability occurs downstream of the Visco Jet.

CHAPTER X

CONCLUDING REMARKS

10.1 General Comments

The original premise for this study was to obtain a better understanding of Joule-Thomson devices used in space based cryogenic fluid management systems and determine if the metastability of single phase cryogenic fluids below the saturation line needed to be considered in the design of these systems. If this behavior was indeed observed, it was desired to see if some intermediate curve might be defined as shown in Figure 22 that could define a minimum practical limit of metastability. So, the questions that need to be answered are (1) did was metastability observed in the present tests, and (2) could the phenomenon be consistently predicted and reproduced? Based on LO_2 and LCH_4 test data from this program, some apparent metastability was indeed observed (in subcooled LCH_4 tests), but was not observed in other tests (NBP LCH_4 tests and all LO_2 tests). Therefore, it does not appear that the present work can define any minimum practical metastability limit for LO_2 and LCH_4 with any certainty. That being said, one needs to consider what other factors may be at play that may have had an influence on results. Reviewing the test procedures and results, the following factors are noted:

1. For all LO_2 tests and the NBP LCH_4 test, the bulk liquid was not deeply subcooled

with respect to the test tank pressure. That is, the transition through the saturation point was very close to the saturation temperature based on Visco Jet inlet pressure.

2. The differential pressure across the Visco Jets was substantially higher for the LO_2 tests than it was for the LCH_4 tests.
3. In the LCH_4 tests, the downstream pressure could be modulated to bring it through the saturation point in a controlled manner, whereas with the LO_2 tests, this was not possible. This may indicate an influence of rate on the process.
4. Metastability was not observed with LO_2, but was in some cases with LCH_4. This may indicate some dependence on fluid. Although there was limited reference in the literature found that would indicate this, the possibility cannot be unilaterally dismissed. However, that study is beyond the scope of this work.

Considering the first two factors listed above, refer to Hendricks[30]. He refers to Benjamin and Miller[34] who postulated that "no vaporization occurred right at the orifice, but that the flow passes through as a liquid in a metastable state and flashes slightly downstream". Hendricks work with LN_2 indicated that a metastable jet downstream of an orifice existed, but that the distance downstream that the metastable jet breaks down is a function of the pressure difference across the orifice. That is, a very large pressure drop across the orifice would result in vaporization very near the orifice, causing a decrease in flow. In our tests, the pressure difference across the Visco Jets for LO_2 tests were as high as 700 kPa, whereas the maximum pressure drop across Visco Jets for LCH_4 tests was only approximately 90 kPa. If there was any metastability in the LO_2 flow, it could have

broken up before reaching the downstream temperature sensor. It is possible that with the lower pressure drop across the Visco Jet with LCH_4, that metastability may have persisted far enough downstream to be sensed by the temperature sensor. For both LO_2 and LCH_4 test configurations, the downstream temperature sensor was located approximately 5 cm downstream of the Visco Jet orifice.

Considering the third factor (the difference in rate of depressurization between LCH_4 and LO_2 tests), it would appear that depressurizing more slowly would be more likely to result in a metastable state downstream of the Visco Jet. However, Shamsundar[39] addresses the rate of depressurization across an orifice, and states that the faster the rate of depressurization and the fewer the sources of heterogeneous nucleation, the closer the liquid can come to the metastable spinodal limit. That is, if the depressurization happens quickly enough, the fluid won't have time to react to the change in pressure by changing state. This runs counter to the present test work's results with LCH_4, as apparent metastability was observed with a slower rate of depressurization. As Shamsundar also noted that the number of sources of heterogeneous nucleation influences metastability, and that a Visco Jet with its multiple passages provides many potential nucleation sites that would promote phase change, it seems reasonable to look elsewhere for reasons for our observations of metastability. To date, no good explanation in the literature has been found that would explain observations from the tests conducted in the present work.

Considering the influence of the fluids themselves, Shamsundar also makes reference to the fact that a slow process *with industrial quality liquid* will vaporize very close to the

saturation point. The LO_2 and LCH_4 used for these tests was relatively high purity (99.9%+ pure). However, each fluid did have in its specification impurities of other atmospheric gas species in the 1 – 100 ppm range, which could have possibly had an effect. That is, if these other species were cold enough to actually freeze, they could have provided nucleation sites that would have enhanced phase transition. Although this possibility is worth considering, it is outside the scope of this work, and may be addressed in future work in this area.

Finally, one needs to consider the possibility of bad data due to an inadequate experimental set up. As previously noted in the LO_2 test results section, the outlet temperature was masked by the bulk fluid temperature, as the outlet of the Visco Jet was not insulated. This can be seen in more detail in data runs in Appendix 13.2. However, the LCH_4 test set up did insulate the outlet. Also, it is noted that the NBP test results showed downstream fluid temperatures tracking saturation temperatures very closely, which validates the downstream temperature reading. The LCH_4 flow rate for both tests was consistent and varied from approximately 20 – 30 slpm, negating the possibility of the different flow rates influencing downstream temperatures. Based on this information, it can be asserted that the temperatures observed in the subcooled LCH_4 test indeed did indicate metastability.

In summary, the data from this test program does not provide enough consistent data to formulate a predictive tool that would quantify a minimum metastable temperature for the fluids tested. However, one still might make some observations and provide some

recommendations for designers to consider when constructing cryogenic TVS systems.

1. In some instances, it appears that a metastable, warm fluid flow can persist for an extended period of time. Presuming that eventually the temperature downstream of the orifice would drop, any time constant for metastability should be considered in design.
2. A greater pressure drop across a J-T device appears to be less prone to any metastability. This observation was based on the lack of any indication of metastability with the LO_2 tests where pressure drop across the orifice ranged from 40 to 730 kPa, as opposed to LCH_4 tests where metastability was indicated with pressure drops in the range of 40 to 90 kPa.
3. The rate at which depressurization occurs may have an influence on the presence of metastability. This is based on the fact that metastable conditions were observed with LCH_4 where the pressure was decreased across the J-T device in a controlled manner. This may influence how the J-T device or other components might be specified.

10.2 Implications for Space Flight TVS Systems

As previously mentioned, J-T devices are key to cryogenic thermal control systems in space flight architecture. Findings from this study indicate that metastable superheated liquid may indeed be present under certain conditions, and system designers should be aware of the implications. Based on the results of this study, a designer should consider the following factors in system design:

1. Higher pressure cryogenic storage systems would appear to be less likely to see any

metastability due to the higher pressure drop across a J-T device.

2. Consideration should be made on where to locate any temperature measurement devices, as any metastable warm liquid may give a false indication of downstream fluid conditions (i.e. – fluid changes state and drops in temperature downstream of the temperature sensor).
3. The physical location of heat exchangers should be such that if there is any metastable flow, it has a chance to change state with a corresponding temperature drop before the heat exchanger.

10.3 Possible Future Work

Inconsistent test results are never as good as a large amount of good data that can be used to develop useful tools for the designer. However, although there were some inconsistent results, one must consider what has been learned from this work, and use that information to help map out what future work would be most useful in providing a better understanding of these J-T devices and the issue of metastability.

These tests were "piggybacked" onto other tests that were being performed at the NASA Glenn Research Center as part of their cryogenic fluid management development program. That is, the Visco Jet test hardware was not optimized for these tests. Nor was the entire system devised solely for the purpose of studying metastable phenomena. Obviously, a test configuration that would consistently produce metastable flow would be ideal. A test configuration that could isolate and study the various factors that influence the onset of metastability would be useful in determining how these factors should best be incorporated into cryogenic fluid system designs. Based on test results observed from

this program, that test configuration might have the following characteristics:

1. Ability to vary the rate of pressure drop across the J-T orifice. Although this was accomplished with the LCH_4 test configuration, it was not so with the LO_2 test.
2. Considering that there may be metastable flow downstream of the orifice, temperature sensors could be located at a number of stations to determine how far this flow might persist downstream.
3. Consider a broader set of test conditions with varying degrees of subcooling. Current tests only looked at test conditions where the liquid was either highly subcooled, or very close to saturation conditions. In addition, higher pressure tests may be of specific interest to NASA, as current cryogenic propellant systems are considering higher pressure storage tanks. As propellant conditions come closer to the critical point, it should be noted that the minimum spinodal temperature comes much closer to the nominal saturation temperature. This is illustrated in Figure 32 which shows the saturation curve and spinodal curves for water[5].
4. Increase the duration of the tests. In the case where apparent metastable flow was observed, the test should have been extended until the downstream temperature started to track the saturation temperature.
5. Future tests should be configured to allow change out of different type J-T devices. The Visco Jets consisted of multiple orifices. Presumably, a single clean orifice may be more prone to metastable phenomenon than a J-T device with multiple passages like the Visco Jet.

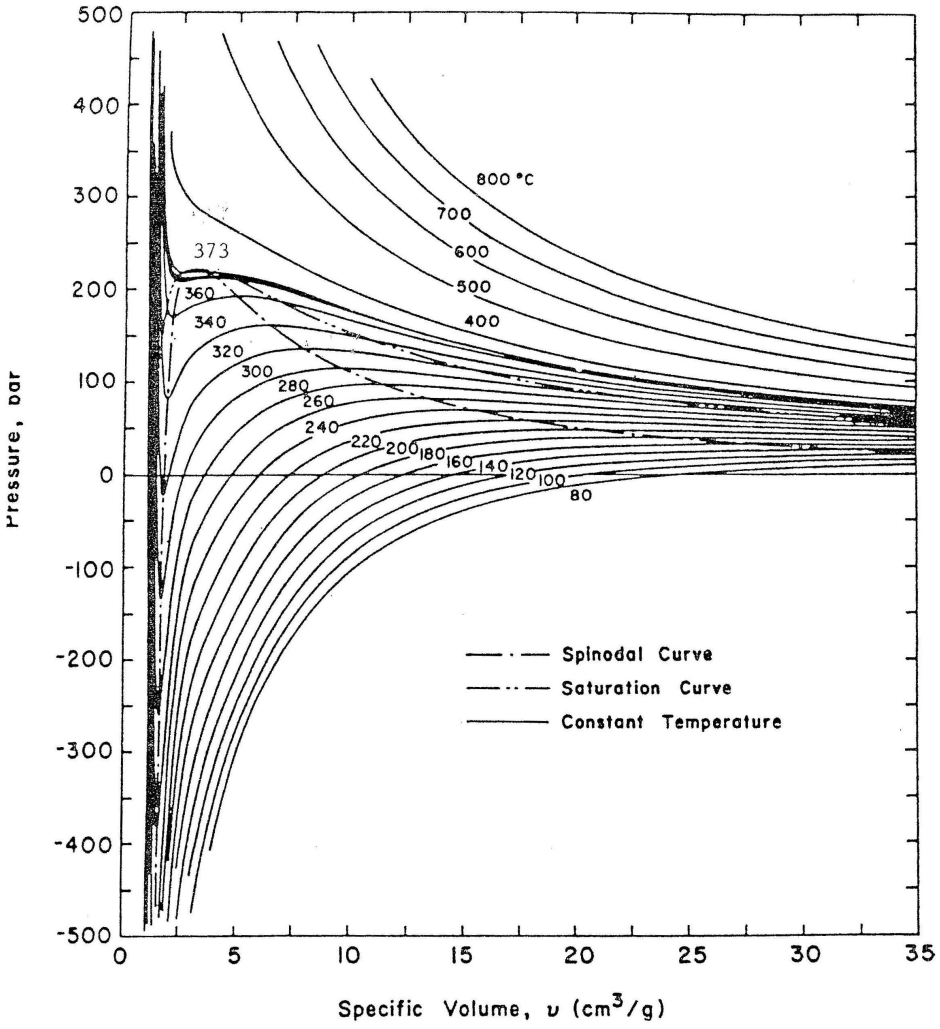

Figure 32 – Saturation curve and Spinodal curves for water

In summary, it is noted that there is abundant literature on metastability from a theoretical and experimental perspective. This body of work to date has largely focused on theoretical limits using precise experimental hardware. The present work has provisionally demonstrated that this effect may also be present in systems that represent real space flight hardware. Further work is recommended to better quantify the factors that may induce metastable flow. These factors being items such as degree of subcooling, rate of process and type of J-T device. This present work has contributed to the general

body of knowledge by observing metastable phenomena in typical cryogenic fluid management systems, and by providing a path for research that will assure that the potential metastable nature of flow through J-T devices is properly incorporated into these system designs.

BIBLIOGRAPHY

1. Papell S.S., Nyland T.W., Saiyed N.H., *Acquisition and Correlation of Cryogenic Nitrogen Mass Flow Data Through a Multiple Orifice Joule-Thomson Device,* NASA TM-103121, 1990

2. Papell S.S., Nyland T.W., Saiyed N.H., *Liquid Hydrogen Mass Flow Through a Multiple Orifice Joule-Thomson Device,* AIAA-92-2881, NASA TM-105583, 1992

3. Lienhard J.H., Karimi A., "Homogenous Nucleation and the Spinodal Line", *Journal of Heat Transfer,* Volume 103, pp 61-64, February 1981

4. Lienhard J.H., "Corresponding States Correlation of the Spinodal and Homogenous Nucleation Limits", *Journal of Heat Transfer Technical Notes,* Volume 104, pp 379-381, May 1982

5. Shamsundar N., Lienhard J.H., "Equations of State and Spinodal Lines – a Review", *Nuclear Engineering and Design,* 141, pp 269-287, 1993, Elsevier Science Publishers

6. Baidakov V.G., Skripov V.P., "Experimental Study of Cryogenic Liquids in the Metastable Superheated State, *Experimental Thermal and Fluid Science*, Volume 5, pp 664-678, Elsevier Science Publishing Co. Inc., 1992

7. Jurns J.M., Kudlac M.T., *NASA Glenn Research Center Creek Road Complex – Cryogenic Testing Facilities*, 2005 Space Cryogenics Workshop, Colorado Springs CO, August 24-26, 2005

8. Wikipedia website, reference to Joule & Thomson collaboration, available at: http://en.wikipedia.org/wiki/William_Thomson%2C_1st_Baron_Kelvin

9. Wikipedia website, reference to Carl Von Linde refrigeration work, available at: http://en.wikipedia.org/wiki/Carl_von_Linde

10. Sterbentz W.H., *Liquid Propellant Thermal Conditioning System Interim Report*, NASA Contractor Report CR-72113, Lockheed Missiles & Space Company Report LMSC-A839783, April 20, 1967

11. Knoll R.H., Stochl R.J., Sanabria R., *A review of candidate multilayer insulation systems for potential use on wet-launched LH_2 tankage for the space exploration initiative lunar missions,* : AIAA 91-2176, NASA-TM-104493, 1991

12. Lin C.S., Hasan M.M., Van Dresar N.T., *Experimental Investigation of Jet-Induced Mixing of a Large Liquid Hydrogen Storage Tank,* AIAA-94-2079, NASA TM-106629, July 1994

13. Lin C.S., Hasan M.M., Nyland T.W., *Mixing and Transient Interface Condensation of a Liquid Hydrogen Tank,* AIAA-93-1968, NASA TM-106201, June 1993

14. Hastings L.J., Flachbart R.H., Martin J.J., Hedayat A., Fazah M., Lak T., Nguyen H., and Bailey J.W., *Spray Bar Zero-Gravity Vent System for On-Orbit Liquid Hydrogen,* NASA TM-2003-212926, October 1993

15. Blatt M.H., Aydelott J.C., *Centaur Propellant Thermal Conditioning System,* AIAA-77-851, July 1977

16. Howard F.S., *Liquid-Hydrogen Boiloff Reliquifier,* NASA Report KSC-11021, June 1977

17. Aydelott J.C., Carney M.J., Hochstien J.I., "NASA Lewis Research Center Low-Gravity Fluid Management Technology Program", IN Man's permanent presence in space Proceedings of the Third Annual Aerospace Technology Symposium, New Orleans, LA, November 7, 8, 1985

18. Aydelott J.C., Rudland R.S., *Technology requirements to be addressed by the NASA Lewis Research Center Cryogenic Fluid Management Facility program,* AIAA 85-1229, 1985

19. Lak T., Wood C., *Cryogenic Fluid Management Technologies for Space Transportation – Zero G Thermodynamic Vent System,* Final Report No. SSD 94M0038, NASA contract NAS8-39202, 1994

20. Lin C.S., Van Dresar N.T., Hasan M.M., "Pressure Control Analysis of Cryogenic Storage Systems", *Journal of Propulsion and Power,* Volume 20, No. 3, May-June 2004, Pages 480-485

21. The Lee Company Web site, "Engineering and Reference Information", accessed 10 April 2007, available at: http://www.theleeco.com/LEEWEB2.NSF/Engineering!OpenView

22. Lebar J.F., *Testing of Multiple Orifice Joule-Thomson Devices in Liquid Hydrogen,* AIAA-1997-3315, presented at 33rd AIAA Joint Propulsion Conference, 1997

23. Jurns J.M., Lekki J.D., *Clogging of Joule-Thomson Devices in Liquid Hydrogen Handling,* AIAA-2006-4877, presented at 42nd AIAA Joint Propulsion Conference, July 2006

24. Nyland T.W., *On the Clogging of Visco Jets and Orifices,* NASA Lewis Research Center, Cleveland, OH, 1992, unpublished

25. Baonza V.G, Alonso M.C., Delgado J.N., “Estimation of the Spinodal Curve for Liquids: Application to 2,3-Dimethylbutane”, *The Journal of Physical Chemistry,* Vol. 98, No. 7, 1994

26. Hasan M.M., Lin C.S., Knoll R.H., Bentz M.D., *Explosive Boiling at Very Low Heat Fluxes: A Microgravity Phenomenon,* NASA TM 106325, presented at ASME 1993 Winter Annual Meeting, Nov. 28 – Dec. 3 1993

27. Simoneau R.J., *Maximum Two-Phase Flow Rates of Subcooled Nitrogen Through a Sharp Edged Orifice,* NASA-TM-X-71760, presented at the Cryogenic Engineering Conference, July 1975

28. Benjamin M.W., Miller J.G., *Trans. ASME,* 63:419, 1941

29. Bailey J.F., *Trans. ASME,* 73:1109, 1951

30. Hendricks R.C., Simoneau R.J., Ehlers R.C., “Choked Flow of Fluid Nitrogen with Emphasis on the Thermodynamic Critical Region”, *Advances in Cryogenic Engineering,* Volume 18, pp 150-161, 1972

31. Henry R.E., Grolmes M.A., Fauske H.K., “Pressure Drop and Compressible Flow of Cryogenic Liquid-Vapor Mixtures”, Chapter 11, *Heat Transfer at Low Temperatures,* Plenum Press, New York, 1975

32. Whalley P.B., “Critical Two-Phase Flow”, Chapter 8, *Boiling, Condensation and Gas-Liquid Flow,* Oxford Scientific Publications, 1987

33. Motil S.M., Meyer M.L., Tucker S.P., *Cryogenic Fluid Management Technologies for Green Propulsion Systems,* AIAA-2007-343, 2007

34. Himpan J., “Die definitive Form der neuen thermischen Zustandsgleichung nest ihren stoffkonstanten von uber 100 verschiedenen Stoffen:, *Monatschefte fur Chemie,* Vol. 86, 1955, pp. 259-268

35. Annamalai K., “Advanced Thermodynamics Engineering”, CRC press, ISBN-10: 0849325536, 2001, page 473

36. Biney P.O., Dong W., Lienhard J.H., “Use of a cubic equation to Predict Surface Tension and Spinodal Limits”, *Journal of Heat Transfer,* Vol. 108, pp. 405-410, May 1986

37. Shamsundar N., Lienhard J.H., “Equations of state and spinodal lines – a review”, *Nuclear Engineering and Design 141,* pp. 269-287, 1993

APPENDICES

APPENDIX A - LCH_4 Test Data

Pressure vs. Time	Temp. vs. Time	Visco Jet Lohm	LCH_4 condition	Bulk Liquid Temp. (K)	Inlet Pressure (kPa)	Outlet Pressure (kPa)	2-phase transition pressure (kPa)	Saturation Temperature based on tank pressure (K)
Figure 33	Figure 34	8200	saturated	112.9	151	60.6 – 124.1	112.3	116.7
Figure 35	Figure 36	8200	subcooled	105.3	137.2	52.4 – 97.2	58.2	115.4

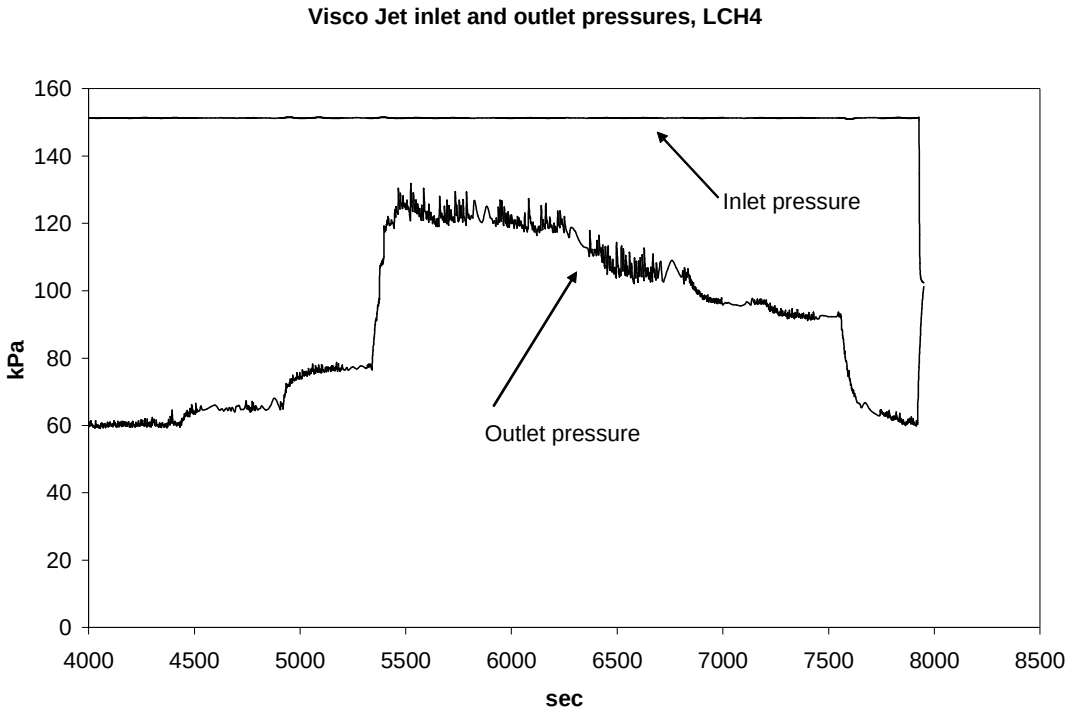

Figure 33

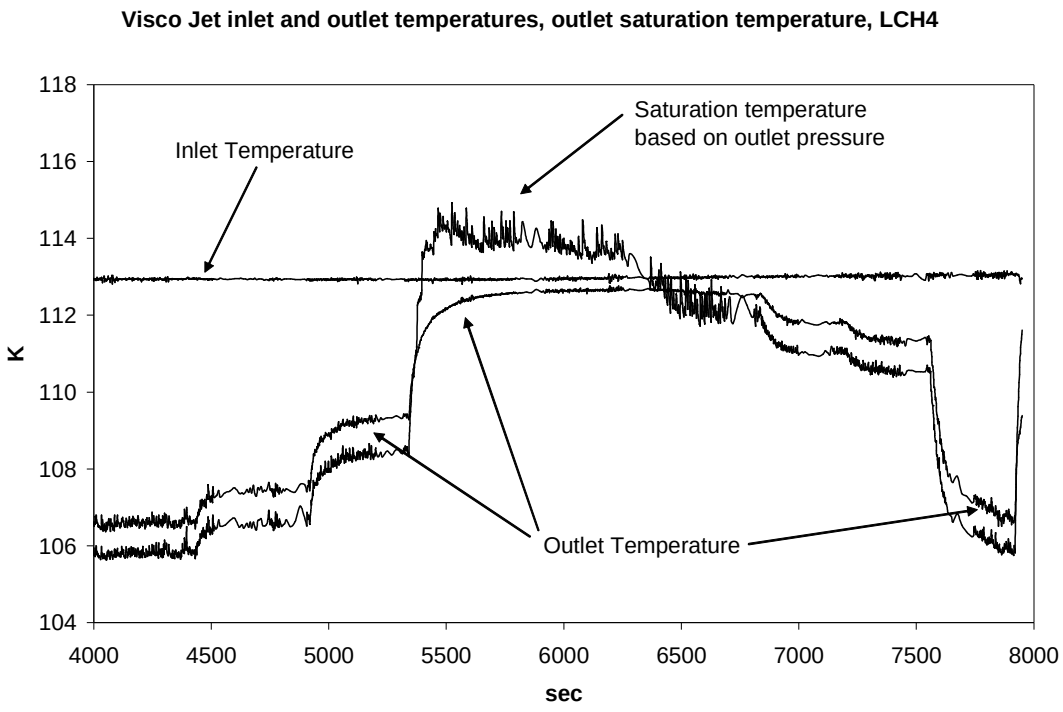

Figure 34

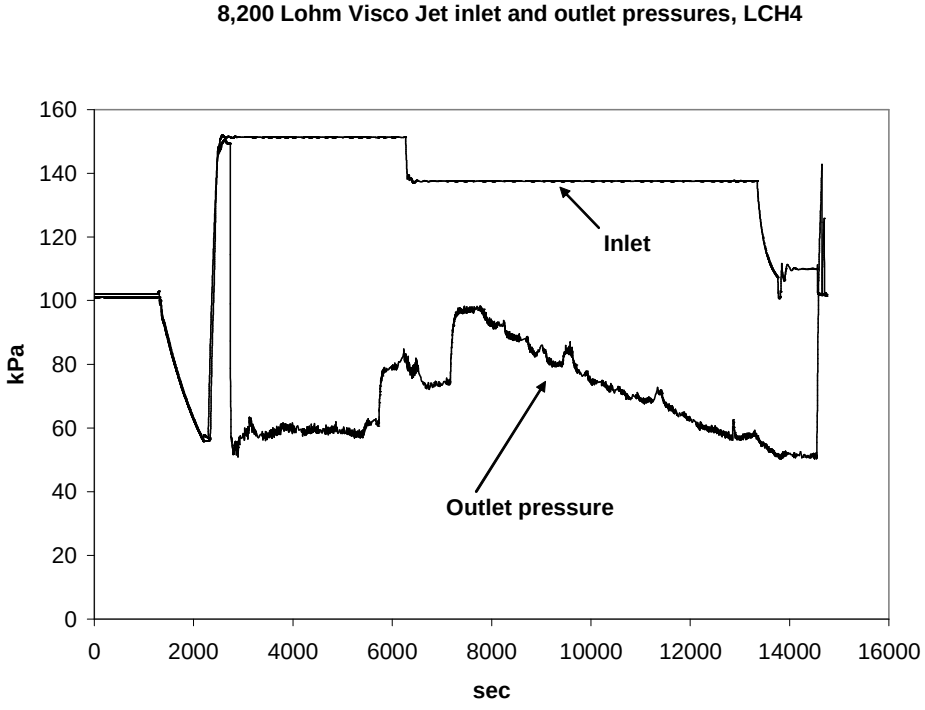

Figure 35

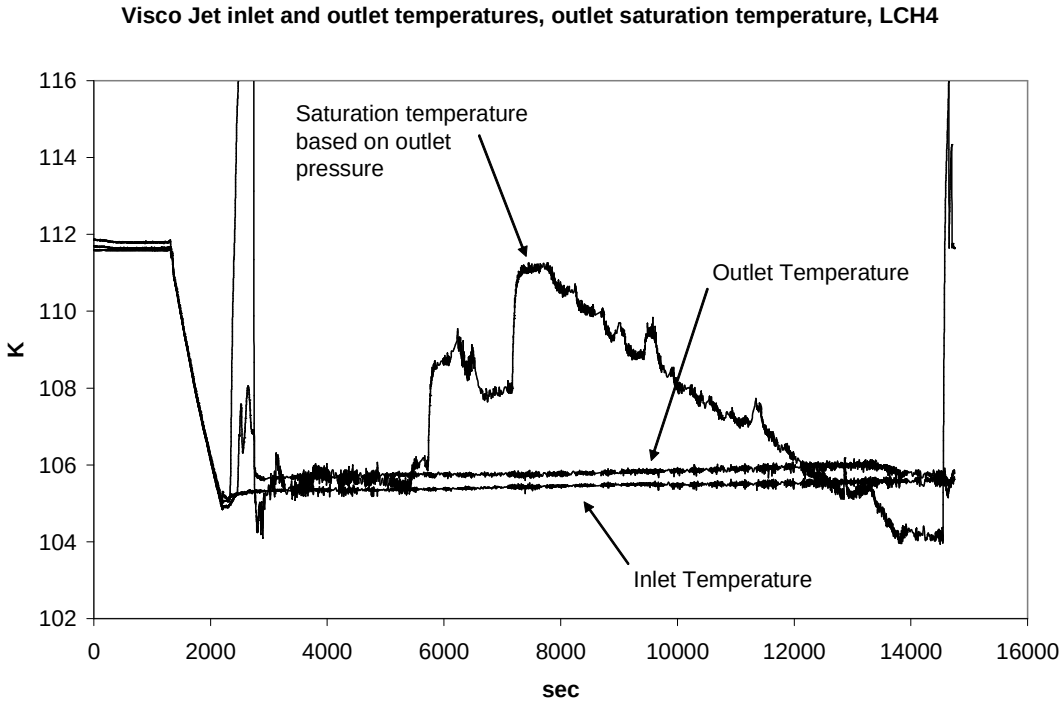
Visco Jet inlet and outlet temperatures, outlet saturation temperature, LCH4
116
114
112
110
108
106
104
102
K
0
2000
4000
6000
8000
10000
12000
14000
16000
sec
Saturation temperature based on outlet pressure
Outlet Temperature
Inlet Temperature

Figure 36

APPENDIX B - LO_2 Test Data

Press. vs. Time	Temp. vs. Time	Visco Jet Lohm Rating	LO_2 condition	Bulk Fluid Temp. (K)	Inlet Press. (kPa)	Outlet Press. (kPa)	2-phase transition pressure (kPa)	Saturation Temperature based on tank pressure (K)	Notes
Figure 37	Figure 38	1350000	Subcooled	93.6	141.3	101.4	142.2	93.5	1
Figure 39	Figure 40	313000	Subcooled	93.7	141.3	102.7	143.7	93.5	2
Figure 41	Figure 42	102000	Subcooled	93.7	142.0	103.4	143.9	93.5	3
Figure 43	Figure 44	11200	Subcooled	93.6	142.7	104.1	142.6	93.6	
Figure 45	Figure 46	3300	Subcooled	93.5	143.3	104.1	142.0	93.6	
Figure 47	Figure 48	102000	Saturated	115.6	835.9	102.7	786.6	116.6	4
Figure 49	Figure 50	3300	Saturated	115.2	834.8	104.1	764.0	116.6	
Figure 51	Figure 52	1350000	Saturated	115.8	835.0	104.1	793.5	116.6	5
Figure 53	Figure 54	313000	Saturated	116.0	834.3	104.8	804.5	116.6	6
Figure 55	Figure 56	11200	Saturated	115.7	833.1	104.1	788.0	116.6	
Figure 57	Figure 58	680	Saturated	115.7	832.9	120.0	790.7	116.6	7
Figure 59	Figure 60	1350000	Saturated	116.0	836.3	102.7	804.5	116.6	8
Figure 61	Figure 62	11200	Saturated	115.7	835.8	103.4	790.2	116.6	
Figure 63	Figure 64	313000	Subcooled	93.3	139.3	104.8	138.6	93.3	

Notes:

1. Figure 38 – outlet temperature drops immediately at T=270 sec to outlet saturation temperature. Subsequent rise to inlet temperature at T=500 is not due to metastability, but due to outlet line being submerged in bulk liquid with no insulation on outlet line. Heat transfer from bulk liquid masks outlet flow temperature. This phenomena is noted for many of the low flow (high Lohm rating) Visco Jets.
2. Figure 40 – see note 1

3. Figure 42 see note 1. At T=260, outlet temperature tracks outlet saturation temperature
4. Figure 48 – similar to Figure 41, except at T=100, outlet temperature is masked by bulk liquid temperature.
5. Figure 52 – see note 1.
6. Figure 54 – see note 1.
7. Figure 57 – outlet pressure increase due to high flow through Visco Jet.
8. Figure 60 – see note 1.

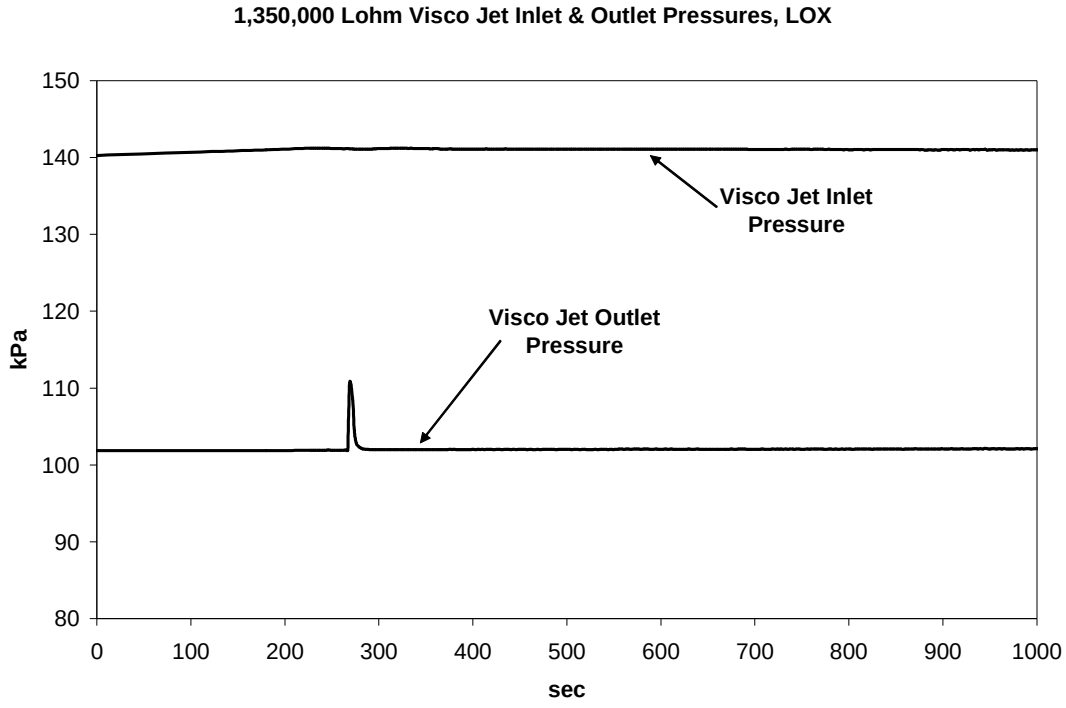

Figure 37

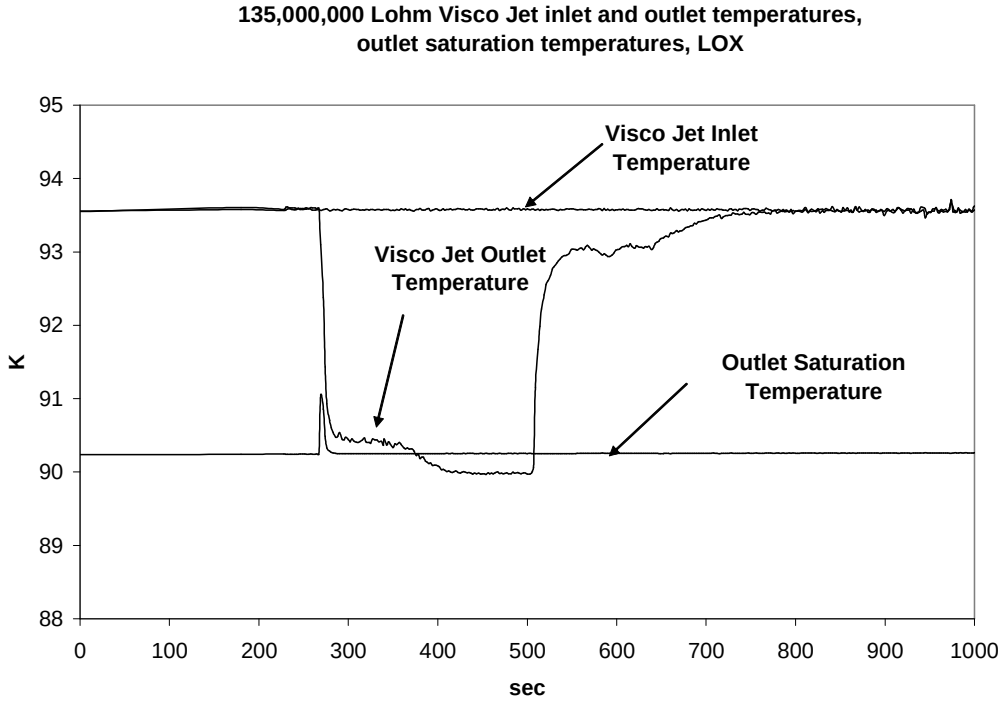

Figure 38

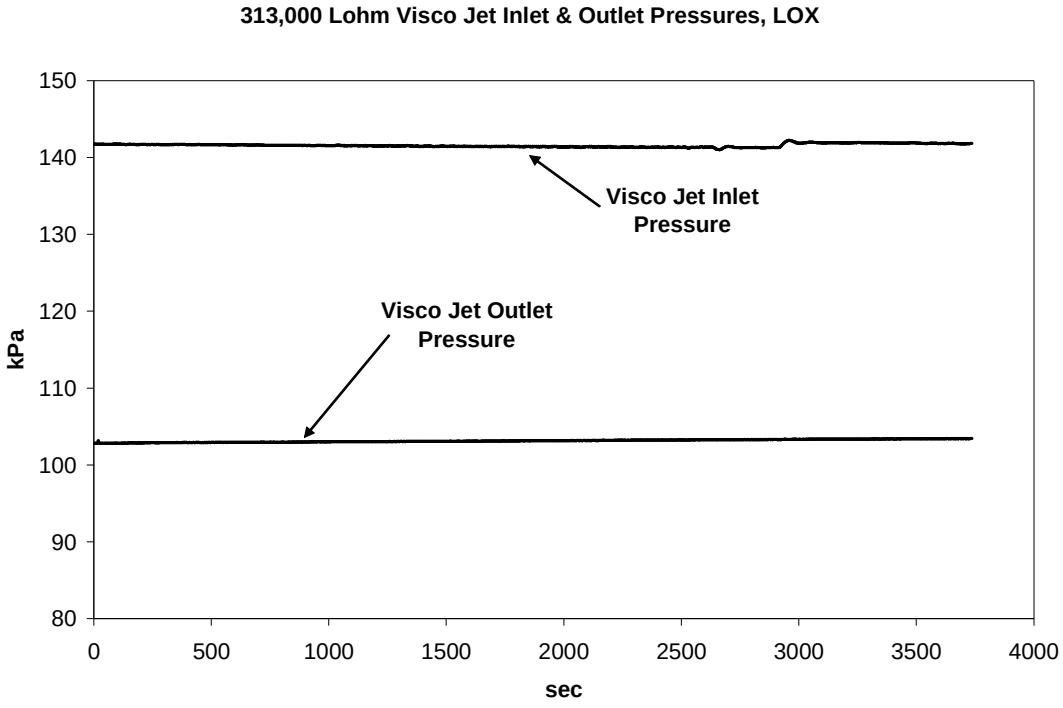

Figure 39

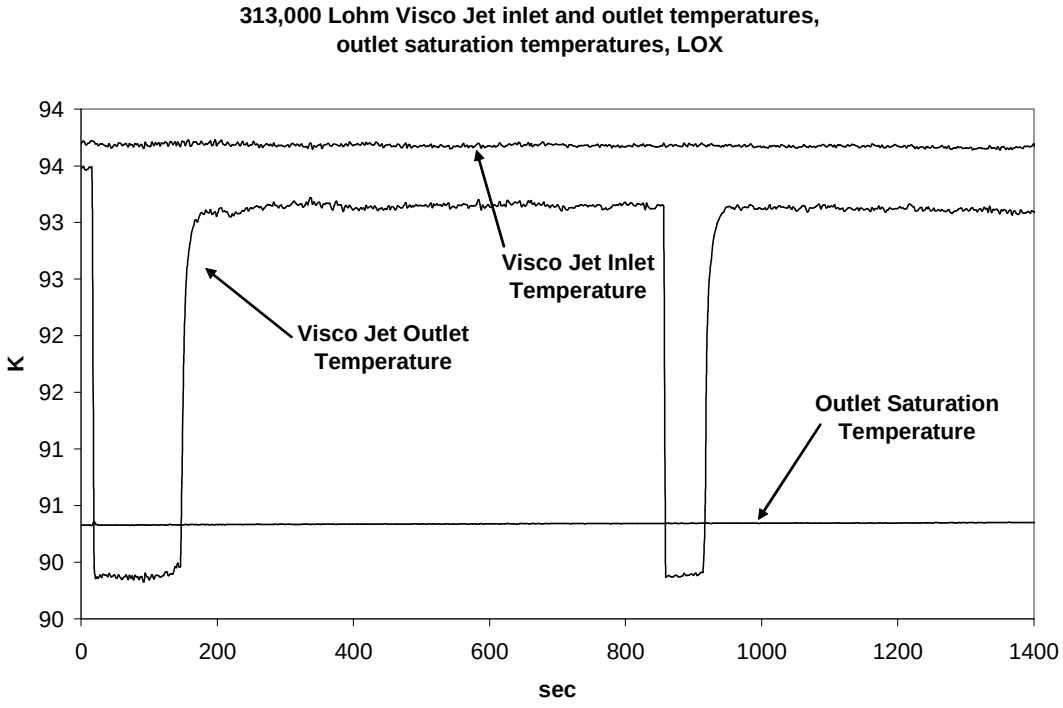

Figure 40

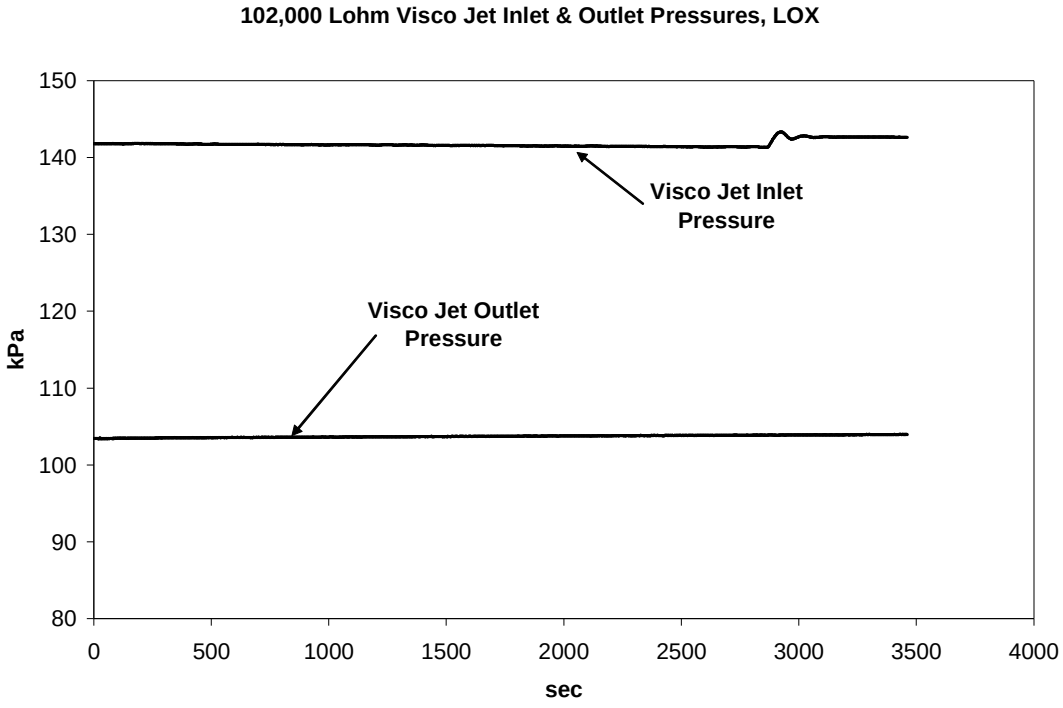

Figure 41

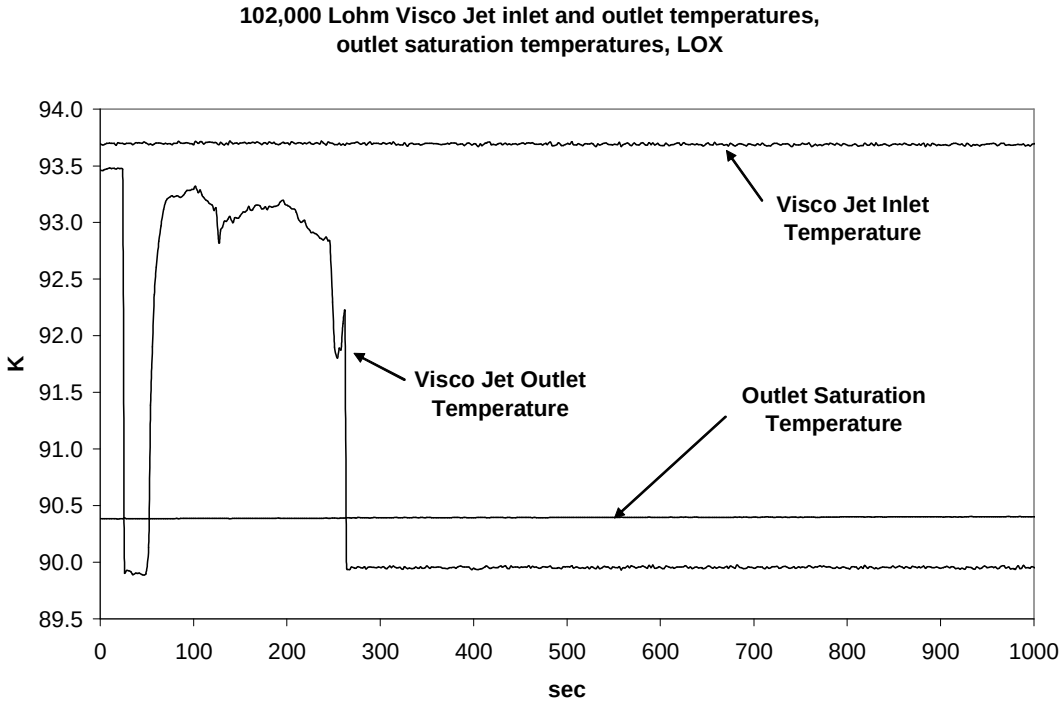

Figure 42

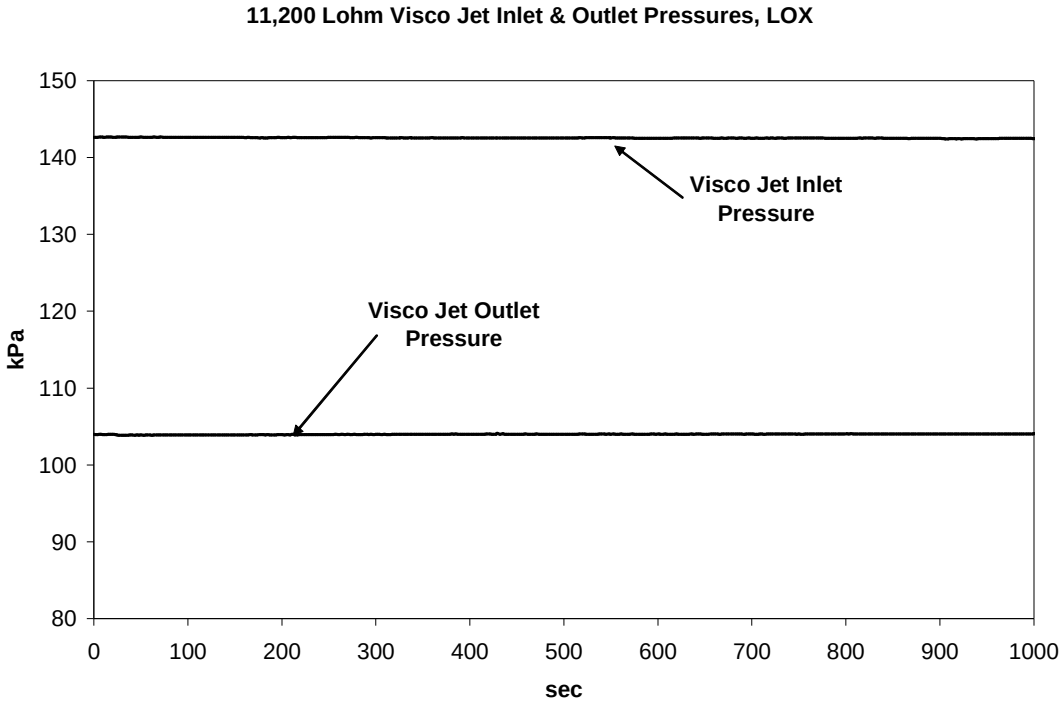

Figure 43

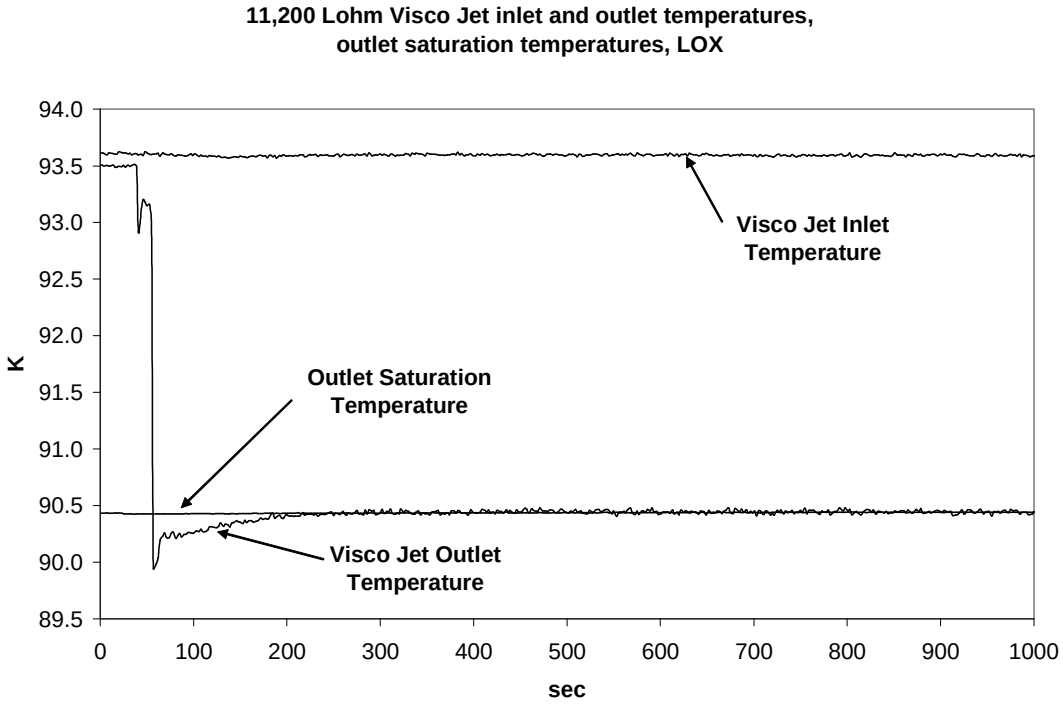

Figure 44

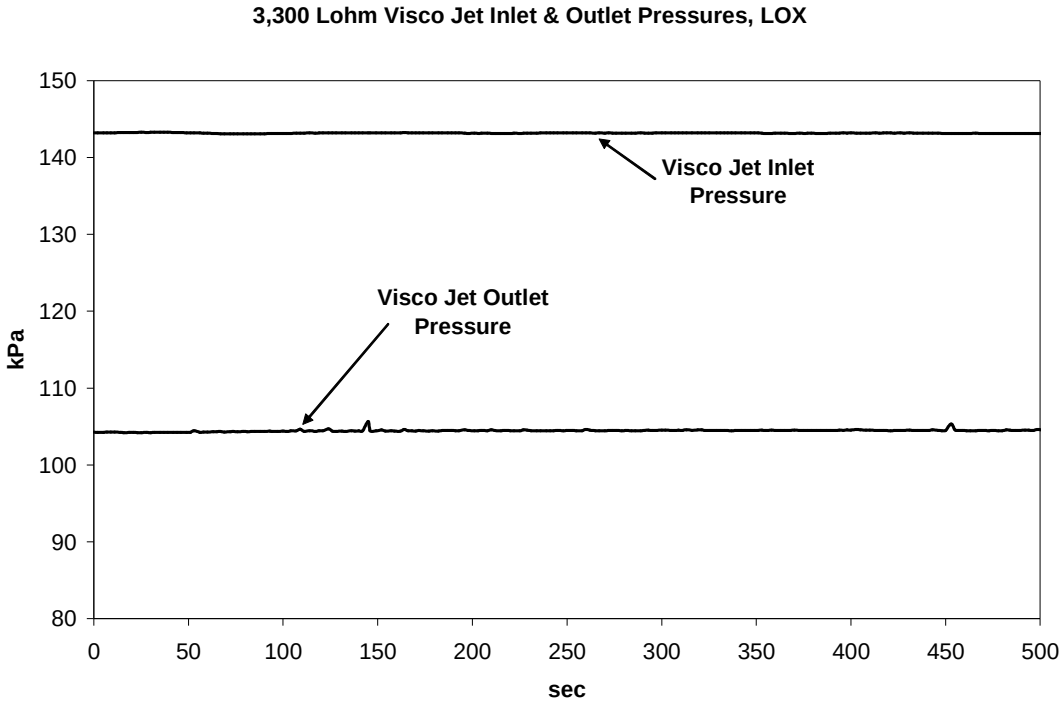

Figure 45

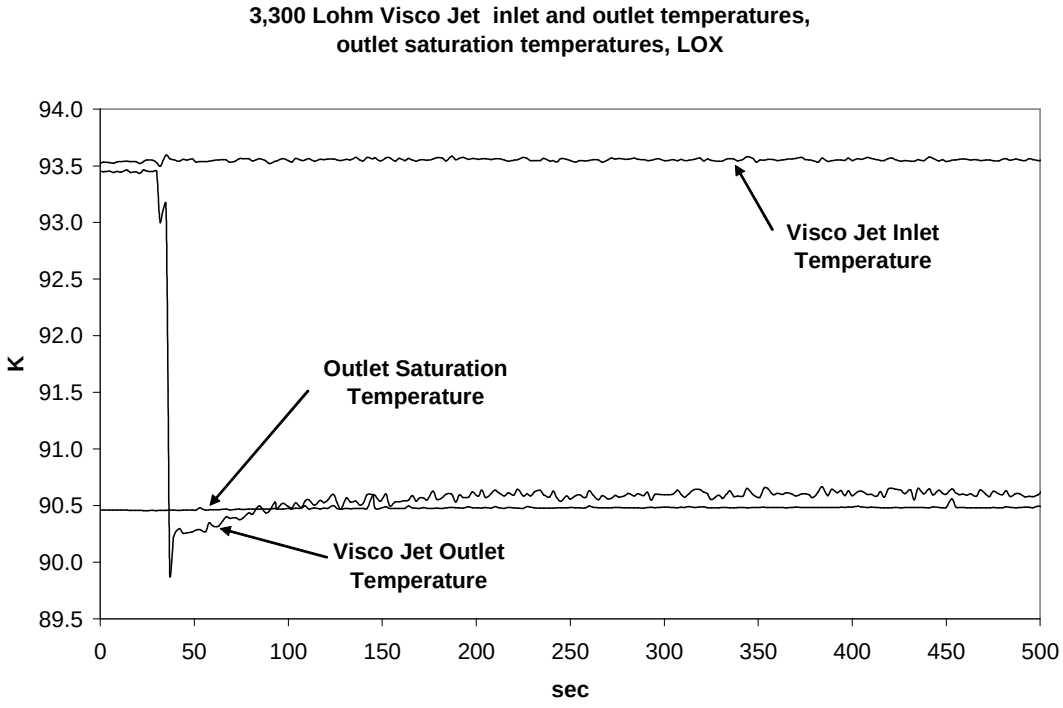

Figure 46

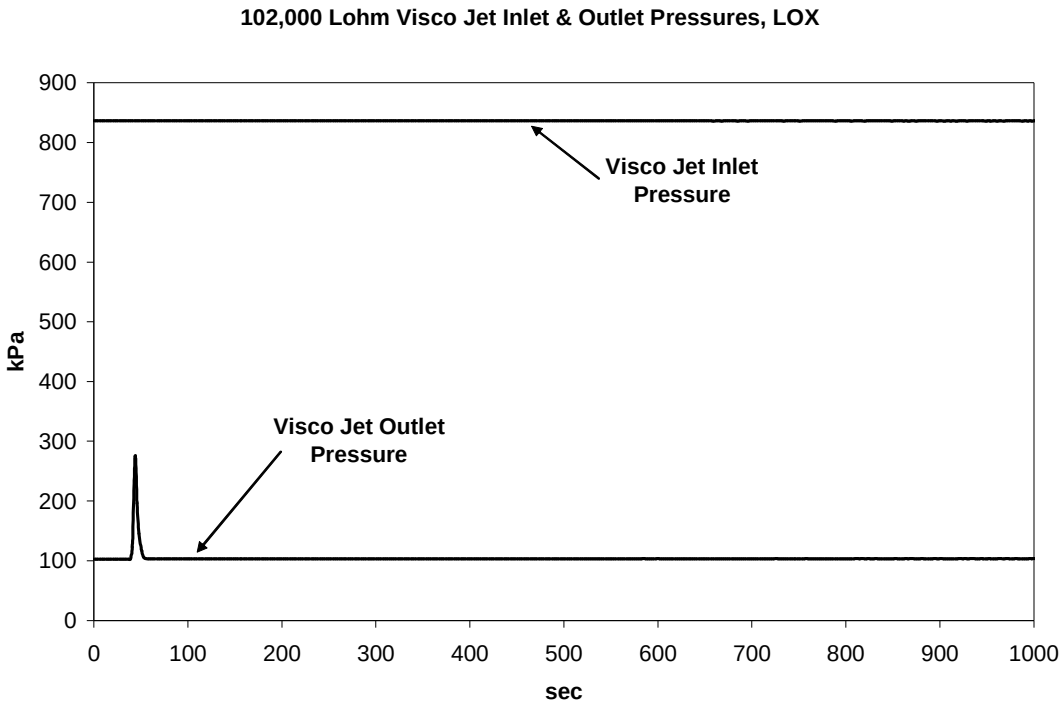

Figure 47

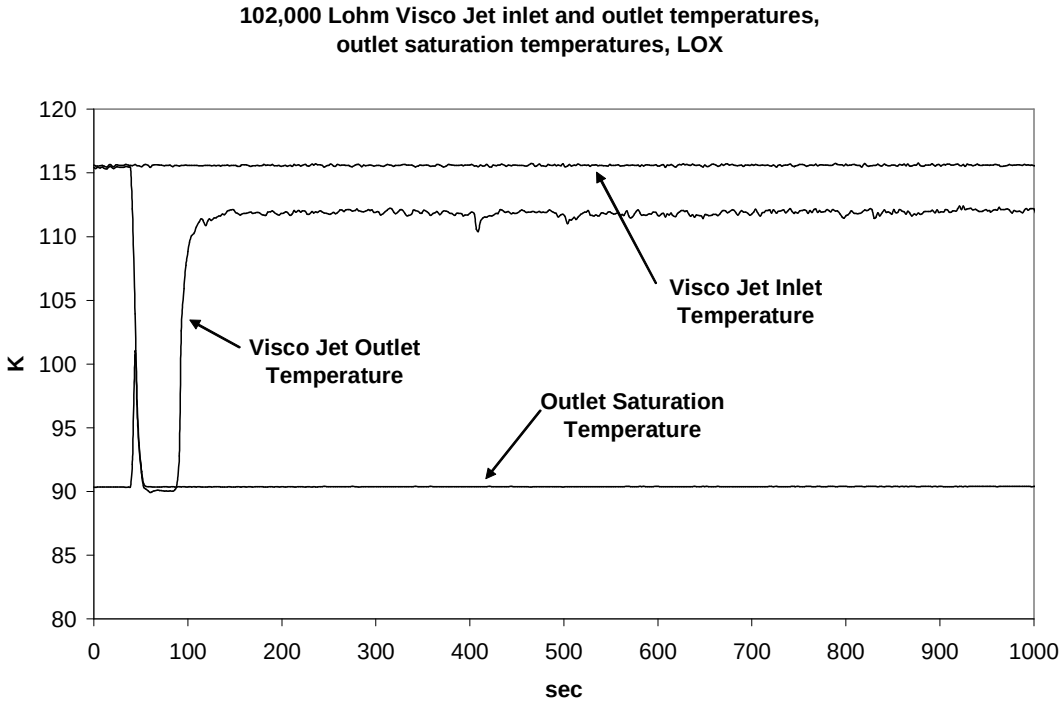

Figure 48

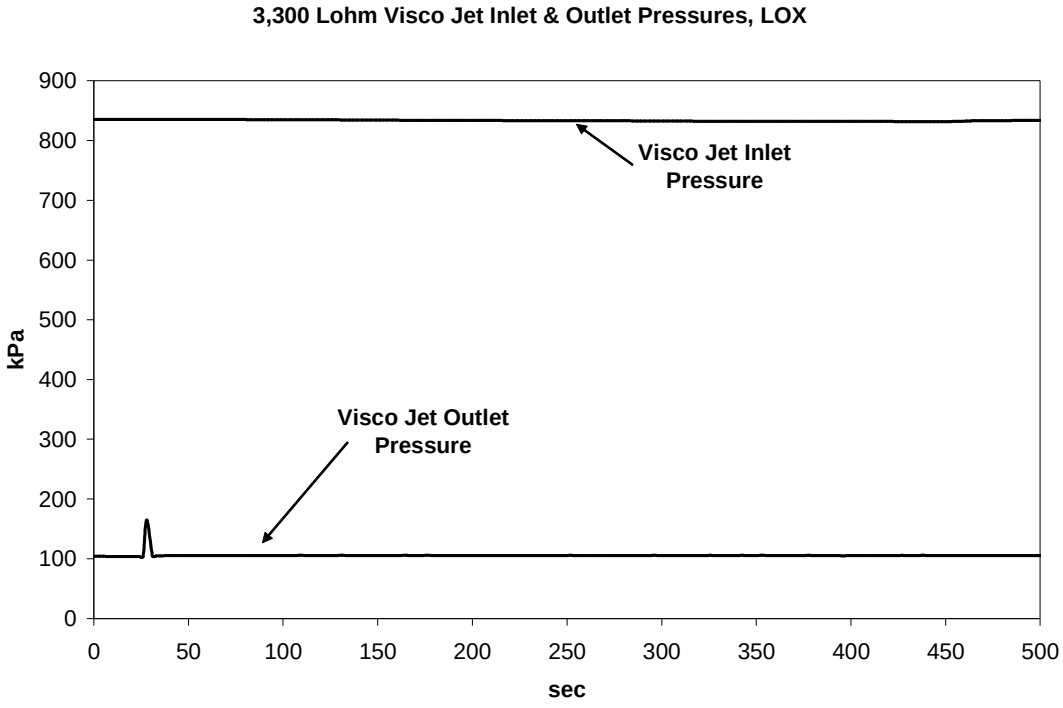

Figure 49

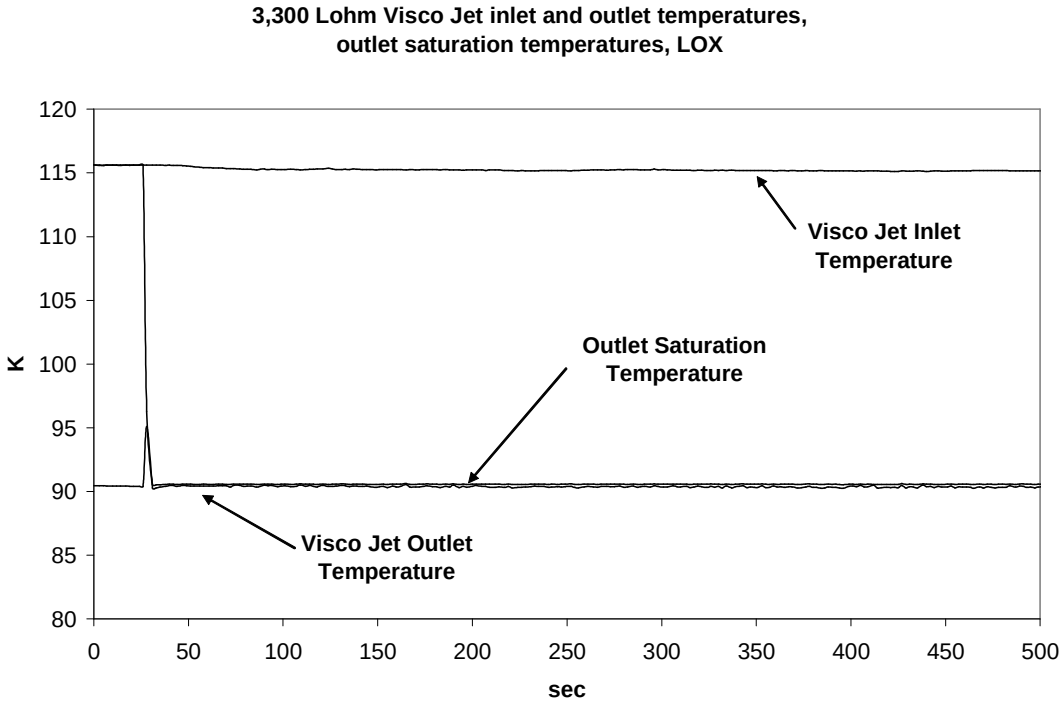

Figure 50

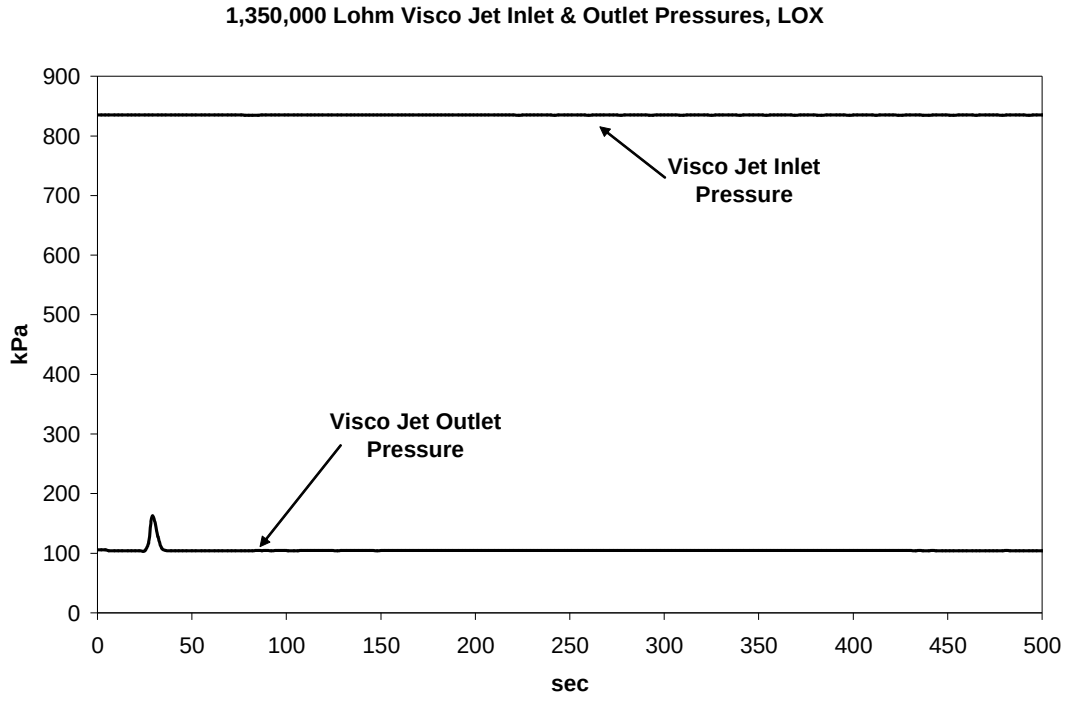

Figure 51

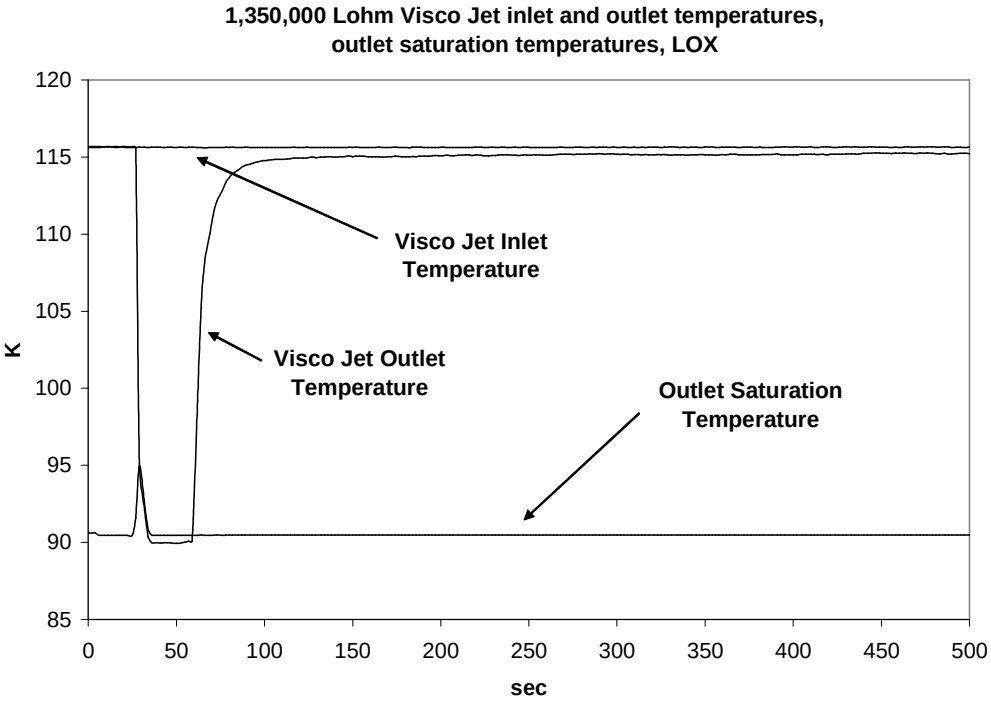

Figure 52

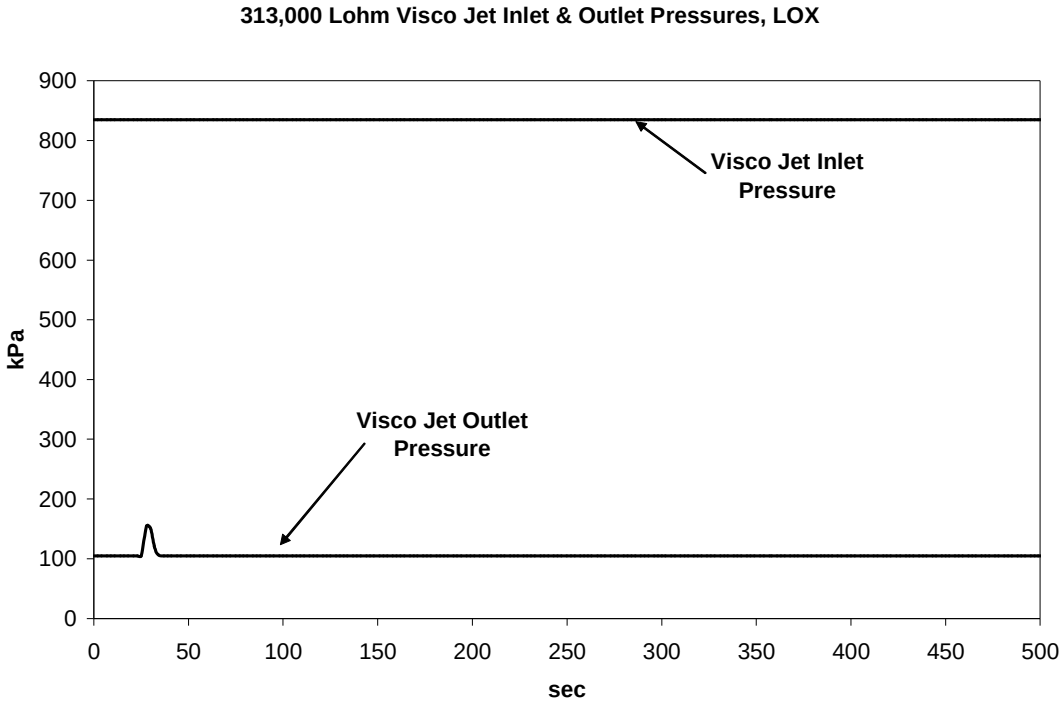

Figure 53

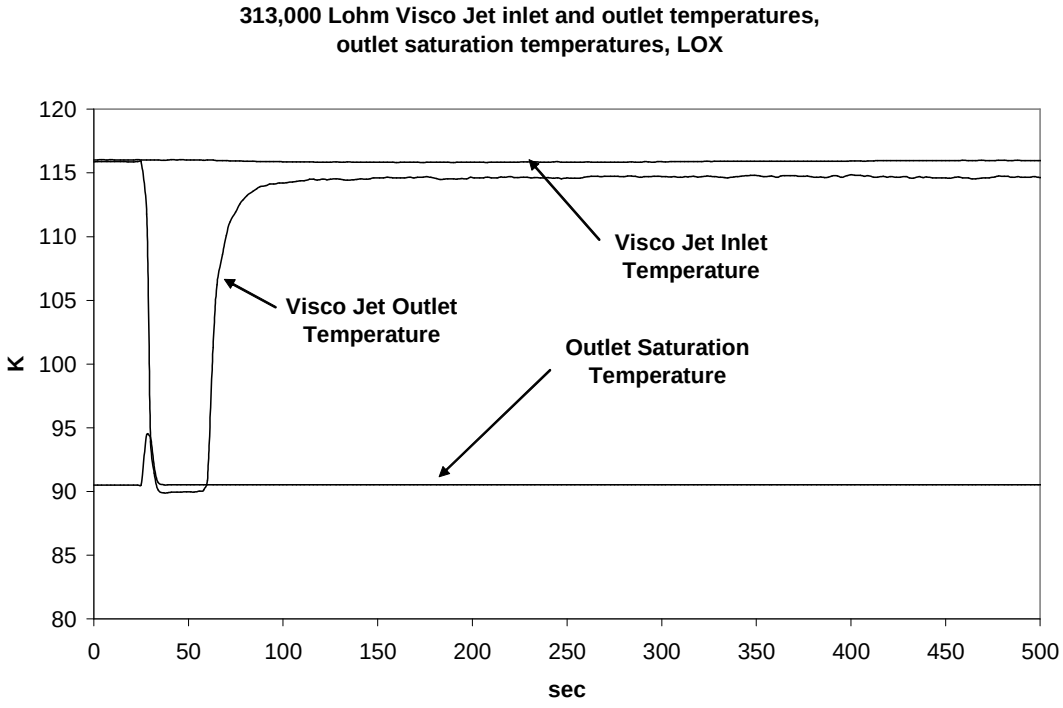

Figure 54

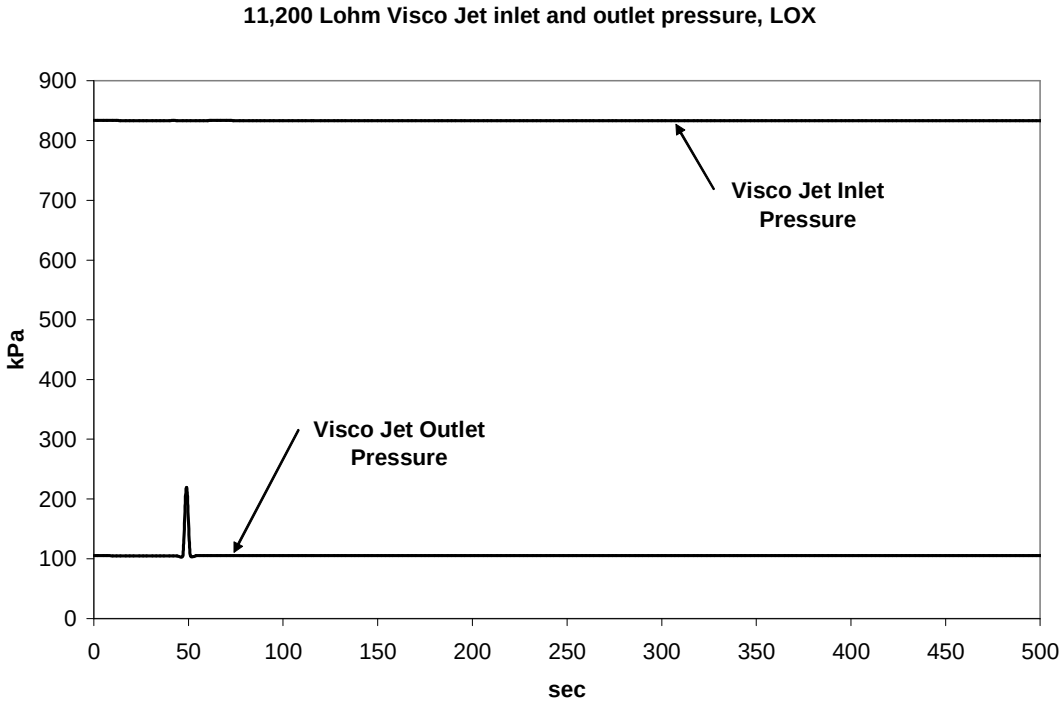

Figure 55

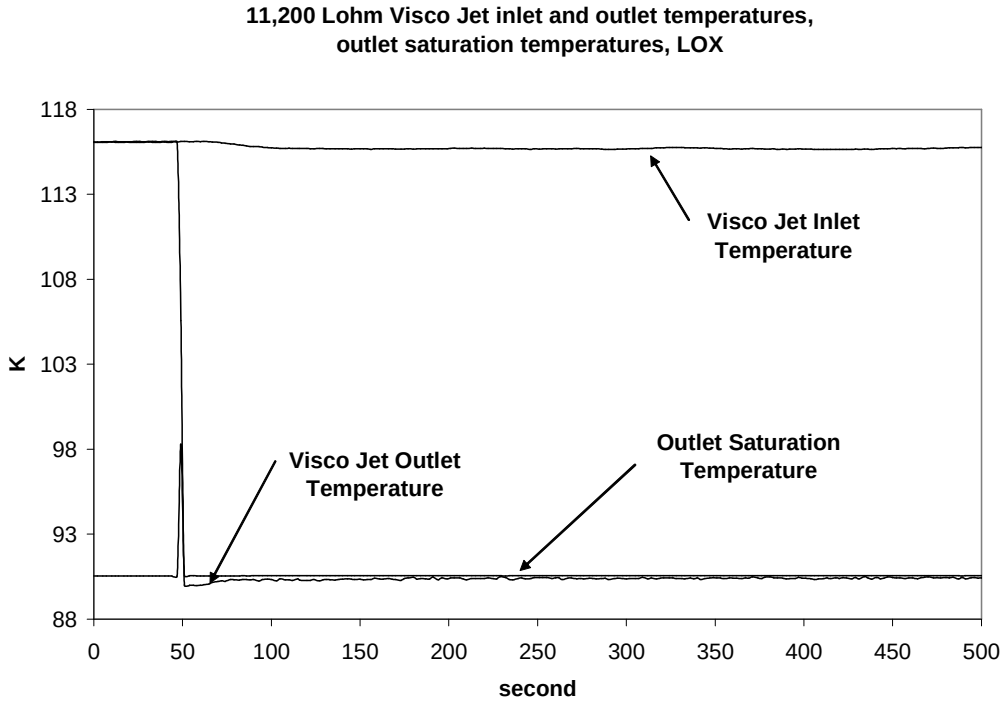

Figure 56

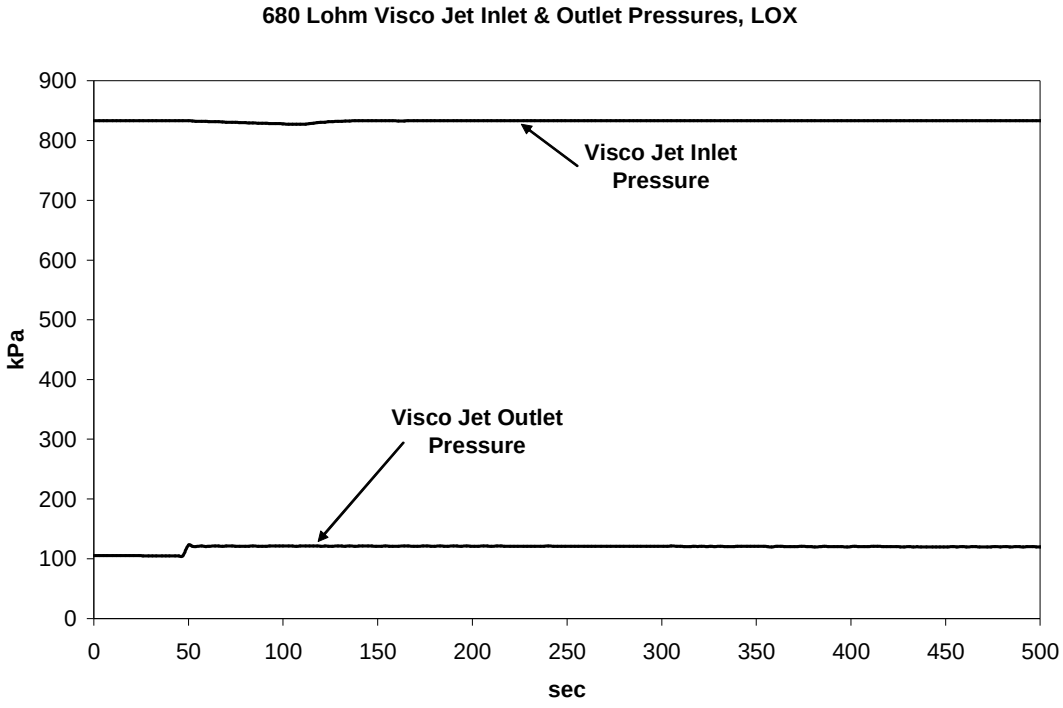

Figure 57

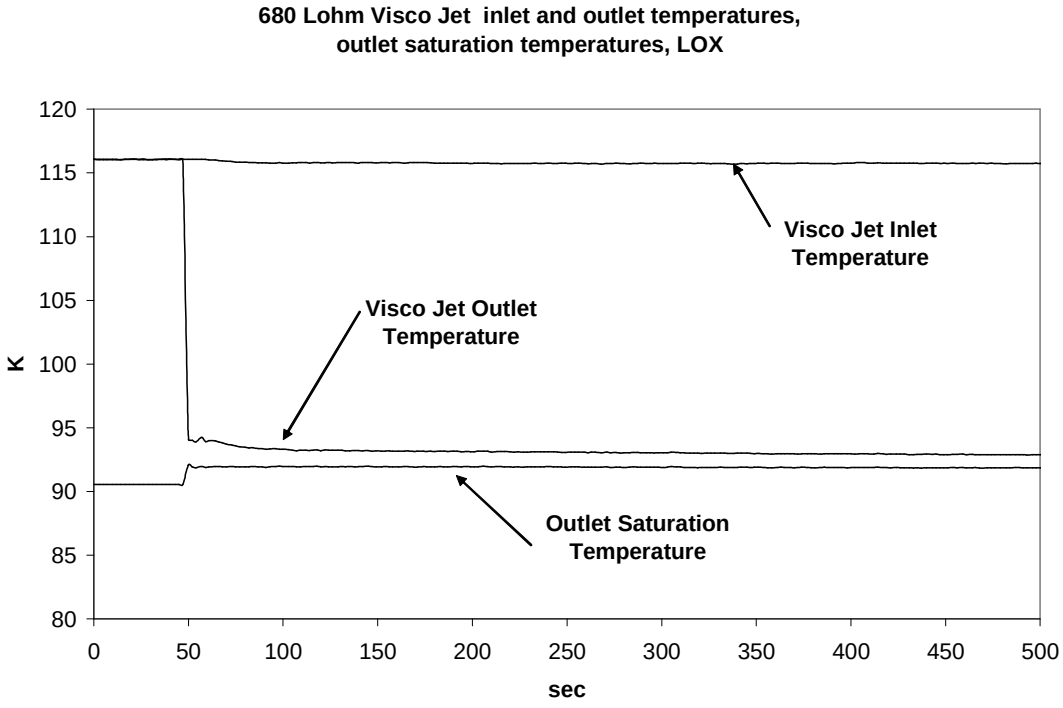

Figure 58

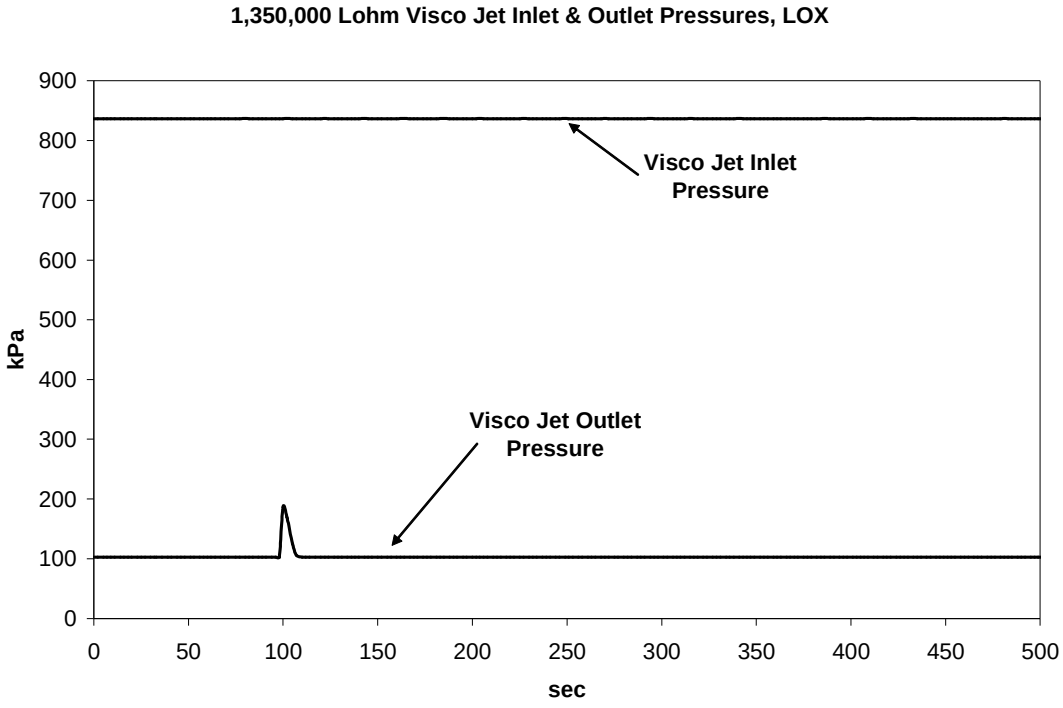

Figure 59

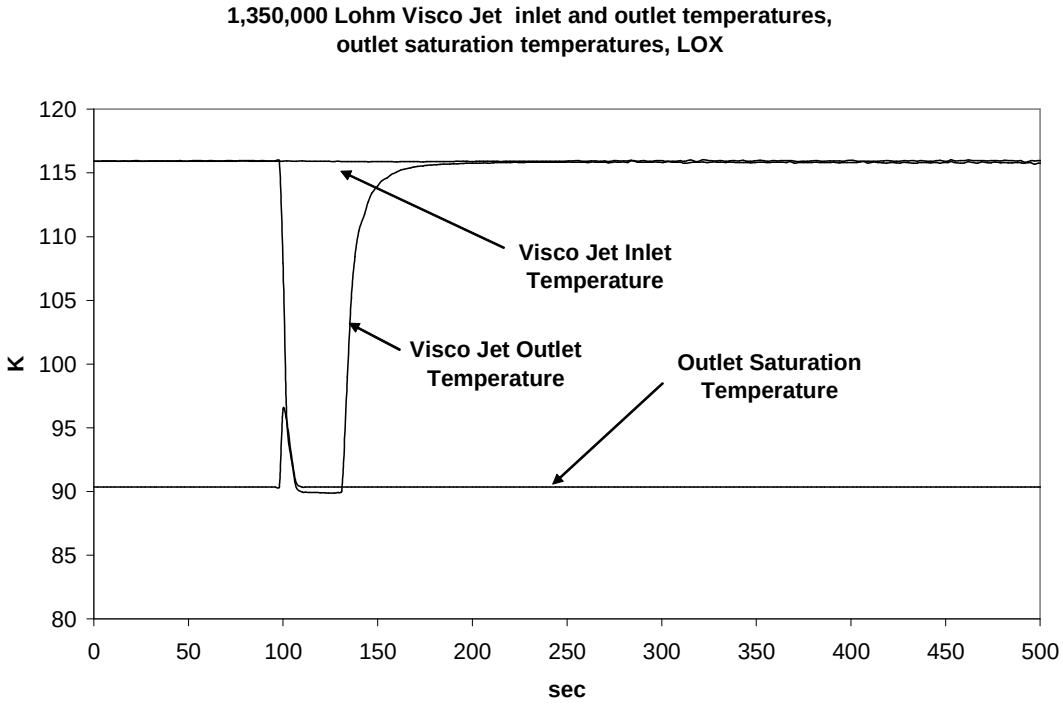

Figure 60

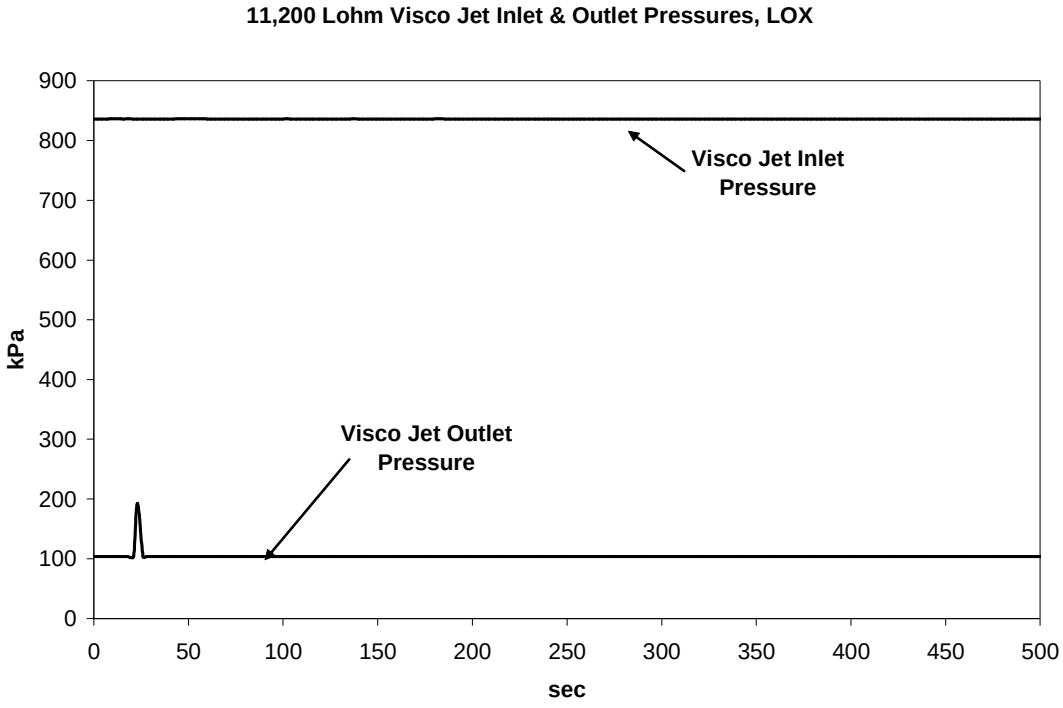

Figure 61

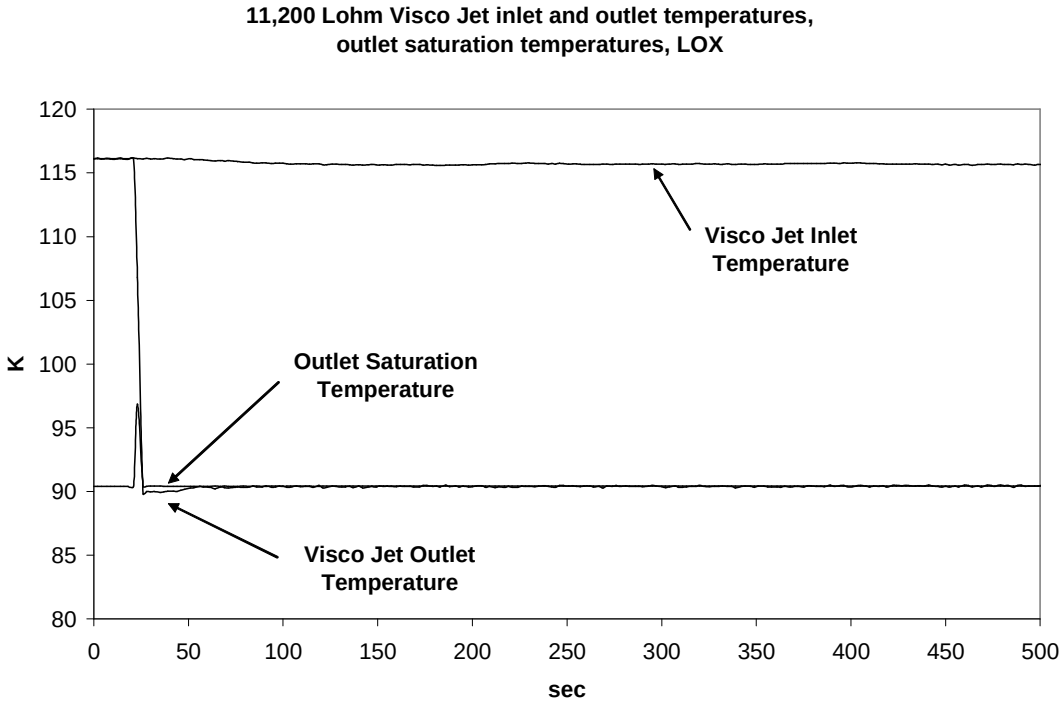

Figure 62

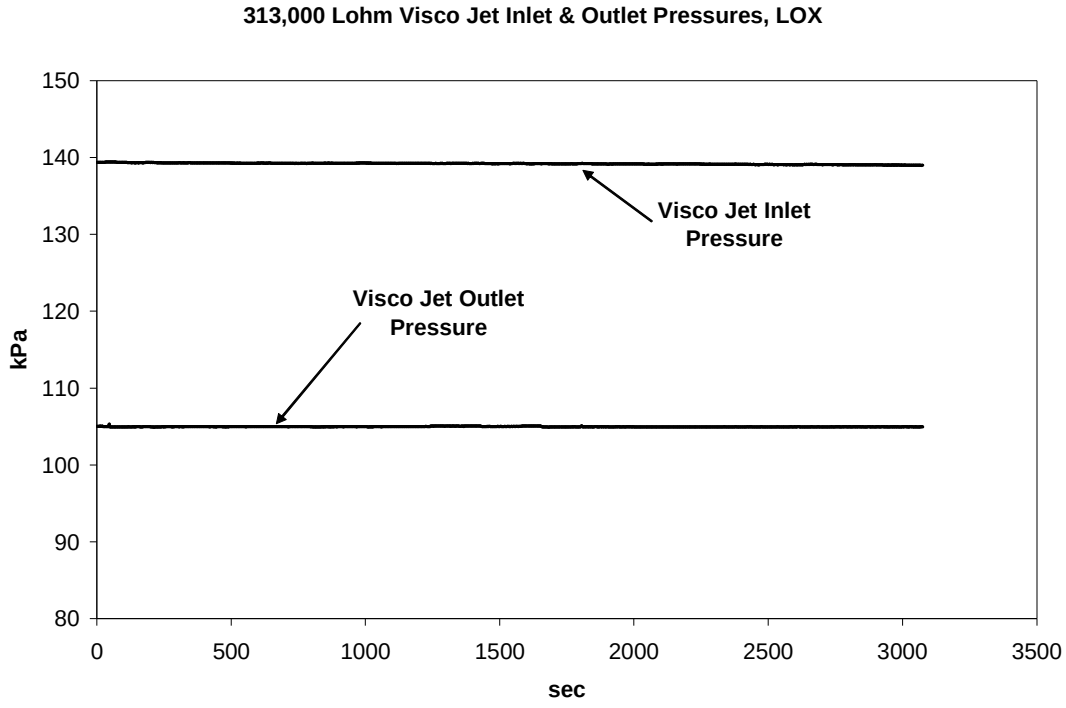

Figure 63

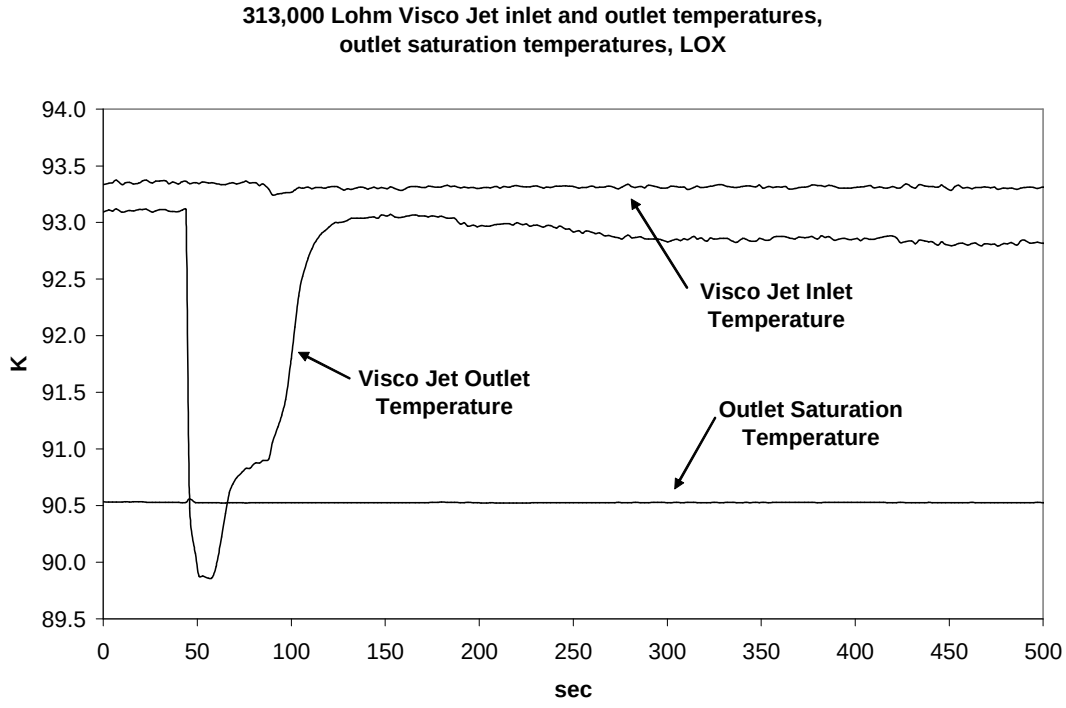

Figure 64

APPENDIX C - CRYOGNEIC FLUID THERMO-PHYSICAL PROPERTIES

Cryogenic fluid thermo-physical properties are available from a number of sources. Fluid properties used for analysis in this test program were obtained from the NIST Standard Reference Database 12, "NIST Thermophysical Properties of Pure Fluids" Version 3.0, 1992, published by the Fluid Mixtures Data Center, Thermophysics Division, NIST, Boulder, CO. This interactive DOS based database program computes thermophysical properties of 17 pure fluids according to the extremely accurate and wide ranging NIST standards reference correlations.

This database has since been commercialized, and is marketed under the name "GASPAK" by Cryodata.com. Cryodata's website is: http://www.cryodata.com/

This data is also available directly from NIST via their interactive website titled "Thermophysical Properties of Fluid Systems", available at: http://webbook.nist.gov/chemistry/fluid/